AD NUMBER
AD872104
LIMITATION CHANGES
TO: **Approved for public release; distribution is unlimited.**
FROM: **Distribution authorized to U.S. Gov't. agencies and their contractors; Critical Technology; JUN 1970. Other requests shall be referred to Air Force Aero Propulsion Laboratory, Wright-Patterson AFB, OH 45433. This document contains export-controlled technical data.**
AUTHORITY
AFAPL ltr, 12 Apr 1972

AFAPL-TR-70-47

AD872104

DESIGN OF MAXIMUM THRUST PLUG NOZZLES FOR FIXED INLET GEOMETRY

Robert P. Humphreys, H. Doyle Thompson, and Joe D. Hoffman

Jet Propulsion Center
Purdue University
Lafayette, Indiana 47907

TECHNICAL REPORT AFAPL-TR-70-47

JUNE 1970

AIR FORCE AERO PROPULSION LABORATORY
AIR FORCE SYSTEMS COMMAND
WRIGHT-PATTERSON AIR FORCE BASE, OHIO

222

NOTICE

When Government drawings, specifications, or other data are used for any purpose other than in connection with a definitely related Government procurement operation, the United States Government thereby incurs no responsibility nor any obligation whatsoever; and the fact that the Government may have formulated, furnished, or in any way supplied the said drawings, specifications, or other data, is not to be regarded by implication or otherwise as in any manner licensing the holder or any other person or corporation, or conveying any rights or permission to manufacture, use, or sell any patented invention that may in any way be related thereto.

Information in this report is embargoed under the U.S. Export Control Act of 1949, administered by the Department of Commerce. This report may be released by departments or agencies of the U.S. Government to departments or agencies of foreign governments with which the United States has defense treaty commitments. Private individuals or firms must comply with Department of Commerce export control regulations.

Copies of this report should not be returned unless return is required by security considerations, contractual obligations, or notice on a specific document.

AFAPL-TR-70-47

DESIGN OF MAXIMUM THRUST PLUG NOZZLES FOR FIXED INLET GEOMETRY

Robert P. Humphreys, H. Doyle Thompson, Joe D. Hoffman

FOREWORD

The present study is part of the program "An Analytical Study of the Exhaust Expansion System (Scramjet Scientific Technology)" being conducted by the Jet Propulsion Center, Purdue University, under United States Air Force Contract No. F33615-67-C-1068, BPSN 7 (63 301206 6205214). The Air Force program monitor was Lt. Gary J. Jungwirth of the Air Force Aero Propulsion Laboratory. This report presents a formulation, numerical solution technique, and a computer program implementing the technique for the optimization of fixed inlet plug nozzles including boundary layer effects. The problem is formulated for isentropic, rotational and isentropic, irrotational flows.

The authors wish to express their appreciation to the Air Force Frank J. Seiler Research Laboratory for its generous contribution of computer time and to Mr. Gearold R. Johnson for his efforts in making the computer program compatible with the computers at Purdue University and Wright-Patterson AFB.

This report was submitted by the authors on 25 May 1970.

Gary J. Jungwirth
1st Lt., USAF
Project Engineer
Ramjet Technology Branch
Ramjet Engine Division
AF Aero Propulsion Laboratory

ABSTRACT

The techniques of the calculus of variations have been used to determine the configuration of an optimum thrust plug nozzle. The problem is formulated for a fixed thrust injection angle and cowl lip radius, and the resulting plug contour is then an optimum for a given upstream geometry. The optimum values of the injection angle and cowl lip radius are determined by a parametric study. The analysis is carried out for rotational and irrotational flows and includes boundary layer effects. A method is presented for each of the problem formulations to determine if a given contour is an optimum and a relaxation technique is used to obtain a solution to the irrotational flow problem.

A computer program which makes use of the design equations for the irrotational flow problem is developed and described. This program is used to carry out a parametric study to determine the optimum cowl lip radius and injection angle when the plug length is fixed. The resulting optimum nozzle is compared to one designed by Rao's Method. The importance of determining the base pressure accurately is illustrated and an example of scramjet nozzle optimization is presented.

TABLE OF CONTENTS

LIST OF TABLES

LIST OF FIGURES

NOMENCLATURE

English Symbols

a	acoustic speed
C_1, C_2	Lagrange multipliers
E'	Cowl lip location
F	fundamental function, Eq. (9)
g	general isoperimetric constraint
G	boundary requirements, Eqs. (10), (11), and (12)
h_o	throat half-height
I	integral to be maximized, Eq. (8)
m	m'/ε
m'	gradient of the nozzle walls at the throat
m''	a mean radius of curvature at the throat
M	Mach number
n	number of generic dependent variables
p_o	total pressure
p	pressure
p_k	z_{k_x}, partial derivative of z_k with respect to x
q_k	z_{k_y}, partial derivative of z_k with respect to y
q	dynamic pressure, $\rho V^2/2$
R	gas constant
T	thrust integral, Eq. (1)
u	x-component of velocity

v y-component of velocity

V velocity modulus = $(u^2 + v^2)^{1/2}$

x spacial coordinate along the axis of symmetry

y spacial coordinate normal to the axis of symmetry

z_k typical generic dependent variable

Greek Symbols

α Mach angle

β angle of inclination of the general flow direction in the throat to the axis of symmetry

γ ratio of specific heats

δ^* a boundary layer thickness

$\delta(\ )$ first variation

δ' $\delta^* \cos\theta$

ε $R^{-1/2}$, where R is a non-dimensional radius of curvature of a meridian section at the throat

ζ_k defined by Eq. (B-6)

η defined by Eq. (B-5), and when used in conjunction with the Moore-Hall analysis η represents the asymmetry of the nozzle profile at the throat

θ flow angle

λ_1, λ_2, λ_3, λ_4 Lagrange multipliers

ξ defined by Eq. (B-4)

ρ density

ρ_d downstream radius of curvature of the plug wall at the throat

τ shear stress

ϕ base pressure contribution to the thrust, Eq. (13)

ψ $(\gamma - 1)/(\gamma + 1)$

Subscripts

b	base
D	evaluated at point D
DE	evaluated along the line DE
E	evaluated at point E
TD	evaluated along the boundary TD
w	evaluated on the nozzle wall
x	partial derivative with respect to x
y	partial derivative with respect to y

Other

$(\dot{\ })$	total derivative with respect to x
*	critical conditions

Blank Page

SECTION I

INTRODUCTION

Conceptually, nonconventional nozzles such as the plug nozzle or the forced deflection nozzle offer advantages that cannot be achieved with conventional nozzles. The plug nozzle, for example, has the potential advantages of throttleability, thrust vector control, altitude compensation, and a shorter (and presumably lighter) nozzle for the same expansion ratio when compared with a conventional axisymmetric nozzle. This type of nozzle is currently operational on General Electric's TF39 and Pratt and Whitney's JT9D jet engines and shows considerable promise for ramjet, scramjet, and rocket engine applications. Because of its potential importance, the problem of maximizing the thrust of a plug nozzle is of considerable interest and is the subject of this investigation.

The concept of applying optimization techniques to design thrust nozzles was introduced by Guderley and Hantsch (1) in 1955. Subsequently, Rao (2) simplified the analysis and developed a basic design procedure that has gained wide acceptance throughout the industry. Rao also applied his formulation to the plug nozzle design problem (3). His formulations (2,3) are limited to a fixed

nozzle length (or, equivalently, a fixed expansion ratio for a conventional nozzle). More recently Guderley and Armitage (4,5) reformulated the problem for the design of axisymmetric nozzles using a more general approach which provides for a wide selection of the form of the geometric constraint that can be imposed on the design. This additional flexibility is achieved only at the expense of a more complex problem formulation and an order of magnitude increase in the complexity of the numerical solution.

The additional potential of the Guderley-Armitage approach was realized when the method was extended by Hoffman and Thompson (6) to include the design of optimum nozzles for gas-particle flows, by Hoffman (7) to include the design of optimum nozzles for reacting nonequilibrium flows, and by Scofield, Thompson, and Hoffman (8) to include the effects of boundary layer drag in the optimization. The essential difference in applying the method to these various types of flows is in the computation of the basic flow field and not in the method itself.

In addition to the references already cited, it is of interest to note that the Soviets are actively engaged in this field of study (9,10,11,12,13). Krayko (9) has extended the work of Guderley and Armitage (4) to the construction of the rear part of a minimum drag body which is restricted in length. His study included two cases: 1) the pressure in the base region of the body is independent of the upstream body contour, and 2) the pressure in the base

region is dependent upon the upstream body contour. Pirumov and Rubtsov (10) have developed a computer program to calculate the flow field in axisymmetric plug and expansion-deflection nozzles using a linear sonic line. References 11, 12, and 13 are works of a similar nature.

The objective of this investigation is to determine the configuration of an optimum thrust plug nozzle, including the throat injection angle, cowl lip radius, and the plug contour, by applying the techniques of the calculus of variations. The problem is formulated for a fixed throat injection angle and cowl lip radius, and the resulting plug is then an optimum for the given upstream geometry. The optimum values of the injection angle and cowl lip radius are then determined by a parametric study.

The first two sections which follow contain the problem formulations. The first is for axisymmetric, steady, rotational* flow and the second is for axisymmetric, steady, irrotational** flow. Section IV contains explanations of the solution procedure and the method of plug contour modification. Section V contains: 1) the results of the

* The isentropic, rotational assumption implies that entropy and total enthalpy are constant on a streamline (see Ref. 14).

** The irrotationality assumption implies that entropy and total enthalpy are constant throughout the flow.

parametric study used to determine the optimum injection angle and cowl lip radius and the corresponding optimum plug contour, 2) a comparison of the optimum nozzle to a nozzle designed by Rao's method for the same conditions, 3) an explanation of the effects of changing the base pressure model, and 4) an example which illustrates the optimization of scramjet nozzles. The final section contains the summary and recommendations.

SECTION II

ROTATIONAL FLOW PROBLEM

1. FLOW MODEL

The plug contour to be optimized is that portion between points T' and D', shown in Figure 1 along with the remaining nozzle geometry. The cowl lip radius, y_E, and the injection angle, β, are prescribed, and the nozzle geometry upstream of the characteristic ET is fixed. The resulting optimum contour is then the best for a given upstream geometry. The region (R) is considered to be an inviscid core bounded by the streamline TD, the right characteristic DE, and the left characteristic ET. The streamline TD is separated from the plug surface by a boundary layer thickness δ^*, measured normal to the streamline. Thus, changes in the streamline TD will affect only the flow in region (R).

The axial thrust to be maximized is obtained by summing the integrated pressure and shear forces on the plug T'D' and the pressure forces acting on the base D'C. The thrust expression, developed in Appendix A, is given by:

$$\frac{T}{2\pi} = -\int_T^D [p(\dot{y} - \dot{\delta}') + \tau]\,(y - \delta')dx + (y_D - \delta'_D)^2 p_b/2 \qquad (1)$$

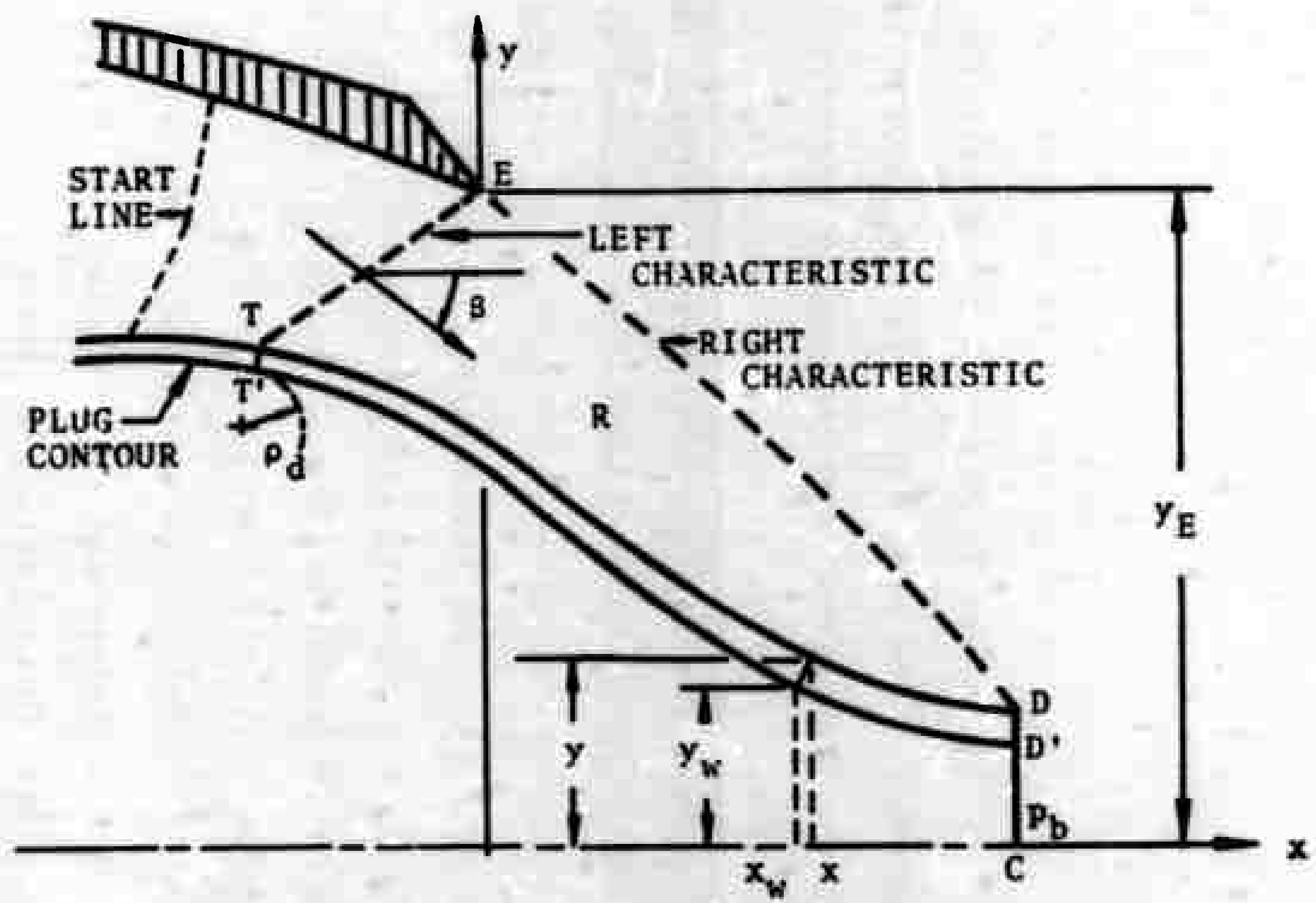

FIGURE 1. NOZZLE GEOMETRY AND COORDINATE SYSTEM

where $\delta' = \delta^* \cos\theta$ and $(\dot{})$ denotes differentiation with respect to x. Equation (1) represents only that portion of the total axial thrust which is to be maximized in the variational problem. The optimization with respect to the injection angle and cowl lip radius is accomplished by a parametric study. Since ambient pressure acts over the area πy_E^2, the altitude for which the nozzle is designed is specified during the parametric study. Thus, it is desired to find the streamline $y = y(x)$ which maximizes Eq.(1) and from which the wall contour can be obtained. However, it is necessary to introduce certain constraints to assure that the results will be physically realizable.

The governing equations for axisymmetric, steady, isentropic, rotational flow are the following:

$$\rho u_x + \rho v_y + u\rho_x + v\rho_y + \rho v/y = 0 \tag{2}$$

$$\rho u u_x + \rho v u_y + p_x = 0 \tag{3}$$

$$\rho u v_x + \rho v v_y + p_y = 0 \tag{4}$$

$$u p_x + v p_y - a^2 u\rho_x - a^2 v\rho_y = 0 \tag{5}$$

where the subscripts x and y denote partial derivatives. Equation (2) is the continuity equation, Eqs.(3) and (4) are the x and y Euler equations, and Eq.(5) is obtained as a result of the entropy being constant on a streamline. The boundary TD is to be a streamline, which requires the dependent variables u and v to be related by

$$u\dot{y} - v = 0 \qquad \text{along TD}$$

This expression is multiplied by $y\rho$ for later convenience in algebriac manipulation

$$y\rho(u\dot{y} - v) = 0 \qquad \text{along TD} \quad (6)$$

In addition to these constraints most engineering applications require the contour to have either a fixed length, a fixed surface area, or to be restricted in some other way. To place a physical limitation on the flow, a general isoperimetric constraint of the form

$$\int_T^D g(y,\dot{y},p)dx = \text{constant} \qquad \text{along TD} \quad (7)$$

is imposed. A fixed length constraint is obtained by setting $g = 1$ and the condition of a fixed surface area by setting $g = (1 + \dot{y}^2)^{1/2}$.

The constraining relations given by Eqs.(2) through (7) are imposed by utilizing Lagrange multipliers. The functional to be optimized becomes

$$I = \iint_R F dy dx + \int_{TDET} G dx + \Phi \qquad (8)$$

where

$$\begin{aligned} F = {} & \lambda_1(\rho u_x + \rho v_y + u\rho_x + v\rho_y + \rho v/y) \\ & + \lambda_2(\rho u u_x + \rho v u_y + p_x) + \lambda_3(\rho u v_x + \rho v v_y + p_y) \\ & + \lambda_4(u p_x + v p_y - a^2 u \rho_x - a^2 v \rho_y) \qquad \text{in R} \quad (9) \end{aligned}$$

$$G = -[f + C_1 g + C_2 y \rho(u\dot{y} - v)] \qquad \text{along TD} \qquad (10)$$

$$G = 0 \qquad \text{along DE} \qquad (11)$$

$$G = 0 \qquad \text{along ET} \qquad (12)$$

$$\Phi = (y_D - \delta'_D)^2 p_b/2 \qquad \text{at D} \qquad (13)$$

$$f = [p(\dot{y} - \dot{\delta}') + \tau](y - \delta') \qquad (14)$$

In the above equations λ_1 through λ_4 are functions of x and y, C_2 is a function of x, and C_1 is a constant.

The functional forms assumed for τ and δ' are

$$\tau = \tau(x) \quad , \quad \delta' = \delta'(x)$$

The base pressure is taken as constant over the base of the plug at an effective value which is determined by the flow properties in the region (R). Further, since the base pressure does not affect the flow properties in the region (R), it must be treated in the variational problem as a constant which is not known a priori. As will be explained in more detail later, the optimum contour is approached in an iterative manner in which the value of the base pressure is recalculated in each iteration.

The optimization procedure is independent of the model used to calculate the base pressure. The particular model used in this investigation and other details of base pressure are discussed in Appendix G. In addition it is assumed that the total temperature and pressure are known

for each streamline crossing the characteristic TE.

2. NECESSARY CONDITIONS

In the calculus of variations there are certain necessary conditions arising out of the first variation which have to be met for an extremal solution to exist. These conditions are the Euler Equations, transversality condition, Erdman-Weirstrass corner condition for corner lines, and the corner condition for corner points on a boundary line. The Erdman-Weirstrass condition will not be investigated since flows in which corner lines arise are not to be considered. When the remaining conditions are satisfied it will be assumed on physical grounds that the resulting nozzle surface is indeed the maximizing solution.

The calculus of variations for a functional of the type shown in Eq.(8) is developed in Appendix B. The details of the application of the calculus of variations are given in Appendices C through E and the results are presented in the next few sections.

a. Euler Equations. The general form of the Euler Equations, obtained for arbitrary variations of the generic dependent variables in the region (R), is given by Eq.(B-13). After application of this equation for each of the generic dependent variables u,v,p, and ρ, and some manipulation as shown in Appendix C, Eqs.(C-5), (C-9), (C-13), and (C-20) are obtained. This set of partial differential equations for

determining the Lagrange multipliers in the region (R) is:

$$-\lambda_2 u_x - \lambda_3 v_x - (\lambda_4/\rho)(p_x - a^2\rho_x) + y\lambda_{1_x} + u\lambda_{2_x} + v\lambda_{2_y} = \lambda_2 v/y \tag{15}$$

$$-\lambda_2 u_y - \lambda_3 v_y - (\lambda_4/\rho)(p_y - a^2\rho_y) + y\lambda_{1_y} + u\lambda_{3_x} + v\lambda_{3_y} = \lambda_3 v/y \tag{16}$$

$$\lambda_4 u_x + \lambda_4 v_y + (\lambda_4 a^2/p)(u\rho_x + v\rho_y) + \lambda_{2_x} + \lambda_{3_y} + u\lambda_{4_x} + v\lambda_{4_y} = 0 \tag{17}$$

$$(\lambda_2/\rho)p_x + (\lambda_3/\rho)p_y + yu\lambda_{1_x} + yv\lambda_{1_y} + a^2\lambda_{2_x} + a^2\lambda_{3_y} = 0 \tag{18}$$

where the subscripts x and y denote partial derivatives.

Equations (2) through (5), together with Eqs. (15) through (18), constitute a system of eight partial differential equations for determining the eight variables $u, v, p, \rho, \lambda_1, \lambda_2, \lambda_3$, and λ_4. As shown in Appendix F, these eight equations form a system of quasi-linear, nonhomogeneous, first-order partial differential equations of the hyperbolic type. Thus, the system can be replaced by an equivalent system of characteristic and compatibility equations. The characteristic system valid along gas streamlines is defined by Eqs. (F-40), (F-47), (F-48), (F-49), and (F-50). These equations are:

$$dy/dx = v/u \tag{19}$$

$$\rho u du + \rho v dv + dp = 0 \tag{20}$$

$$dp - a^2 d\rho = 0 \tag{21}$$

$$-\lambda_2 du - \lambda_3 dv + y d\lambda_1 + u d\lambda_2 + v d\lambda_3 = (\lambda_2 dx + \lambda_3 dy)(v/y) \tag{22}$$

$$(v\lambda_2 - u\lambda_3)dv + (\lambda_2/\rho)dp - (\lambda_4 u a^2/\rho)(\gamma - 1)d\rho + yud\lambda_1$$

$$-a^2 u d\lambda_4 = -(\lambda_4 a^2 v/y)dx \tag{23}$$

The system of equations valid along gas Mach lines is made up of Eqs. (F-42),(F-57), and (F-58). These equations are:

$$dy/dx = \tan(\theta \pm \alpha) \tag{24}$$

$$a^2(vdu - udv) \pm (a^2/\rho)\text{ctn}\ \alpha\ dp = (a^2 v/y)(udy - vdx) \tag{25}$$

$$\lambda_2 du + \lambda_3 dv - (\lambda_4/\rho)(dp + a^2 d\rho) - yd\lambda_1 \pm \tan\alpha\ (vd\lambda_2$$

$$-ud\lambda_3) = \mp \tan\alpha\ (\lambda_3 dx - \lambda_2 dy)(v/y) \tag{26}$$

The upper sign in Eqs.(24), (25), and (26) refers to left-running Mach lines and the lower sign to right-running Mach lines.

b. Transversality Conditions. The general transversality condition is given by Eq.(B-14). A detailed development of the transversality conditions is presented in Appendix D. The following is a summary of the results:

(1) Along ET. There can be no variations in u,v,p, ρ,x, or y along ET (see Figure 1) since the location of this line and the flow properties along it are determined by the

fixed upstream geometry. Therefore, the transversality conditions along ET are satisfied identically.

(2) Along DE. Application of Eq.(B-14) along DE results in the four equations (D-4) through (D-7). These four equations can be combined to yield the equation of a right-running characteristic which can be used to replace any of the four equations. Thus, DE is required to be a right-running characteristic along which Eqs.(D-4),(D-5), and (D-7) must be satisfied in addition to the characteristic equation which is used to replace Eq.(D-6). These equations are:

$$y\dot{y}\lambda_1 + (u\dot{y} - v)\lambda_2 = 0 \tag{27}$$

$$y\lambda_1 - (u\dot{y} - v)\lambda_3 = 0 \tag{28}$$

$$y\lambda_1 - a^2\lambda_4 = 0 \tag{29}$$

$$(u^2 - a^2)\dot{y}^2 - 2uv\dot{y} + (v^2 - a^2) = 0 \tag{30}$$

(3) Along TD. When Eq.(B-14) is applied along TD, Eqs.(D-14),(D-18), and (D-31) result. These equations are as follows:

$$\lambda_1 = C_2 \tag{31}$$

$$u\lambda_3 - v\lambda_2 + uf_p + ug_pC_1 = 0 \tag{32}$$

$$\begin{aligned} dC_2/dx = {} & (y - \delta')(du/dx + \dot{\delta}'dv/dx)/y \\ & -[C_1\ (\rho ug_p dv/dx - g_y + d(g_y)/dx]/(y\rho u) \\ & + \tau/(y\rho u) \end{aligned} \tag{33}$$

where

$$f_p = (\dot{y} - \dot{\delta}')(y - \delta') \tag{34}$$

c. <u>Corner Conditions</u>. The corner conditions are discussed in detail in Appendix E. Points E and T are considered to be fixed, thus the corner condition is satisfied identically at these two points. The condition which must be satisfied at point D is given by Eq.(B-16). Application of this equation yields Eqs.(E-12) and (E-13) which are:

$$[(y - \delta')(p\dot{\delta}' - \tau) + C_2\rho u y\dot{y} - C_1(g - \dot{y}g_{\dot{y}})]_{TD} = 0 \tag{35}$$

$$[p(y - \delta') + C_1 g_{\dot{y}} + C_2\rho y u]_{TD} = (y_D - \delta'_D)p_b \tag{36}$$

3. METHOD OF SOLUTION

The equations obtained from the variational problem can now be applied in a straightforward manner to determine if a given contour is an optimum. A contour for the plug is assumed and the flow field calculated by the method of characteristics. However, this requires an initial-value line along which the flow properties are known.

In the problem formulation it has been assumed, perhaps naively, that the initial conditions from which the method of characteristic solution can be initiated are provided or can be readily calculated. This is consistent with the fact that the optimization method is independent of the method of obtaining initial conditions, and only requires that the initial conditions represent a physically possible flow that

is compatible with the governing equations for the supersonic flow field. Thus, the same optimization procedure is used for a scramjet, for which the initial conditions at the nozzle entrance are provided either from measured data or from a theoretical analysis of the flow through the combustor, and for a subsonic burning engine for which the initial conditions can be determined from a transonic flow analysis.

Once the flow field has been calculated, values of the Lagrange multipliers λ_1 through λ_4 can be determined at point D from Eqs.(27),(29),(31),(32),(35), and (36). Starting at point D, values of these multipliers can be evaluated along TD using Eqs.(22),(23),(31),(32), and (33). Then, utilizing the characteristic net (see Figure 2) developed in evaluating the flow field, the Lagrange multipliers in the region (R) can be determined.

Starting at point 1 near the base of the plug, the initial data known along TD can be used, along with Eq.(26) which is valid along the two Mach lines intersecting at point 2, and Eqs.(27) and (29) which are valid along DE, to determine the Lagrange multipliers λ_1 through λ_4 at point 2. The values of λ_1 through λ_4 can be determined at point 3 by applying Eq.(26) along the Mach lines intersecting at point 3 and Eqs.(22) and (23) along the gas streamline passing through points 2 and 3. Point 5 can be determined in the same manner as point 2. The Lagrange multipliers can be determined throughout the region (R) by continuing this procedure.

Note that Eq.(28) was not used in the above procedure but

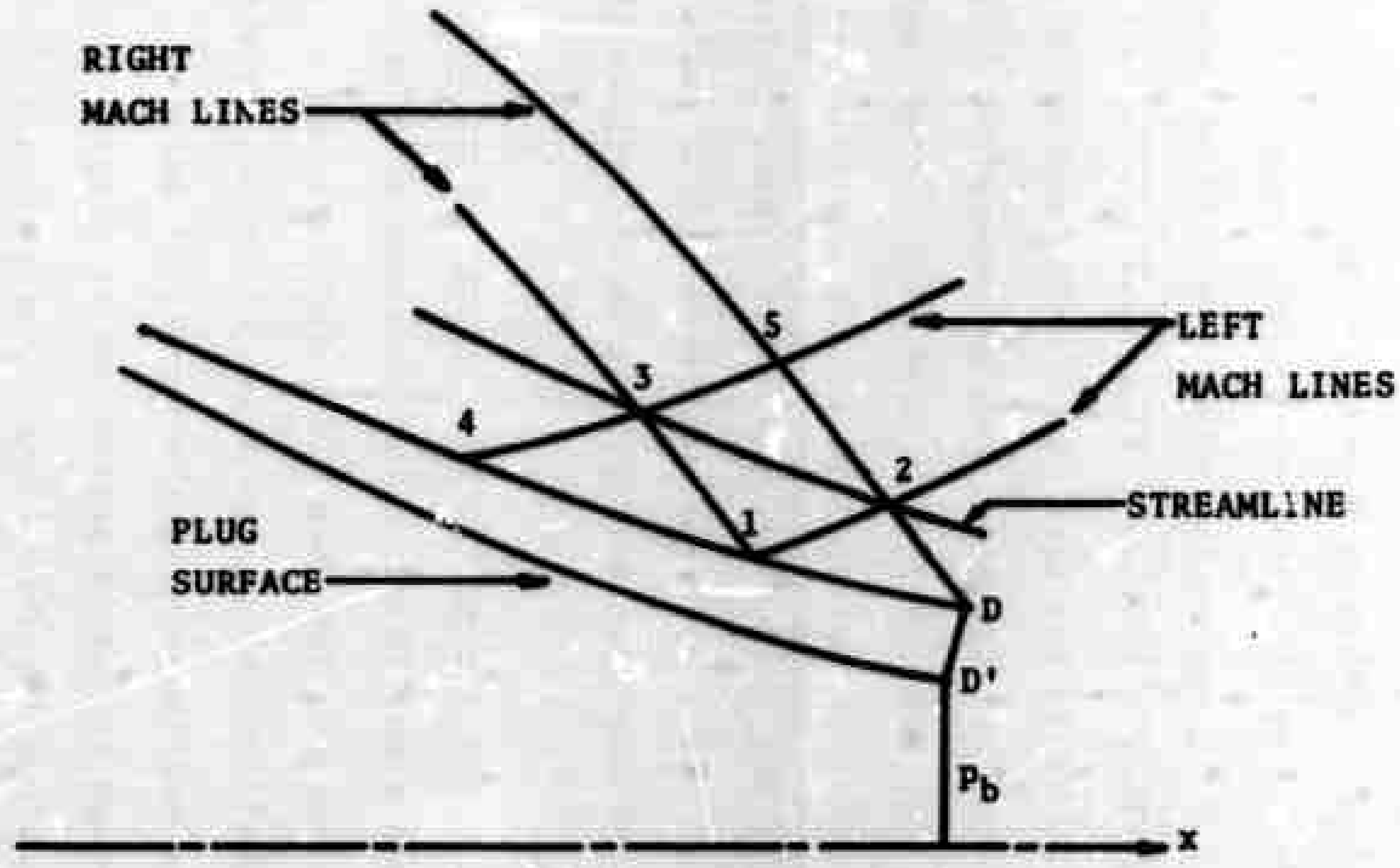

FIGURE 2. CHARACTERISTIC NET

must be satisfied along DE. This relation then serves as a means of checking whether a given contour is an optimum. If the contour is not an optimum, it must be modified to satisfy Eq.(28).

Contour modification techniques have been developed by Guderley and Armitage (5) and Scofield et al.(8) for irrotational flow. Even though the current problem is more complex, it appears that a similar contour modification technique could be developed to obtain an optimum plug contour.

It is possible to significantly simplify the calculation procedure by considering a problem which is slightly more restrictive than the present one and yet retains the significant features of the optimization, thereby providing considerable insight into the design and operation of optimum plug nozzles. This problem is considered in the next section.

SECTION III

IRROTATIONAL FLOW PROBLEM

1. FLOW MODEL

The problem to be considered here is one in which the flow in region (R)(see Figure 1) is irrotational. The thrust to be maximized in the variational problem is given by Eq.(1) which is repeated here for convenience:

$$\frac{T}{2\pi} = -\int_T^D [p(\dot{y} - \dot{\delta}') + \tau](y - \delta')dx + (y_D - \delta_D')^2 p_b/2 \quad (37)$$

Here again, the optimum values of the injection angle and cowl lip radius are obtained from a parametric study.

The basic difference between this problem formulation and the one presented in Section II is in the governing equations of motion. For the flow field to be isentropic, it must satisfy the irrotationality condition:

$$u_y - v_x = 0 \quad (38)$$

The flow field must also satisfy the continuity equation

$$(y\rho u)_x + (y\rho v)_y = 0 \quad (39)$$

where the subscripts indicate partial derivatives. Along the nozzle wall the dependent variables are related through the

equation for a streamline which is:

$$y\rho(u\dot{y} - v) = 0 \tag{40}$$

Also, a general isoperimetric constraint is imposed along TD.

$$\int_T^D g(y,\dot{y},p)dx = \text{constant} \tag{41}$$

The constraining relations given by Eqs.(38),(39),(40) and (41) are again imposed by means of Lagrange multipliers such that the functional to be maximized becomes

$$I = \iint_R F dy dx + \oint G dx + \Phi \tag{42}$$

where

$$F = \lambda_1(u_y - v_x) + \lambda_2[(y\rho u)_x + (y\rho v)_y] \qquad \text{in R} \quad (43)$$

$$G = -[p(\dot{y}-\dot{\delta}') + \tau](y-\delta') + \lambda_3 y\rho(u\dot{y} - v) + \lambda_4 g \quad \text{along TD} \; (44)$$

$$G = 0 \qquad \text{along DE} \; (45)$$

$$G = 0 \qquad \text{along ET} \; (46)$$

$$\Phi = (y_D - \delta_D')^2 p_b/2 \qquad \text{at D} \quad (47)$$

In the above equations λ_1 and λ_2 are functions of x and y, λ_3 is a function of x, and λ_4 is a constant.

In addition it is assumed that the total temperature and pressure are known. Since the flow is isentropic the functional relations

$$p = p(u,v) \quad \rho = \rho(u,v) \quad a = a(u,v) \quad \alpha = \alpha(u,v)$$

are valid. Thus, the dependent variables are the velocity components u and v.

2. NECESSARY CONDITIONS

The calculus of variations can be applied to Eq.(42) in a manner similar to the previous case to determine the conditions necessary to an extremal solution. These conditions are as follows:

a. Euler Equations.

$$\lambda_{1_y} + y\rho(1 - u^2/a^2)\lambda_{2_x} - y\rho(uv/a^2)\lambda_{2_y} = 0 \tag{48}$$

$$\lambda_{1_x} + y\rho(uv/a^2)\lambda_{2_x} - y\rho(1 - v^2/a^2)\lambda_{2_y} = 0 \tag{49}$$

In the region of supersonic flow these equations are a system of hyperbolic, partial differential equations with characteristic directions which correspond to the characteristic directions of the basic flow field. The compatibility equations are

$$d\lambda_1 \mp y\rho \operatorname{ctn} \alpha \, d\lambda_2 = 0 \tag{50}$$

Equations (50) are valid along the characteristics of the basic flow field, defined by

$$dy/dx = \tan(\theta \pm \alpha) \tag{51}$$

The upper sign in Eqs.(50) and (51) refers to left-running characteristics and the lower sign to right-running characteristics.

b. Transversality Conditions.

(1) Along TD. Along this line variations in u,v,x, and y can be treated as arbitrary and independent which results in three equations:

$$\lambda_2 = \lambda_3 \tag{52}$$

$$\lambda_1 = \rho u(y - \delta')(\dot{y} - \dot{\delta}') + \lambda_4 \rho u g_p \tag{53}$$

$$\dot{\lambda}_3 = (y - \delta')(du/dx + \dot{\delta}' dv/dx)/y - (\lambda_4/y)[g_p \dot{v} - (g_y - dg_{\dot{y}}/dx)/(\rho u)] + \tau/(y\rho u) \tag{54}$$

(2) Along DE. Along the exit characteristic, DE, variations in u,v,x, and y can be treated as arbitrary and independent. This results in two equations which can be combined to yield the equation of a right-running characteristic. This equation can be used to replace one of the two original equations. Thus, DE is required to be a right-running characteristic along which the following equation must be satisfied:

$$\lambda_1 - \lambda_2 y\rho \text{ ctn } \alpha = 0 \tag{55}$$

(3) Along ET. Since no variations in the gas properties or in x and y are allowed upstream of the left-running characteristic ET, the transversality condition is satisfied identically along this line.

c. Corner Conditions.

As in the previous case, corner conditions are obtained at point D only. The two conditions which must be satisfied at this point are:

$$[(y - \delta')(p\dot{\delta}' - \tau) - \lambda_4(g - \dot{y}g_{\dot{y}}) + \lambda_3 y\rho u\dot{y}]_{TD} = 0 \qquad (56)$$

$$[p(y - \delta') + \lambda_3 y\rho u + \lambda_4 g_{\dot{y}})_{TD} = (y_D - \delta_D')p_b \qquad (57)$$

3. METHOD OF SOLUTION

The solution procedure for this problem is similar to that of the previous case, but is somewhat less complicated. First, the flow field is solved by the method of characteristics. The characteristics have directions given by Eq.(51) and the compatibility relations valid along these lines are

$$d\theta \mp \text{ctn}\,\alpha\, dV/V \pm [(\sin\theta \sin\alpha)/(y \sin(\theta\pm\alpha)]dy = 0 \qquad (58)$$

The upper sign refers to left-running characteristics and the lower sign to right-running characteristics. Once the flow field is known, Eqs.(52),(56), and (57) can be used to solve for λ_1 and λ_2 at point D.

Starting from point D, Eqs.(52),(53), and (55) can be used to evaluate λ_1 and λ_2 along TD. The plug surface TD then serves as an initial-value line from which to start the method of characteristics solution for λ_1 and λ_2 in the region (R). These two multipliers have the same characteristic directions as the flow field, and their compatibility relations are given by Eqs.(50).

Equation (55) must be satisfied along the exit characteristic, DE, and serves as a check to determine whether or not a given contour is an optimum. If Eq.(55) is not satisfied then the contour must be modified. As mentioned earlier, contour modification techniques have been developed

for the type of flow under consideration, but were applied to converging-diverging nozzles.

4. RAO'S RESULT A SPECIAL CASE

It is of interest to note that the current formulation contains the results of Rao(3) as a special case. If the axial length is held constant, then $g = 1$, and

$$g_p = g_y = g_{\dot{y}} = 0$$

Neglecting the wall shear stress and boundary layer thickness, Eq.(54), valid along TD, becomes

$$d\lambda_3/dx = du/dx$$

or since $\lambda_2 = \lambda_3$ on TD,

$$\lambda_2 - \lambda_{2D} = u - u_D$$

$$\lambda_2 = \lambda_{2D} + V \cos\theta - V_D \cos\theta_D \qquad (59)$$

Equation (53), which is also valid on TD, becomes

$$\lambda_1 = y\rho V \sin\theta \qquad (60)$$

For any velocity distribution $u(x,y)$, $v(x,y)$ that satisfies the flow equations, the two pairs of functions

$$\lambda_1 = \text{const} \qquad \lambda_2 = \text{const}$$

$$\lambda_1 = y\rho V \sin\theta \qquad \lambda_2 = V\cos\theta$$

satisfy the partial differential equations(48) and(49) which

are valid throughout the flow field. Thus, Eqs.(59) and (60) must also be valid along DE where Eq.(55) applies. Substitution of Eqs.(59) and (60) into Eq.(57) yields

$$y\rho V \sin\theta - y\rho \operatorname{ctn}\alpha \,(\lambda_{2_D} + V\cos\theta - V_D\cos\theta_D) = 0$$

which reduces directly to

$$\frac{V\cos(\theta+\alpha)}{\cos\alpha} = \text{const} \tag{61}$$

Equations (50) and (55) can be combined to yield

$$\lambda_1 = (Cy\rho \operatorname{ctn}\alpha)^{1/2}$$

where C is a constant. Substituting this into Eq.(60) yields

$$y\rho V^2 \sin^2\theta \tan\alpha = \text{const} \tag{62}$$

Equations (61) and (62) must be satisfied along the exit characteristic DE and are identical to the equations obtained by Rao. At point D Rao obtained the corner condition

$$(p - p_b)\operatorname{ctn}\alpha/(1/2\rho V^2) = -\sin 2\theta \tag{63}$$

This equation can also be obtained by neglecting the wall shear and boundary layer thickness in Eqs.(53) and (57), and by substituting Eqs.(52) and (53) into Eq.(55). This results in

$$\lambda_3 = v/\text{ctn}\ \alpha \tag{64}$$

which must be satisfied at point D. This result is then substituted into the corner condition, Eq.(57), which reduces directly to Eq.(63).

The problem formulated in Section III, neglecting the boundary layer thickness, has been programmed in Fortran IV. Correction for boundary layer thickness can be made to the optimized contour by using the displacement thickness to adjust the wall coordinates. The numerical techniques, including the method of contour modification, are discussed in the next section.

SECTION IV

NUMERICAL METHODS

1. SOLUTION PROCEDURE

The solution procedure consists of estimating what the optimum contour should be, analyzing the contour to see if it is an optimum, and modifying the contour if it is not an optimum. In order to analyze the contour it is necessary to first solve the flow field by the method of characteristics which requires a start line. The computer program contains two options for this purpose. The start line can either be read in from data cards or generated internally. The internally generated start line is obtained from either a modified Moore-Hall (16) transonic flow analysis or an isentropic flow analysis in which the Mach number is assumed to be constant along a straight line. The details of the Moore-Hall analysis and the necessary modifications are discussed in Appendix H. In any case, the start line will always be from point A to point E' shown in Figure 3.

Before going into the details of how the flow field is calculated, the conditions at point T(see Figure 1) need to be examined. In the problem formulation, point T was considered to be fixed and thus variations in the plug contour are only allowed downstream of point T. As a result, in

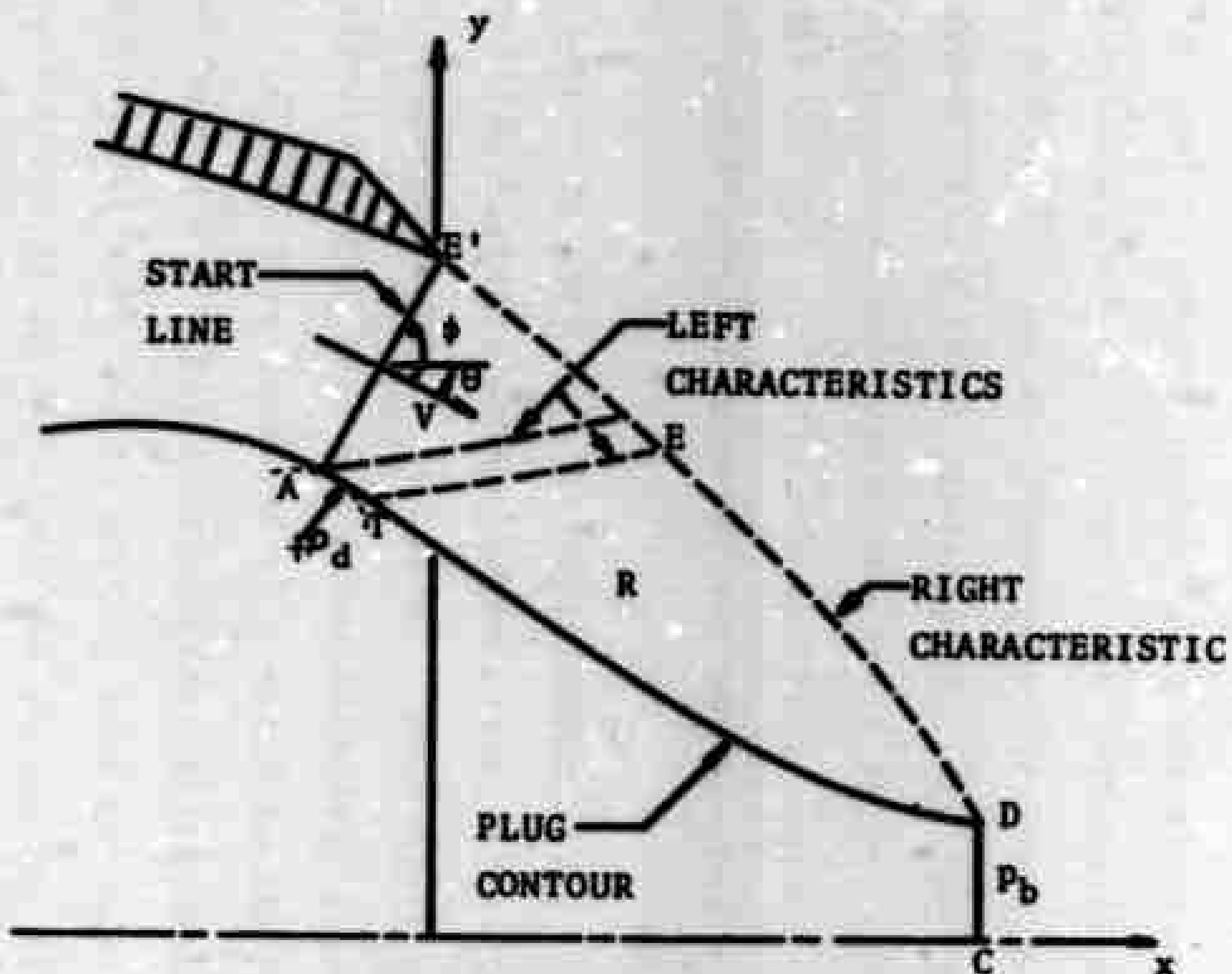

FIGURE 3. NOZZLE GEOMETRY WITH A SPECIFIED THROAT RADIUS

carrying out the optimization process, the contour must be modified, and consequently, a sharp corner can arise at point T. It is thus necessary to specify the plug curvature in this region. The actual nozzle will then follow this contour up to a certain, but not predetermined, point. As a result, point T, shown in Figure 3, is located so that no discontinuity in the plug contour arises as the contour modification is carried out. Point E is then located along the left characteristic originating at point T rather than being on the cowl lip. In general, point T will always be downstream from point A and can never move upstream of point A during the contour modification process. The calculation of the flow field must be carried out in recognition of this situation.

The flow field calculations are started by evaluating the flow properties along right characteristics which originate at the start line. These calculations continue down the right characteristics until the left characteristic which originates at point A is reached(see Figure 3). The properties along this left characteristic are stored to avoid recalculating this portion of the flow field each time the plug contour is adjusted. Thus, as point T moves during the iteration procedure it is necessary to calculate the flow field from the left characteristic originating at point A to the new point T.

Once the flow properties upstream of and along the left characteristic TE are evaluated, TE is divided into (NPTS-1)

equally spaced points and the data are curve fitted. However, an option is provided in the program so that the first (NS-1) points can have closer spacing than the remaining points. Thus, the grid size can be varied in the region (R). The flow calculations in the region (R) proceed from T to E down the right characteristics until the plug contour TD is reached.

Once the flow field is known it is possible to evaluate the Lagrange multiplier field by starting at point D and solving Eqs.(52), (56), and (57) for λ_1 and λ_2. The transversality conditions (52), (53), and (54) are then used to evaluate λ_1 and λ_2 along TD. Thus, the surface TD can be used as an initial-value line from which to start the method of characteristics solution for λ_1 and λ_2 in (R). Again starting at point T and proceeding towards E, λ_1 and λ_2 are evaluated up the right characteristics starting from the plug surface and stopping when the left characteristic TE is reached. Equation (55) is evaluated as λ_1 and λ_2 are obtained along the exit characteristic. No iteration procedure is required to obtain λ_1 and λ_2 in (R) since Eqs.(50) are valid along the characteristics of the basic flow field which is known. Thus, in finite difference form Eqs.(50) are algebraic equations.

In general Eq.(55) will not be satisfied by the first guess for the optimum surface and it is then necessary to calculate a new wall contour. In calculating the new contour it is convenient to consider Eq.(55) as an error

function such that

$$E = \lambda_1 - \lambda_2 y \rho \operatorname{ctn} \alpha \tag{65}$$

Changes in the wall contour are designed to drive E to zero as rapidly as possible and upon this premise a new wall is constructed. This method of contour modification is referred to as a relaxation technique and was developed by Scofield, Thompson, and Hoffman (8). The details of the method are described in the next section.

After the new wall contour is obtained the calculation procedure starts over again, beginning from the stored left characteristic which originates at point A. This iteration procedure continues until the error function E is reduced to an acceptable value near zero.

2. RELAXATION TECHNIQUE

The wall modification procedure or wall relaxation must, above all, produce rapid convergence. The entire procedure is designed with this in mind.

In order to change the wall contour it must first be determined how changes in the contour affect the error function given by Eq.(65). To do this the wall angle θ is chosen as the independent variable and the error function E as the dependent variable. Theoretically the wall angle can be incremented at a point on the wall, the flow field and Lagrange multiplier field recalculated, and the change in the error function along DE evaluated. This procedure

could be repeated until every wall point had been incremented and the corresponding changes in the error function found. This would result in an n x n matrix (n = number of wall points) relating changes in the wall angle to changes in the error function. This can be written in partial derivative form as

$$\frac{\partial E_i}{\partial \theta_j} = \frac{E_i - E_{io}}{\theta_j - \theta_{jo}} \qquad (i, j = 1,\ldots,n) \tag{66}$$

where E_{io} and θ_{jo} are the initial values of E_i and θ_j.

Once these partial derivatives are known, a truncated Taylor series could be used to relate changes in the wall angle to changes in the error function such that

$$E_i - E_{io} = \left.\frac{\partial E_i}{\partial \theta_j}\right|_{\theta_{jo}} (\theta_j - \theta_{jo}) \quad (i, j = 1,\ldots,n) \tag{67}$$

Since the desired value of the error function is zero, Eqs. (67) could be used to solve for the value of the wall angle that will drive the error function to zero. Thus,

$$\Delta\theta_j = -E_{io}/(\partial E_i/\partial \theta_j)\Big|_{\theta_{jo}} \qquad (i, j = 1,\ldots,n) \tag{68}$$

In theory Eqs.(68) could be solved, but in practice this could be difficult when a large number of wall points are involved.

In their investigation of the problem for conventional nozzles, Scofield, Thompson, and Hoffman (8) found that it could be assumed that there is an independent relationship

between changes in the wall angle and changes in the error function which lie on the same right-running characteristic. That is, the main effect on E due to a change in the wall angle propagates down the right-running characteristic which originates at that point. This same type of assumption was found to be valid for the plug nozzle when applied along left-running characteristics originating at the wall. Thus, Eqs.(68) reduce to n simple independent equations which can be solved for $\Delta\theta$ at each of the n wall points.

$$\Delta\theta_i = -E_{io}/(\partial E_i/\partial\theta_i) \qquad (i = 1,\ldots,n) \qquad (69)$$

Since the problem is nonlinear, the final solution must be approached iteratively. The wall angles for the (r + 1) iteration are given by

$$\theta_i^{(r+1)} = \theta_i^r + \Delta\theta_i \qquad (i = 1,\ldots,n) \qquad (70)$$

The procedure just described is a simple method of adjusting the wall contour but would require considerable time if carried out in all of its detail. Scofield, Thompson, and Hoffman (8) used two methods to reduce the computer running time and both are used in the current program. First it was noted that a nearly linear relationship exists between the partial derivatives $\partial E_i/\partial\theta_i$ and the corresponding wall axial coordinate x. Because of this linear relationship it is possible to calculate the partial derivatives at a few points (typically ten) and then fit a straight

line through these points by the method of least squares. The remaining partial derivatives can be taken from the fitted straight line and thereby reduce the time required for calculating $\partial E_i/\partial \theta_i$. The second method used to reduce the program running time is by recalculating the partial derivatives only after several iterations rather than after each iteration.

Two other controls are included in the program to assure rapid convergence and to prevent oscillations. These controls are: 1) application of a weighting factor to the wall angle corrections and 2) allowing a maximum change of 5° in the wall angle at a point.

The error function, wall angle corrections, and partial derivatives have been plotted in Figures 4, 5, and 6 to illustrate how the program progressively reduces the error function and modifies the plug contour. These figures have been plotted from the results of Sample Case No. 1 which is discussed in Appendix K. Figure 4 is a plot of the error function, E, after each iteration. As can be seen, the error associated with the first guess for the optimum surface is very large but reduces rapidly. The iteration procedure continues until the absolute value of the error function divided by the local value of λ_1 is less than 0.001. This criterion for an acceptable solution was met after 11 iterations. Figure 5 is a plot of the wall angle corrections, $\Delta\theta$, after each iteration. As might be

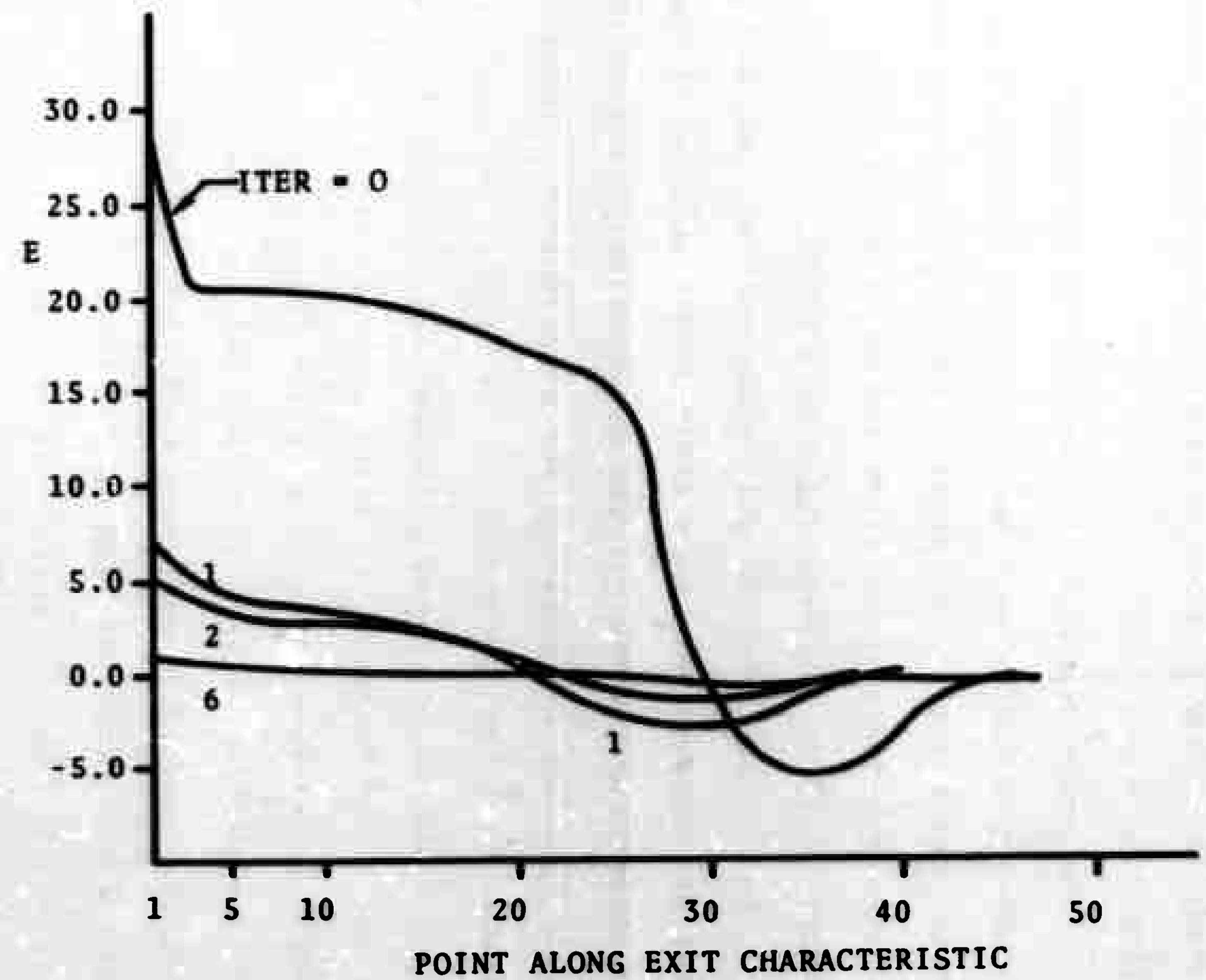

FIGURE 4. REDUCTION OF THE ERROR FUNCTION

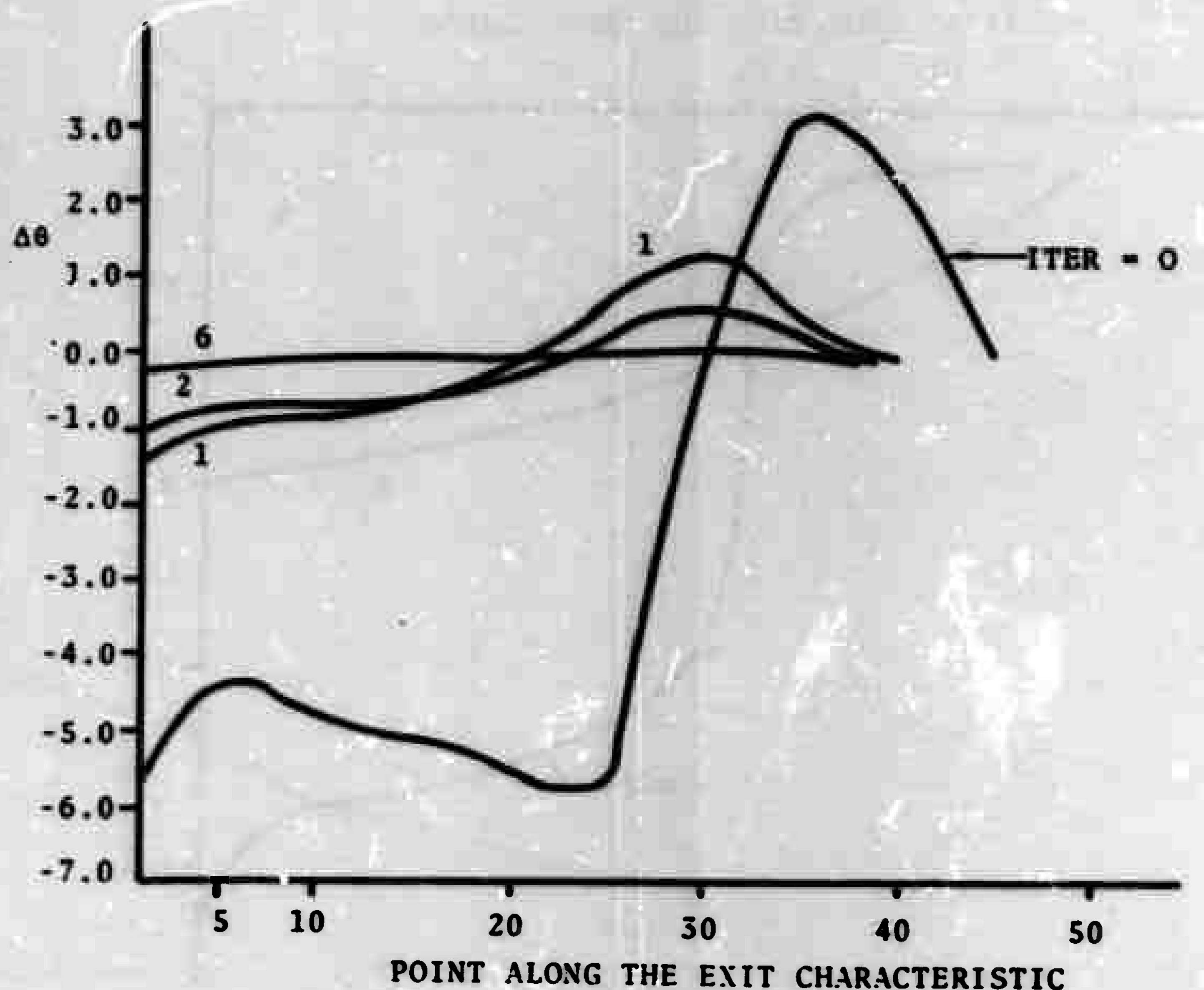

FIGURE 5. BEHAVIOR OF THE WALL ANGLE CORRECTIONS

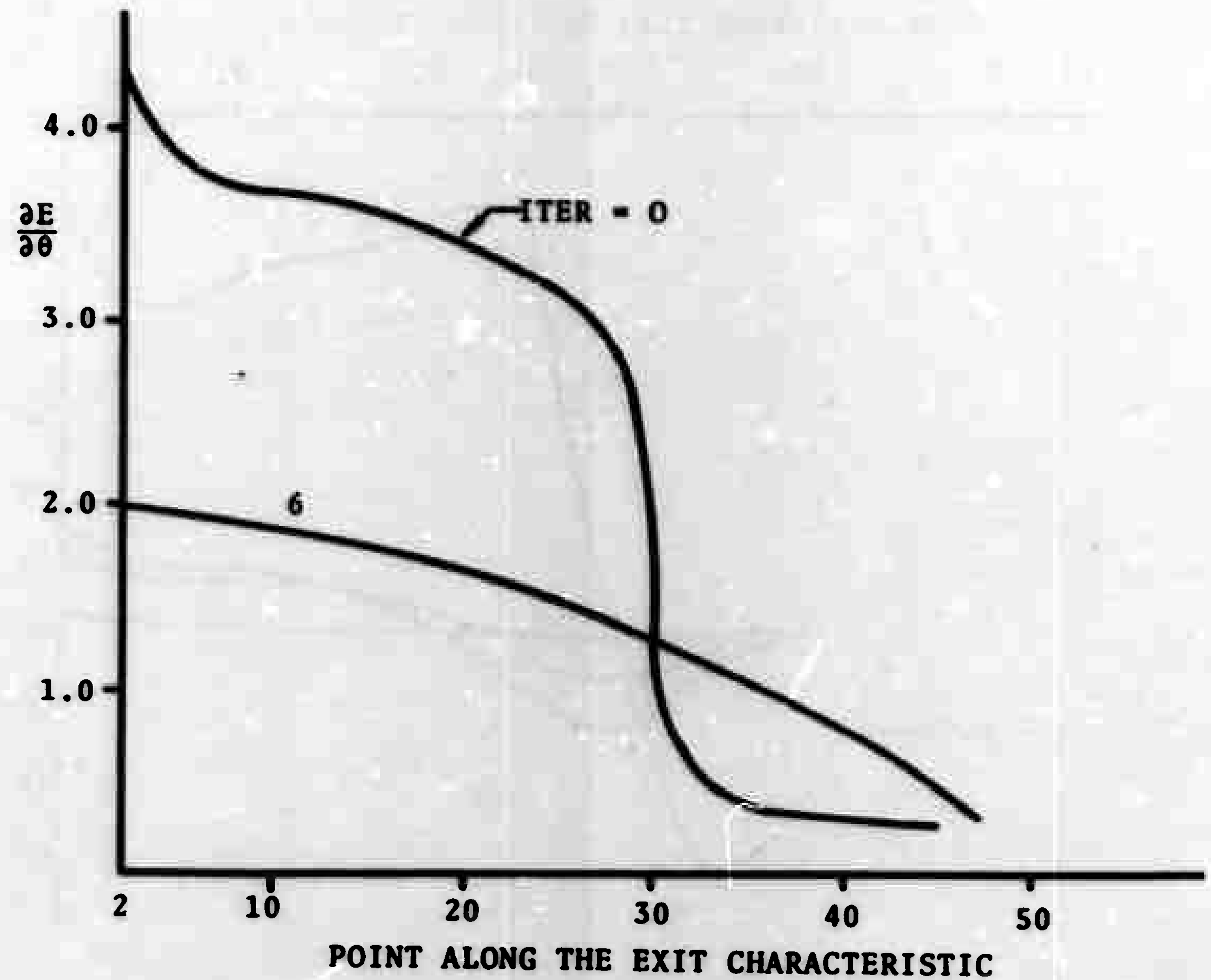

FIGURE 6. BEHAVIOR OF THE ERROR FUNCTION DERIVATIVE

expected, the wall angle corrections are large for the first guess of the optimum contour but decrease rapidly as the error function decreases. The partial derivatives of the error function with respect to the wall angle, $\partial E/\partial \theta$, were calculated for the first guess and again after 5 iterations. These results are shown in Figure 6. It should be noted in each of these figures that the number of wall points on the contour which is to be optimized may change from iteration to iteration. This occurs as the program seeks the specified length and specified number of wall points.

The details concerning the computer program and its operation, including input, output, failure modes, and listings are given in Appendices J, K, and L.

SECTION V

RESULTS

The formulations of Sections II and III assume specified values for the cowl lip radius and initial injection angle. Since both of these parameters have a significant influence upon the total thrust of plug nozzles, it may be desirable, in some cases, to determine the optimum values of these quantities. To illustrate how this can be done, a parametric study was carried out to determine the optimum cowl lip radius and injection angle for a given length nozzle. The purpose of this section is to present the results of the parametric study and to compare the optimum nozzle to one designed by Rao's method (3) for the same mass flow rate and ambient pressure. The effect of changing the base pressure model is illustrated, and an example of the optimization of scramjet nozzles is presented.

1. PARAMETRIC STUDY TO DETERMINE THE OPTIMUM COWL LIP RADIUS AND INJECTION ANGLE

A Fortran IV computer program was written for the irrotational flow problem presented in Section III. The program accounts for the wall shear stress, but does not account for the boundary layer thickness. A correction for the boundary layer thickness can be made to the optimized

contour by displacing the wall contour by the magnitude of the boundary layer thickness.

As mentioned in Section II, the thrust maximized in the variational problem does not represent the total axial thrust. The total thrust is given by the equation

$$\frac{T}{2\pi} = \int_A^E [p + \rho V^2 \frac{\sin(\phi - \theta)}{\sin\theta} \cos\phi] y dy - y_E^2\, p_a/2$$
$$- \int_A^D [p\dot{y} + \tau] y dx + y_D^2\, p_b/2 \qquad (71)$$

where the angles ϕ and θ are shown in Figure 3. The last two terms in Eq. (71) are obtained by neglecting the boundary layer thickness in Eq. (37). The first term accounts for the pressure and momentum forces across the initial-value line EA, the second term accounts for the ambient pressure, the third term is the pressure thrust generated by the plug contour, and the last term is the plug base thrust. The cowl lip radius and injection angle will influence the first two terms while the contour optimization presented in Section III is used to maximize the last two terms for a specific choice of cowl lip radius and injection angle. However, as explained in Section IV, the radius of curvature of the plug between points A and T is specified a priori, and as a result, this portion of the nozzle wall will not necessarily be an optimum. Thus, the plug contour generated by the present technique yields a thrust maximum for the specified inlet. To determine the best overall nozzle when no constraints are placed on the cowl lip radius and injection angle, these two

quantities can be varied parametrically and the optimum plug contour can be obtained for each set of these quantities. The maximum thrust nozzle is then selected from this group of nozzles. Such a parametric study is presented in this section.

The parametric study was conducted for a nozzle which has a mean radius of curvature at the throat of 0.705 in., a downstream radius of curvature of 0.5 in., and a length from point T to point D (see Figure 3) of 12.0 in. The mass flow rate, ambient pressure, and incompressible skin friction coefficient were selected as 148.08 lbm/sec, 14.7 psia, and 0.002, respectively. The engine was assumed to operate with a chamber pressure of 500.0 psia and a chamber temperature of 6000.0°R. The exhaust products were assumed to have a gas constant of 56.0 (ft-lbf)/(lbm-°R) and a ratio of specific heats of 1.23. The constants for the base pressure model were selected as AA = 0.846 and AB = 1.3. Each of the above parameters is an input to the computer program which is described in Appendices J,K, and L. These appendices should be consulted for additional details concerning how these parameters are used in the program. The nozzle was designed for a subsonic burning engine, thus the start line described in Appendix H was used. As the cowl lip radius and injection angle are changed, the throat height, $2h_0$, is varied in order to keep the mass flow rate constant. A total of 20 computer runs were made to determine the optimum cowl lip radius and

injection angle. The results of these runs are presented in Table 1.

The data in Table 1, except the last set where $\beta = -34°$ and $y_E = 7.55$ in., are plotted in Figures 7 and 8. Figure 7 is a plot of thrust as a function of cowl lip radius with the injection angle as a parameter, and Figure 8 is a plot of thrust as a function of injection angle with the cowl lip radius as a parameter. From Figure 7, it was determined that the optimum cowl lip radius would be approximately 7.55 in., and the optimum injection angle was determined from Figure 8 to be approximately -34°. One final computer run was made using these values for the cowl lip radius and injection angle. This run resulted in a thrust of 32,881 lbf., which is the maximum of the total of 21 designs. The coordinates and slope of the resulting optimum contour are given in Table 2 and plotted in Figure 9. Two other contours of the same length have also been plotted in Figure 9 for comparison to the optimum. One contour is 0.5 in. above the optimum at point D and the other is 0.5 in. below the optimum at the same point. As expected, both contours produced a lower thrust than the thrust of the optimum contour. The upper contour produced a thrust of 32,556 lbf. and the lower contour produced 32,601 lbf.

Thus, it is possible to determine the optimum values for both the cowl lip radius and injection angle even though these quantities were fixed in the variational problem

TABLE 1. PARAMETRIC STUDY DATA

INJECTION ANGLE (DEGREES)	COWL LIP RADIUS (IN)	THRUST (lbf)
-31.00	7.00	32,803
-31.00	7.50	32,853
-31.00	8.00	32,813
-31.00	8.50	32,699
-33.00	7.00	32,811
-33.00	7.50	32,874
-33.00	8.00	32,842
-33.00	8.50	32,731
-35.00	7.00	32,808
-35.00	7.50	32,877
-35.00	8.00	32,846
-35.00	8.50	32,747
-37.00	7.00	32,791
-37.00	7.50	32,869
-37.00	8.00	32,847
-37.00	8.50	32,753
-39.00	7.00	32,763
-39.00	7.50	32,844
-39.00	8.00	32,829
-39.00	8.50	32,741
-34.00	7.55	32,881

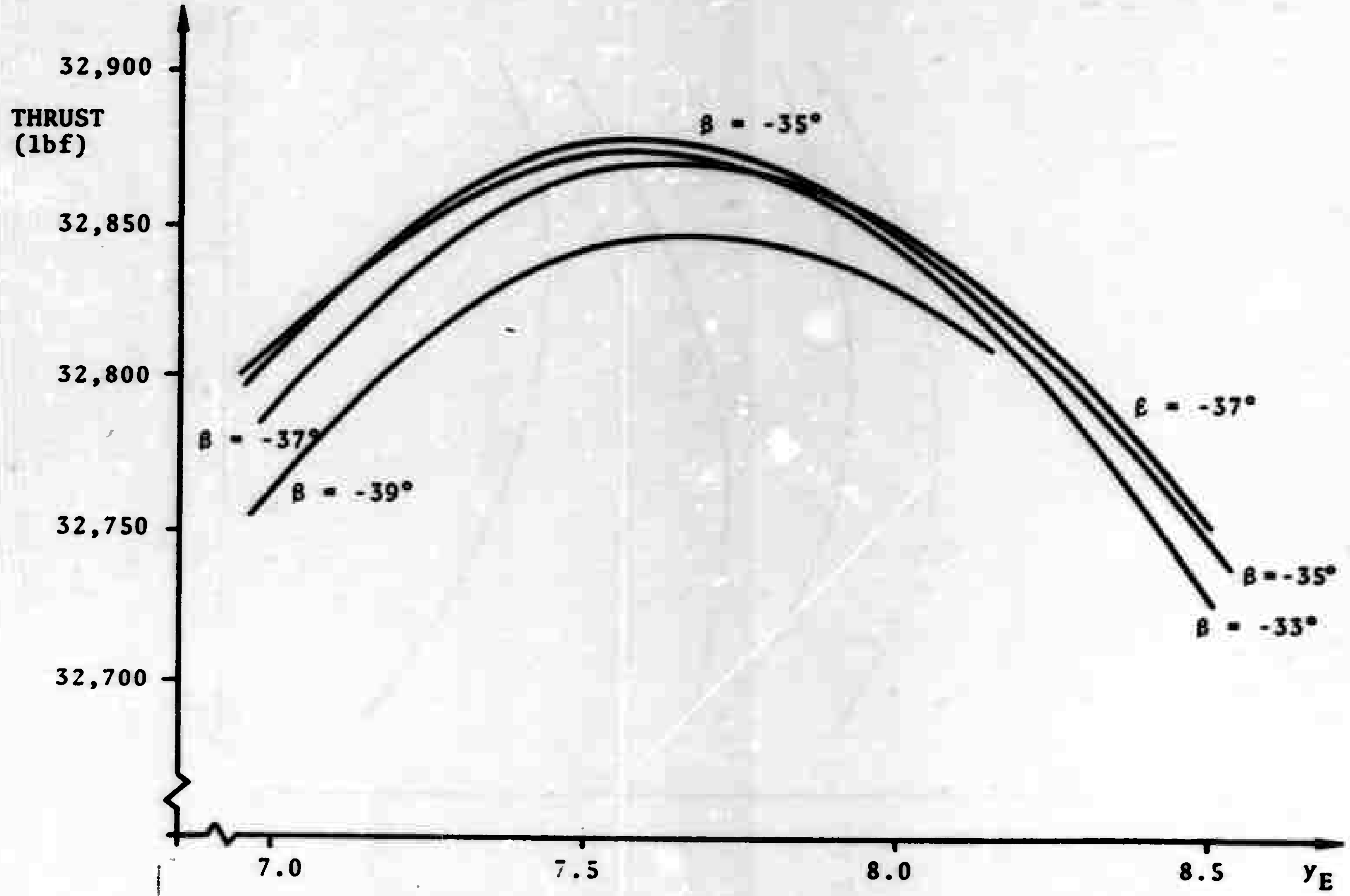

FIGURE 7. THRUST VS. COWL LIP RADIUS

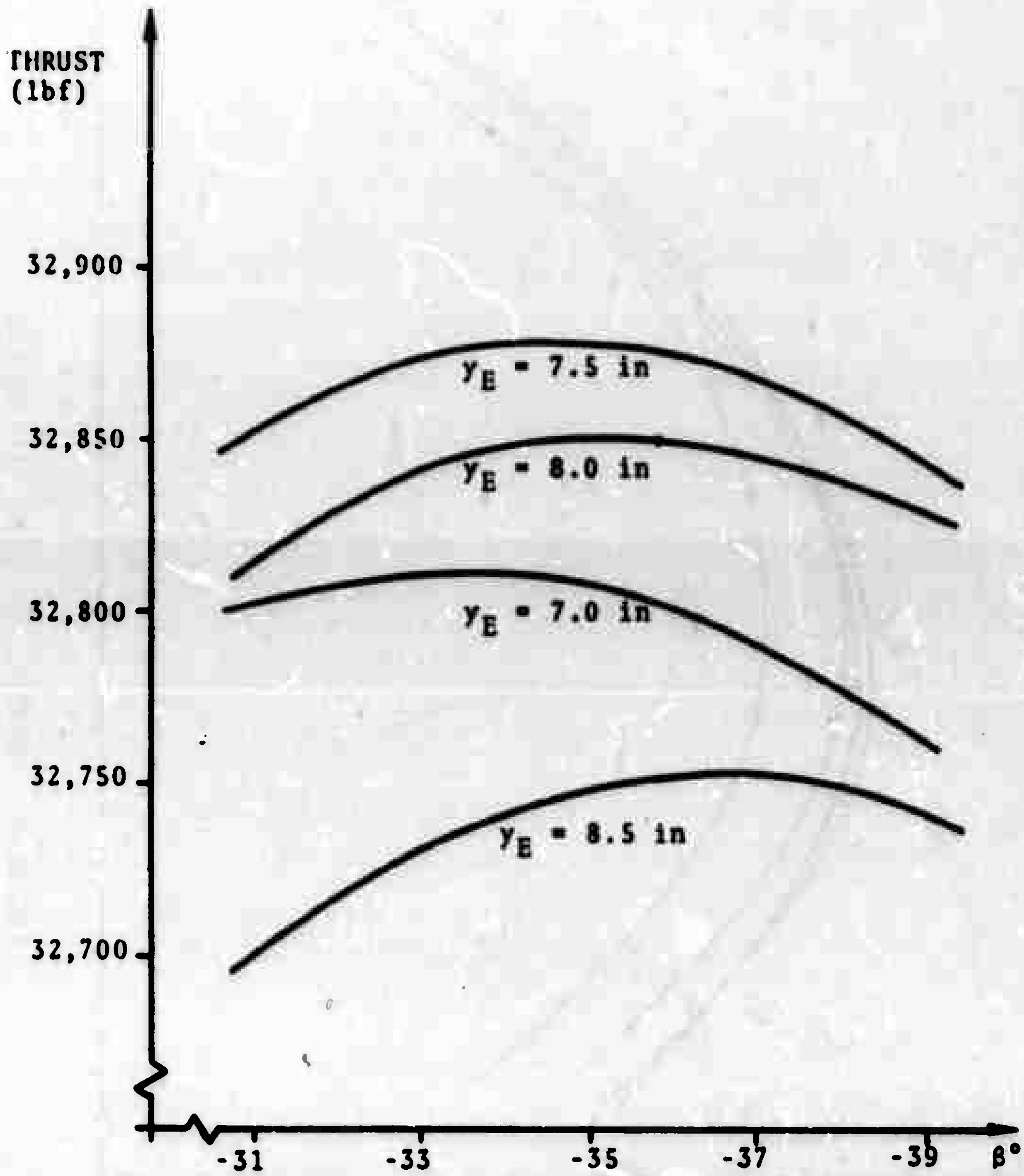

FIGURE 8. THRUST VS. INJECTION ANGLE

TABLE 2. COORDINATES OF THE OPTIMUM PLUG CONTOUR

$\gamma = 1.23$ $\qquad$ $P_o = 500.0$ psia

$R = 56.0 \frac{ft - lbf}{lbm - {}^\circ R}$ $\qquad$ $T_o = 6000\ {}^\circ R$

x(in)	y(in)	θ°
-0.56069	6.71874	-36.25027
-0.55023	6.71087	-37.75027
-0.53999	6.70272	-39.25027
-0.52996	6.69430	-40.75027
-0.52016	6.68563	-42.25027
-0.51059	6.67670	-43.75027
-0.50125	6.66753	-45.25027
-0.49216	6.65811	-46.75027
-0.48331	6.64846	-48.25027
-0.40216	6.55777	-48.02999
-0.29091	6.43493	-47.64577
-0.03515	6.15846	-46.81925
0.29695	5.81585	-44.30856
0.99456	5.21035	-37.84839
2.10220	4.45395	-31.24354
3.01742	3.93915	-27.61354
5.08714	2.98654	-22.22618
6.75042	2.35672	-19.37574
8.85315	1.67387	-16.70496
11.51707	0.95441	-13.26458

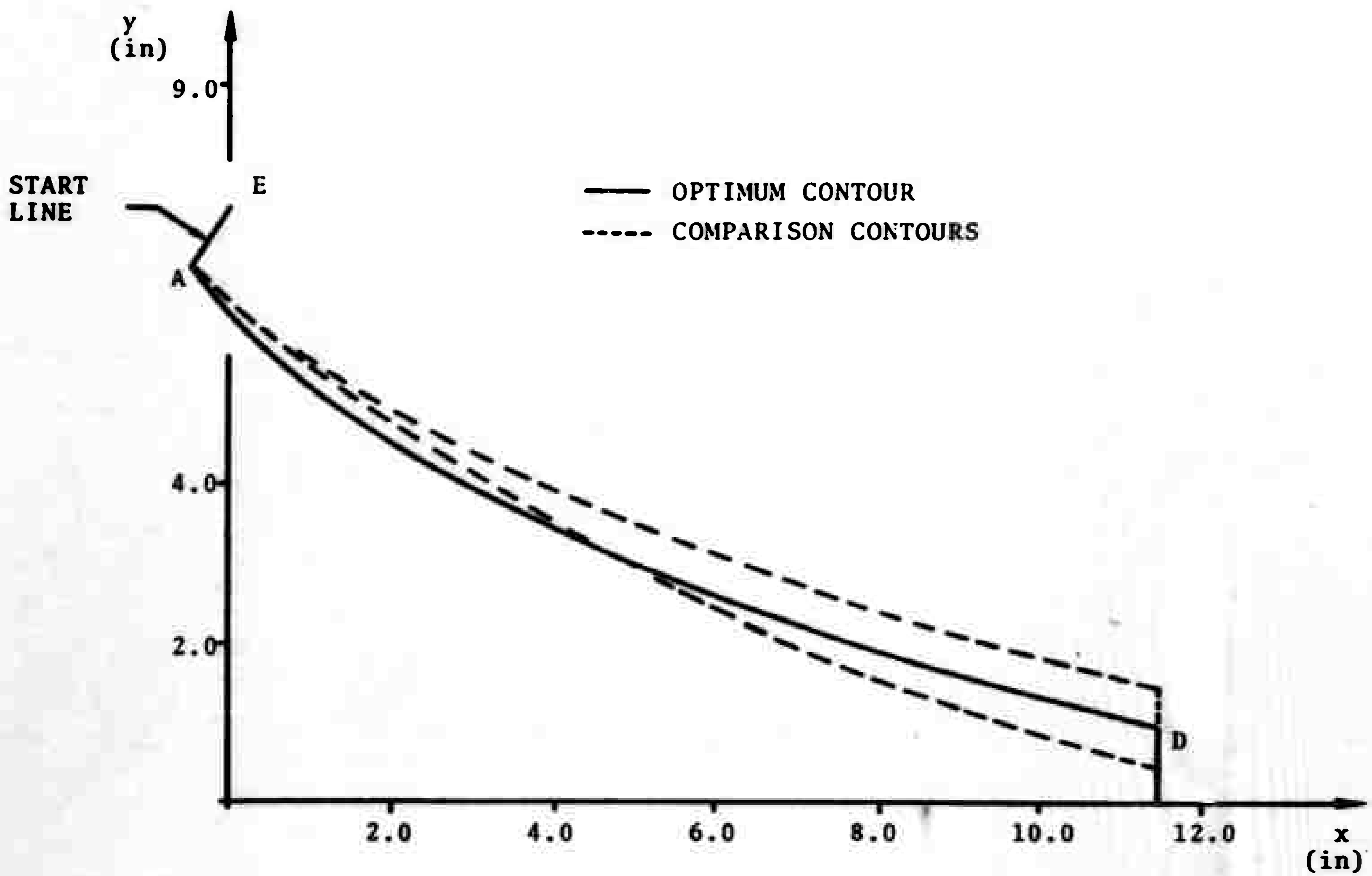

FIGURE 9. OPTIMUM CONTOUR

formulation. This approach to the problem is also useful in cases where either the cowl lip radius or injection angle is dictated by other considerations. This situation could arise, for example, when the cowl lip radius is limited by the vehicle size, but no restrictions are placed on the injection angle. The best injection angle for the given cowl lip radius could be obtained from a plot such as Figure 8.

2. COMPARISON TO RAO NOZZLES

Since the current formulation contains the results of Rao (3) as a special case, it is of interest to compare the nozzles designed by the two methods.

a. Rao Results. The design equations obtained by Rao were programmed in order to compare his technique with the current formulation. A comparison was made with the same mass flow rate, plug length, ambient pressure, thermodynamic properties, and base pressure model as those employed in the parametric study. The Rao method yields an optimum cowl lip radius of 8.33 in. and an optimum injection angle of approximately -58.5° with a resulting thrust of 34,253 lbf. The coordinates and slope of the resulting optimum contour are given in Table 3 and plotted in Figure 10. By comparing the data in Table 3 with that in Table 2, it can be seen that the contour obtained by Rao's method lies above the contour obtained from the parametric study. In order to compare the

TABLE 3. COORDINATES OF THE RAO CONTOUR

$\gamma = 1.23$	$p_o = 500.0$ psia
$R = 56.0 \dfrac{ft - lbf}{lbm - °R}$	$T_o = 6000°R$

x(in)	y(in)	θ°
-0.63971	7.60953	-60.69463
-0.52553	7.41133	-59.26745
-0.38991	7.19374	-56.76264
-0.28105	7.03417	-54.62384
-0.11511	6.81327	-51.56682
0.08454	6.57580	-48.37210
0.26305	6.38348	-45.92900
0.54982	6.10414	-42.64770
0.80980	5.87499	-40.18842
1.11665	5.62702	-37.74413
1.75877	5.16641	-33.72519
2.24216	4.85831	-31.35732
3.03421	4.40556	-28.40556
4.04195	3.89898	-25.23198
5.33714	3.33063	-12.27169
6.55991	2.85772	-20.07902
8.07079	2.33921	-17.86199
9.28531	1.96623	-16.29294
11.51781	1.37506	-13.25333

shapes of these two contours, the contour which resulted from the parametric study was also plotted in Figure 10. However, 0.42065 in. was added to the y-coordinates of the contour obtained from the parametric study so that the two contours would match at point D. As can be seen from Figure 10, the two contours are almost identical in shape except in the throat region, the most significant difference being in the injection angle and cowl lip radius. Since the start line or sonic line assumptions for these two models are not the same, it was suspected that the differences in the results were caused by the dissimilarities in the start lines. The results of an investigation to determine if this was indeed the case are presented in the next section.

b. Importance of Start Line. Since Rao assumed a linear sonic line along which the flow direction is constant, an attempt was made to duplicate his results by using such a start line along which the Mach number was slightly greater than unity. The cowl lip radius and injection angle were fixed at the values found for the optimum Rao nozzle and the wall shear stress was set equal to zero since Rao did not account for this in his formulation. The general flow condition produced by a parallel uniform flow with the flow direction toward the axis of symmetry is one of compression. Unless the Mach number along the start line is increased to approximately 1.5, the compression results in subsonic Mach numbers in the throat region. However, the assumption of a

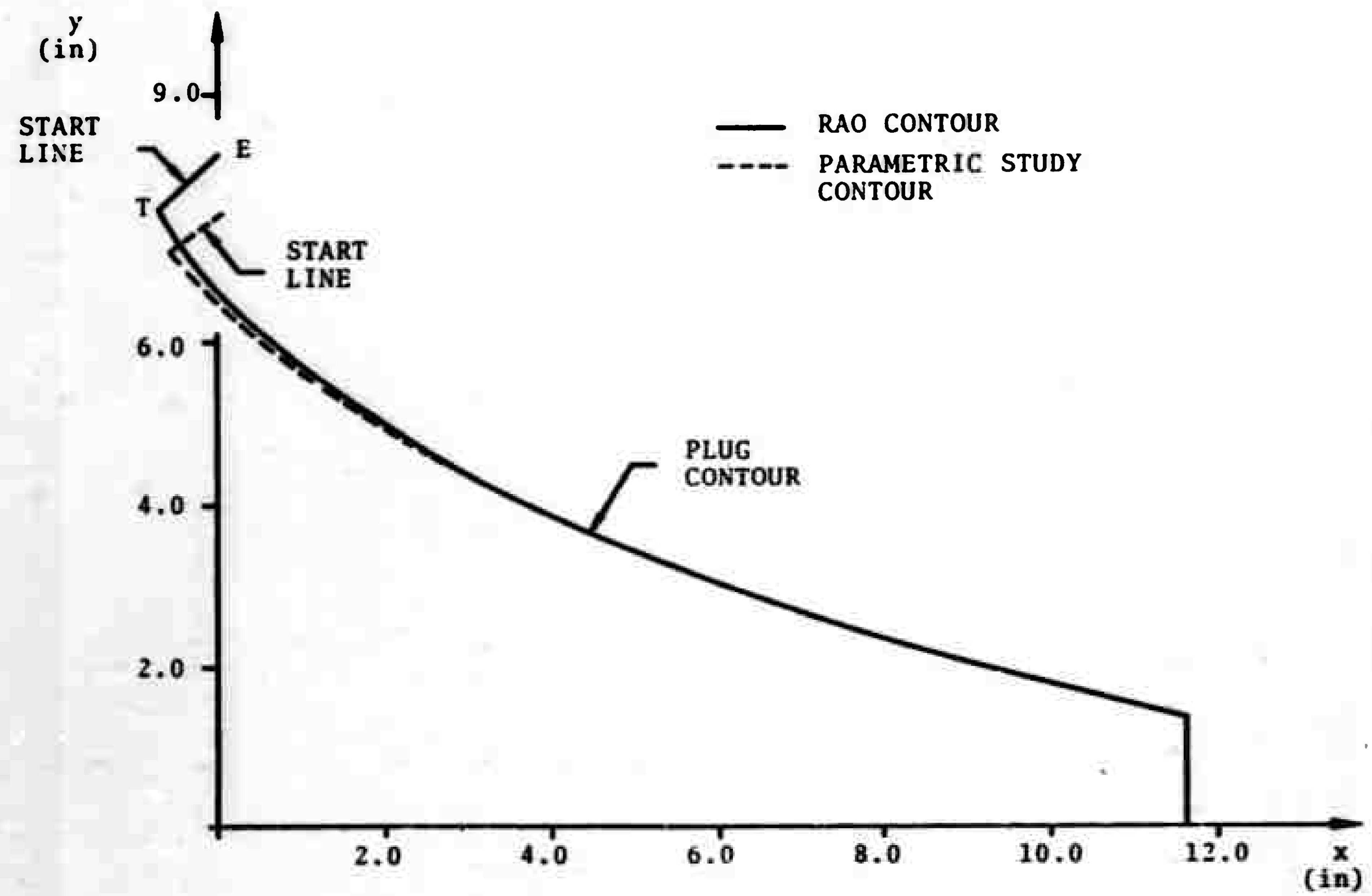

FIGURE 10. CONTOUR COMPARISON

Mach number greater than one along the start line implies that the flow has passed through the minimum area and should be expanding. This requires the flow direction to become more negative along the start line, EA. By decreasing the flow direction from 3 to 6 degrees along the start line, the compression problem was eliminated. Typically, the flow direction at point E was fixed at -56.0° and decreased uniformly to -62.0° at point A. The resulting plug contour matched the Rao contour reasonably well but the thrust was approximately 2700 lbf. lower.

One final attempt was made to duplicate Rao's results. A right-running characteristic near the throat was taken from the Rao nozzle flow field and used as a start line. This start line produced a contour almost identical to Rao's. The y-coordinate at point D was 0.1364 in. lower than Rao's, and the thrust was 34,373 lbf. compared to 34,375 lbf. for Rao's nozzle.

These results indicate that the start line assumptions are very important in the design of optimum plug nozzles, and approximations in this region should be carefully evaluated.

3. EFFECT OF THE BASE PRESSURE MODEL

Another possible source of error in plug nozzle design is the base pressure model. The importance of the base pressure model is illustrated in this section.

After the parametric study was completed and the optimum nozzle configuration determined, the equation used to calculate the base pressure was changed from Eq. (G-1) to Eq. (G-2) to determine the effect of the base pressure model. All other parameters were set at the values used for the parametric study, and the cowl lip radius and injection angle were set at their optimum values of 7.55 in. and -34°. The coordinates and slope of the resulting contour are given in Table 4 and plotted in Figure 11. The contour obtained from the parametric study is also plotted in Figure 11. As can be seen from this figure, the base pressure model has a considerable effect upon the shape of the plug contour. The base height, y_D, increased from 0.954 in. to 2.34 in. and the wall slope at point D increased from -13.26° to -3.08°. In addition, the thrust increased to 32,965 lbf. because of the higher base pressure. Since the thrust has changed, it is expected that the optimum cowl lip radius and injection angle will also be different. Thus, in addition to a direct thrust contribution on the plug base, the value of the base pressure significantly influences the shape of the optimum contour.

4. OPTIMIZATION OF SCRAMJET NOZZLES

The methods and results presented to this point are applicable to supersonic combustion engines as well as to those which burn subsonically. However, the starting conditions for these two applications are not the same. An

TABLE 4. COORDINATES OF AN OPTIMUM CONTOUR FOR THE ALTERNATE BASE PRESSURE MODEL

$\gamma = 1.23$ $\quad$ $p_o = 500.0$ psia

$R = 56.0 \dfrac{ft - lbf}{lbm - {}^{\circ}R}$ $\quad$ $T_o = 6000°R$

x(in)	y(in)	θ°
-0.56069	6.71874	-36.25027
-0.55023	6.71087	-37.75027
-0.53999	6.70272	-39.25027
-0.52996	6.69430	-40.75027
-0.52016	6.68563	-42.25027
-0.51059	6.67670	-43.75027
-0.49819	6.66442	-45.75027
-0.44272	6.60622	-46.29203
-0.33777	6.49721	-45.88483
-0.19453	6.35086	-45.35040
-0.00101	6.15730	-44.66440
0.34386	5.83114	-41.57284
0.90107	5.38449	-36.00408
1.72398	4.85222	-30.05107
2.55635	4.41335	-25.69669
3.61048	3.95442	-21.49032
4.92072	3.49325	-17.40459
6.53289	3.05192	-13.30646
8.49709	2.66542	- 9.02277
11.58406	2.34099	- 3.08106

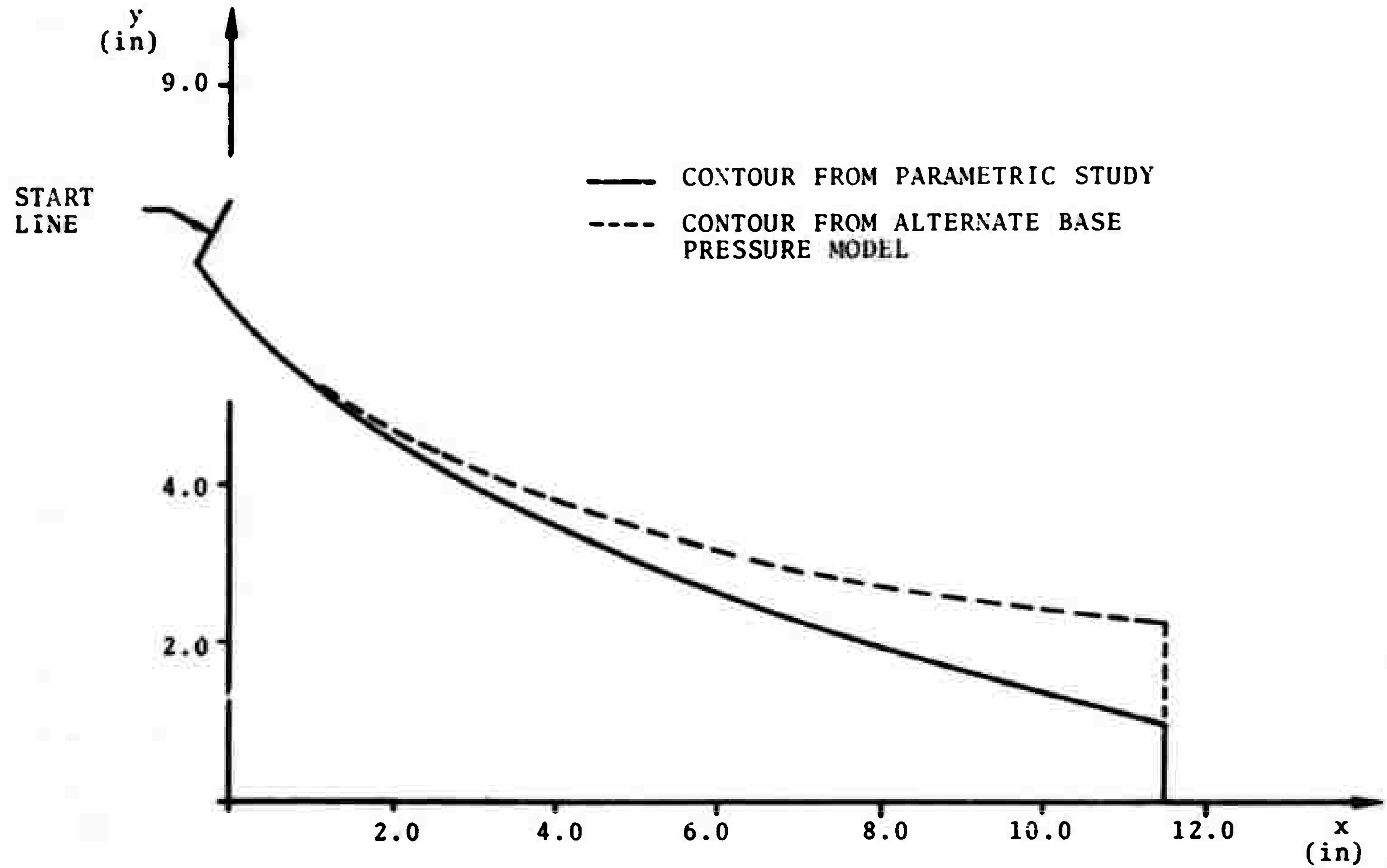

FIGURE 11. OPTIMUM CONTOUR FOR ALTERNATE BASE PRESSURE MODEL

illustration of the optimization of scramjet nozzles is presented in this section.

The flow conditions at the entrance to scramjet nozzles are expected to be nonuniform in nature and well within the supersonic range. The nonuniform nature of the flow is produced by the inlet effects and the combustion process. As was demonstrated in the parametric study, it is advantageous in the case of subsonic burning engines to inject the exhaust gases toward the axis of symmetry. This may not be feasible for scramjets since the flow throughout the engine is supersonic and would require a compression turn. The losses inherent in the resulting shock could outweigh any advantages to be gained. A detailed analysis would have to be carried out before any definite conclusions could be drawn, but for the purpose of illustrating the design of a scramjet nozzle, the injection angle was assumed to be zero. The start line was assumed to be a straight line along which the Mach number had a constant value of 1.5. The downstream radius of curvature was selected as 0.5 in. and the length from point T to point D was chosen as 8.0 in. The mass flow rate, ambient pressure, and incompressible skin friction coefficient were given values of 50.0 lbm/sec, 14.7 psia, and 0.002, respectively. The engine chamber conditions were selected as p_o = 500.0 psia and T_o = 6000°R. The exhaust products were assumed to have a gas constant of 56.0 (ft-lbf)/(lbm-°R) and a ratio of specific heats of 1.23.

The constants for the base pressure model were selected as AA = 0.846 and AB = 1.3. Finally, the cowl lip radius was fixed at 6.0 in. The coordinates and slope of the optimum contour which resulted from these data are given in Table 5 and plotted in Figure 12. This contour produced a thrust of 9722 lbf.

As these results indicate, the contour follows the specified radius of curvature at the nozzle inlet until the slope reaches -39.5°. The contour then begins to flatten out and the slope at point D is about the same as obtained in the previous cases. The maximum wall slopes obtained are less than those calculated for the other cases, due to the design constraint which requires the initial injection angle to be zero. Should moderate injection angles be permissible, a parametric study, such as presented at the beginning of this section, could be performed to obtain the best overall design.

TABLE 5. COORDINATES OF AN OPTIMUM SCRAMJET NOZZLE

$\gamma = 1.23$	$P_o = 500.0$ psia
$R = 56.0 \frac{ft - lbf}{lbm - {}^\circ R}$	$T_o = 6000^\circ R$

x(in)	y(in)	θ°
0.00000	5.56647	0.00000
0.02181	5.56600	-2.50000
0.04358	5.56457	-5.00000
0.06526	5.56219	-7.50000
0.08682	5.55888	-10.00000
0.10822	5.55462	-12.50000
0.12941	5.54944	-15.00000
0.15035	5.54333	-17.50000
0.17101	5.53632	-20.00000
0.19134	5.52841	-22.50000
0.21131	5.51963	-25.00000
0.23087	5.50998	-27.50000
0.25000	5.49949	-30.00000
0.26865	5.48817	-32.50000
0.28679	5.47605	-35.00000
0.30438	5.46315	-37.50000
0.31804	5.45228	-39.50000
0.32071	5.45007	-39.89710
0.45381	5.34156	-38.42232
0.76198	5.11254	-34.84466
1.51175	4.65257	-28.66838
2.50288	4.16818	-23.76215
3.47465	3.77417	-20.52422
4.92358	3.28370	-17.04437
7.03519	2.71383	-13.31267
8.32071	2.43250	-11.39107

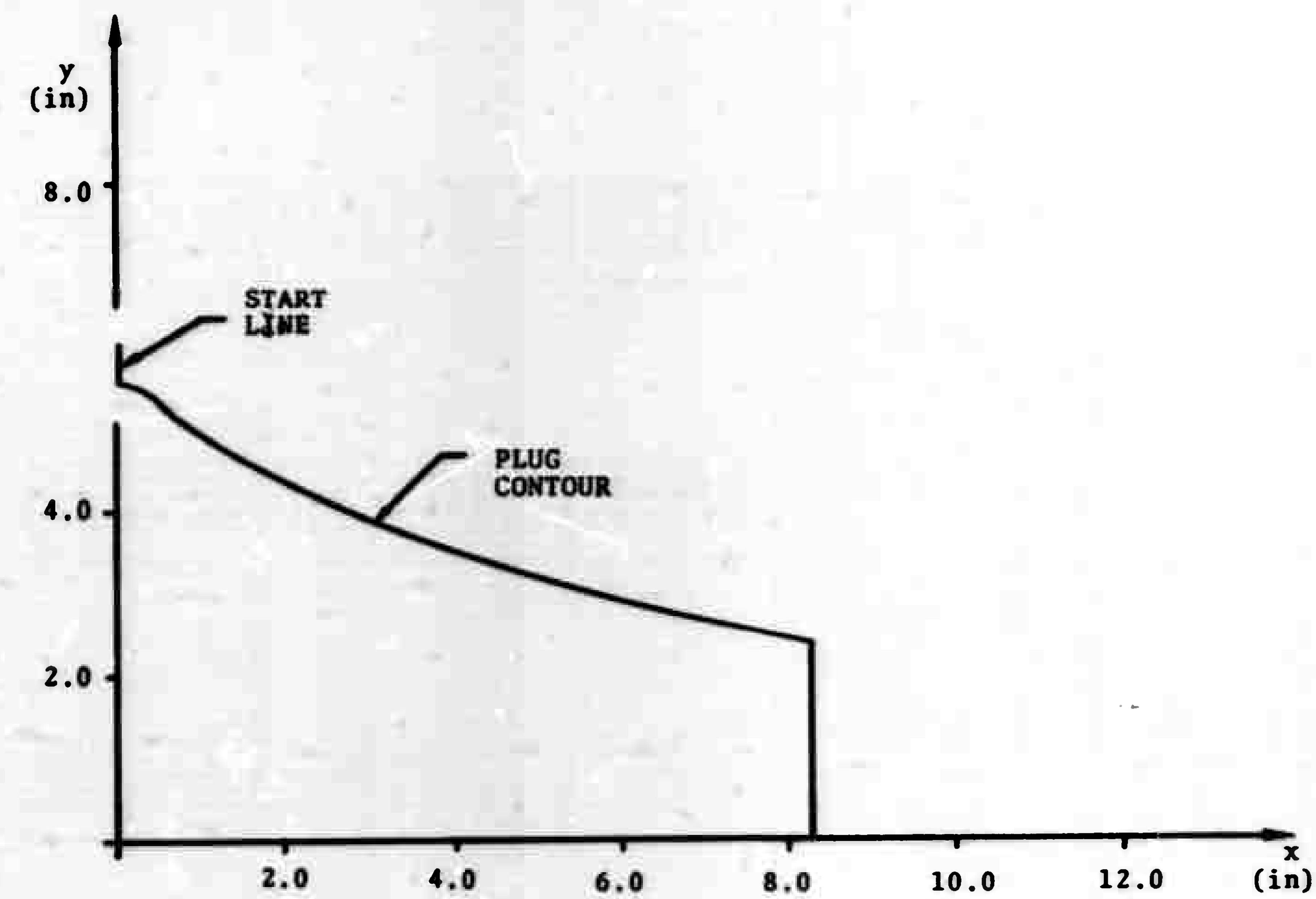

FIGURE 12. OPTIMUM SCRAMJET NOZZLE

SECTION VI

SUMMARY AND RECOMMENDATIONS

An analysis has been presented for the optimization of plug nozzle contours with boundary layer effects accounted for in the optimization. The solution makes no particular assumption about the upstream nozzle geometry but simply requires the flow conditions along a start line to be available in order to initiate the flow field solution. The results can then be applied to supersonic burning engines as well as to those which burn subsonically. The problem was formulated for rotational and irrotational flow. A general isoperimetric constraint was imposed upon the plug contour in the region of supersonic flow. A complete set of partial differential equations with sufficient boundary conditions was obtained for determining the flow properties and Lagrange multipliers. A method was presented for each of the problem formulations to determine if a given contour was an optimum and a relaxation technique was used to obtain a solution to the irrotational flow problem.

The design equations for the irrotational flow problem were programmed in Fortran IV and the computer program was described. This program was used to carry out a parametric

study to determine the optimum cowl lip radius and injection angle when the isoperimetric constraint is one of fixed length. The resulting optimum nozzle was compared to one designed by Rao's method. The importance of determining the base pressure accurately was illustrated and an example of scramjet nozzle optimization was presented.

During this study it has become apparent that several aspects of the plug nozzle optimization problem could benefit from additional work. First, the analytical methods of determining the transonic flow conditions in subsonic burning engines need to be verified experimentally. The flow conditions at the throat determine to a large extent the best injection angle and affect the flow conditions along the exit characteristic. Second, there is a need for a base pressure model which has direct application to plug nozzles. The importance of determining the base pressure accurately has been demonstrated but one finds very little base pressure data in the literature which is directly applicable to plug nozzles. Third, it would be desirable to include the ambient pressure and injection angle in the problem formulation, thereby removing the need for a parametric study to determine the optimum cowl lip radius and injection angle.

REFERENCES

1. Guderley, G. and Hantsch, E., "Beste Formen fur Achsensymmetrische Uberschallschubdusen," Z. Flugwiss, Vol. 3, 1955, pp. 305-313.

2. Rao, G. V. R., "Exhaust Nozzle Contour for Optimum Thrust," Jet Propulsion, Vol. 28, 1958, pp. 377-382.

3. Rao, G. V. R., "Spike Nozzle Contour for Optimum Thrust," Ballistic Missile and Space Technology, Vol. 2, edited by C. W. Morrow, Pergamon Press, New York, 1961, pp. 92-101.

4. Guderley, K. G. and Armitage, John V., "A General Method for the Determination of Best Supersonic Rocket Nozzles," Paper presented at the Symposium on Extremal Problems in Aerodynamics, Boeing Scientific Research Laboratories, Seattle, Washington, December 3-4, 1962.

5. Guderley, K. G. and Armitage, J. V., "General Approach to Optimum Rocket Nozzles," Chap. 11, Theory of Optimum Aerodynamic Shapes, edited by Angelo Miele, Academic Press, New York, 1965.

6. Hoffman, Joe D. and Thompson, H. Doyle, "A General Method for Determining Optimum Thrust Nozzle Contours for Gas-Particle Flows," AIAA Journal, Vol. 5, No. 10, Oct. 1967, pp. 1886-1887.

7. Hoffman, Joe D., "A General Method for Determining Optimum Thrust Nozzle Contours for Chemically Reacting Gas Flows," AIAA Journal, Vol. 5, No. 4, April 1967, pp. 670-676.

8. Scofield, M. Peter, Thompson, H. Doyle and Hoffman, Joe D., "Thrust Nozzle Optimization Including Boundary Layer Effects," Air Force Aero Propulsion Laboratory, Wright-Patterson Air Force Base, Ohio, Report No. AFAPL-TR-67-158, Dec. 1967.

9. Krayko, A. N., "Solution of Variational Problems in Supersonic Gas Dynamics," Prikladnaya Matematika i Mekhanika, Vol. 30, No. 2, 1966, pp. 312-320.

10. Pirumov, U. G. and Rubtsov, V. A., "Calculation of Axisymmetric Supersonic Plug Nozzles," AN SSSR, Mechanics and Machines, No. 6, 1961, pp. 17-37.

11. Gajewski, T., "Gas Dynamics of a Variable Supersonic Plug Nozzle," Tecknika Lotaicza i Astronautyczna, No. 4, 1967, pp. 12-16.

12. Gogish, L. V. and Stephanov, G. Yu., "Classification and Approximate Method for Profiling Plug Nozzles," AN SSSR Mikhanika Zhidkosti i Gaza, No. 4, 1966, pp. 166-171.

13. Pilipko, N. K., "A Method of Shaping a Supersonic Nozzle with an Internal Cone," Izvestiya Kiyevskogo Politekhnicheskogo Instituta, Sbornik Trudov Teplotekhnicheskogo Fakul' teta, Vol. 30, No. 1, pp. 38-52.

14. Von Mises, Richard, Mathematical Theory of Compressible Fluid Flow, Academic Press, New York, 1958, pp. 9-11.

15. Miele, Angelo, "Generalized Approach to the Calculus of Variations in Two Independent Variables," Chap. 4, Theory of Optimum Aerodynamic Shapes, edited by Angelo Miele, Academic Press, New York, 1965.

16. Moore, A. W. and Hall, I. M., "Transonic Flow in the Throat Region of an Annular Nozzle with an Arbitrary Smooth Profile," Aeronautical Research Council Report 26-543, Jan. 4, 1965.

17. Hoffman, Joe D., "Optimum Thrust Nozzle Contours for Chemically Reacting Gas Flows," Jet Propulsion Center, Purdue University, Report No. TM-66-3, April 1966.

18. Shapiro, Ascher M., The Dynamics and Thermodynamics of Compressible Fluid Flow, Vol. I, The Ronald Press Company, New York, 1953, pp. 595-608.

19. Courant, R. and Hilbert, D., Methods of Mathematical Physics, Vol. II, Interscience Publishers, 1962, Chapter V, p. 407.

20. Chapman, D. R., "An Analysis of Base Pressure at Supersonic Velocities and Comparison with Experiments," NACA TR-1051, 1951.

21. Korst, H. H., "A Theory for Base Pressure in Transonic and Supersonic Flow," Journal of Applied Mechanics, Vol. 23, No. 1, March 1956, pp. 593-600.

22. Scherberg, M. G. and Smith, H. E., "An Experimental Study of Supersonic Flow Over a Rearward Facing Step," AIAA Journal, Vol. 5, No. 1, June 1967, pp. 51-56.

23. Donaldson, I. S., "On the Separation of a Supersonic Flow at a Sharp Corner," AIAA Journal, Vol. 5, No. 6, June 1967, pp. 1086-1088.

24. Mueller, T. J., "Determination of the Turbulent Base Pressure in Supersonic Axisymmetric Flow," AIAA Paper 67-446 presented at the 3rd Propulsion Joint Specialist Conference, Washington, D. C., July 17-21, 1967.

25. Charwat, A. F. and Schneider, L., "Effect of the Boundary-Layer Profile at Separation on the Evaluation of a Wake," AIAA Journal, Technical Note, Vol. 5, No. 6, June 1967, pp. 1188-1190.

26. Crocco, L. and Lees, L., "A Mixing Theory for the Interaction Between Dissipative Flows and Nearly Isentropic Streams," Journal of the Aeronautical Sciences, Vol. 19, No. 10, Oct. 1952, pp. 649-676.

27. Lykoudis, P. S., "A Review of Hypersonic Wake Studies," AIAA Journal, Vol. 4, No. 4, April 1966, pp. 577-587.

28. Sedney, R., "Review of Base Drag," Ballistic Research Laboratories" Report No. 1337, Oct. 1966.

29. Marik, R. H. and Hosack, G. A., "Theoretical Prediction of Base Pressure in Aerospike Nozzles," AIAA 2nd Propulsion Joint Specialist Conference, Colorado Springs, Colorado, June 13-17, 1966. Confidential.

30. Grahm, A. R., NASA Plug Nozzle Handbook, Developed by General Electric under NASA Contract NAS9-3748.

31. Users Manual for the External Drag and Internal Nozzle Performance Deck. Prepared by Pratt & Whitney Aircraft under USAF Contract No. AF33(615)-3128, 1968.

32. Rom, J., "Analysis of the Near-Wake Pressure in Supersonic Flow Using the Momentum Integral Method," Journal of Spacecraft, Vol. 3, No. 10, October 1966, pp. 1504-1509.

33. Panov, I. A. and Shvets, A.I., "Investigation of the Base Pressure Near the Trailing Edge of Axisymmetric Bodies in Supersonic Flow," Priklandnaza Mekhanika, Vol. 2, No. 6, 1966, pp. 105-111.

34. Hopkins, D. F. and Hill, D. E., "Transonic Flow in Unconventional Nozzles," AIAA Journal, Vol. 6, No. 5, May 1968, pp. 838-842.

35. Leipman, H. W. and Goddard, "Note on the Mach Number Effect Upon the Skin Friction of Rough Surfaces," Journal of the Aeronautical Sciences, Vol. 24, 1957, p. 784.

APPENDIX A

DERIVATION OF THE THRUST EXPRESSION

The axial thrust to be maximized is obtained by summing the integrated pressure and shear forces on the plug T'D' (see Figure 1) and the pressure acting on the base D'C. Consider the forces acting on the plug surface segment shown in Figure A-1. The segment, of length ds, when rotated about

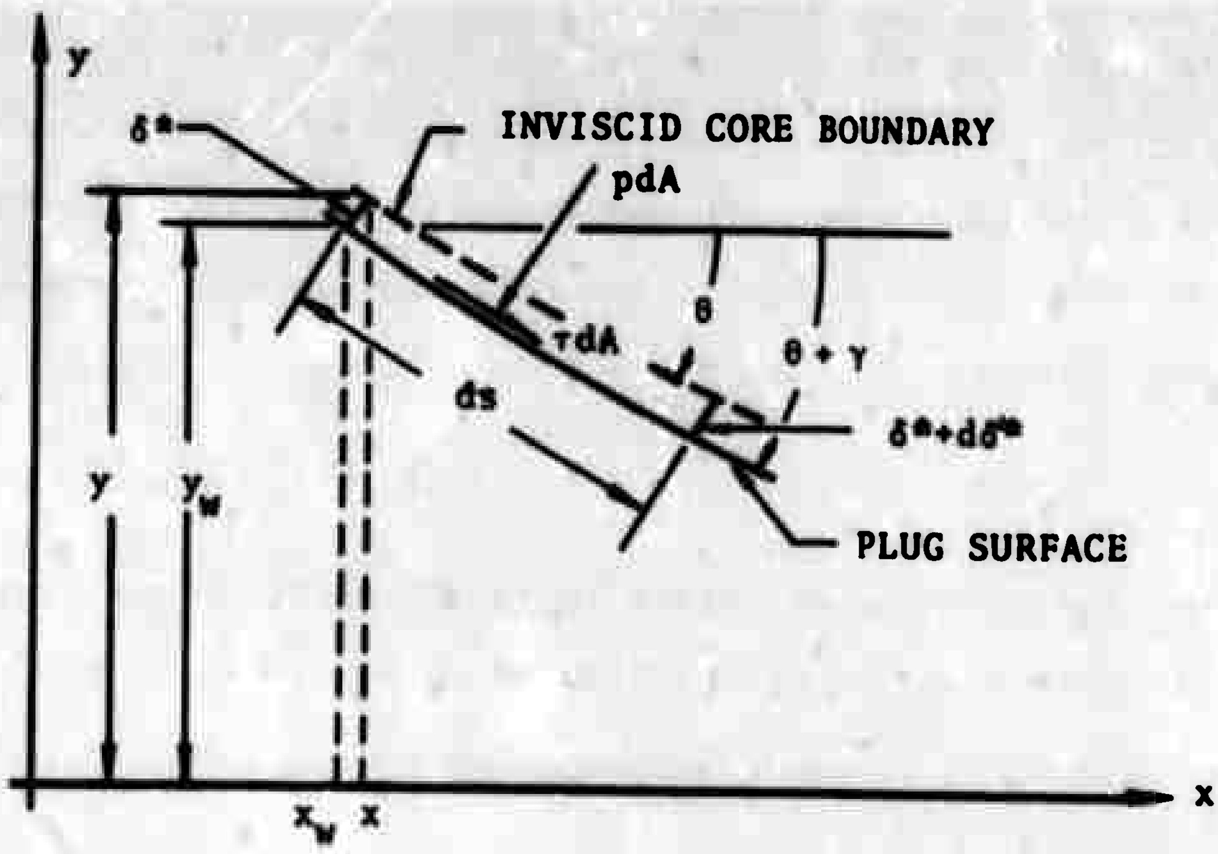

FIGURE A-1. PLUG NOZZLE THRUST SEGMENT

the x-axis sweeps out an area given by

$$dA = 2\pi\, y_w\, ds \tag{A-1}$$

The coordinates (x,y) locate a point on the boundary of the inviscid core (Figure A-1) and (x_w, y_w) locate a corresponding point on the plug surface. The relationship between these two sets of coordinates is given by:

$$x_w = x + \delta^* \sin \theta \qquad \text{(A-2)}$$

$$y_w = y - \delta^* \cos \theta \qquad \text{(A-3)}$$

where δ^* is a boundary layer thickness measured normal to the boundary of the inviscid core.

It will be assumed that the pressure which exists at a given point on the boundary of the inviscid core is the same at the corresponding wall point. The force due to pressure acts normal to the surface and can be written as pdA. The force due to shear must also be considered. This force acts parallel to the wall and is written as τdA. The thrust to be considered is due to the axial components of these two forces. Thus,

$$dT = pdA \sin (\theta + \gamma) + \tau dA \cos (\theta + \gamma) \qquad \text{(A-4)}$$

where the positive direction is to the right. Equations (A-1) and (A-3) can be substituted in Eq. (A-4) to yield

$$\begin{aligned} dT = {} & p2\pi(y - \delta') \, ds \sin (\theta + \gamma) \\ & + \tau 2\pi(y - \delta') \, ds \cos (\theta + \gamma) \end{aligned} \qquad \text{(A-5)}$$

where $\delta' = \delta^* \cos \theta$. It is apparent from Figure A-1 that

$$dy = ds' \sin \theta \qquad dx = ds' \cos \theta \tag{A-6}$$

$$dy_w = ds \sin (\theta + \gamma) \tag{A-7}$$

where ds and ds' are related as shown in Figure A-2. The relationship between them can be expressed as:

$$ds' = ds \cos \gamma \tag{A-8}$$

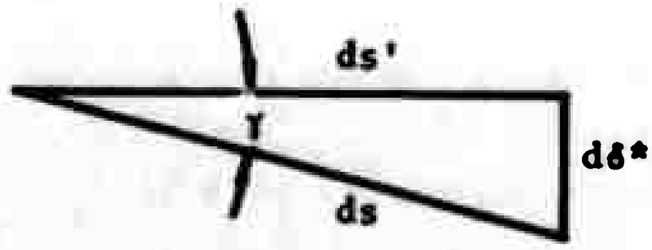

FIGURE A-2. THRUST SEGMENT-INVISCID CORE BOUNDARY RELATIONSHIP

If the boundary layer thickness, δ^*, is small, then γ will also be small. Thus, for small γ:

$$\cos \gamma = 1$$

$$\sin \gamma = \gamma$$

Therefore, from Eq.(A-8) and the trigonometric identities

$$ds' = ds \tag{A-9}$$

$$\sin (\theta + \gamma) = \sin \theta + \gamma \cos \theta \tag{A-10}$$

$$\cos (\theta + \gamma) = \cos \theta - \gamma \sin \theta \tag{A-11}$$

Substitution of Eq.(A-9) into Eqs.(A-6) yields

$$dy = ds \sin \Theta \qquad dx = ds \cos \Theta \tag{A-12}$$

and substitution of Eqs.(A-3), (A-9), and (A-10) into Eq. (A-7) yields

$$d(y - \delta') = ds \sin \Theta + \gamma \cos \Theta \, ds \tag{A-13}$$

Using Eqs.(A-10) and (A-11), Eq.(A-5) can be written as

$$\frac{dT}{2\pi} = p(ds \sin \Theta + \gamma \cos \Theta \, ds)(y - \delta')$$

$$+ \tau(ds \cos \Theta - \gamma \sin \Theta \, ds)(y - \delta') \tag{A-14}$$

which, upon substitution of Eq.(A-10), reduces directly to

$$\frac{dT}{2\pi} = [p(1 + \frac{\gamma}{\tan \Theta}) \, dy + \tau(1 - \gamma \tan \Theta) dx](y - \delta') \tag{A-15}$$

Since the effect of wall shear on thrust is being considered, it is desirable to retain those terms which are of the order of τ or lower. Thus, the term $\tau\gamma \tan \Theta$ can be dropped since it is of an order higher than τ. By considering Eq.(A-13), Eq.(A-15) can be written as

$$\frac{dT}{2\pi} = [p(\dot{y} - \dot{\delta}') + \tau](y - \delta')dx \tag{A-16}$$

where $(\dot{\ })$ indicates the total derivative with respect to x. The final axial thrust expression is obtained by integrating Eq.(A-16) from T to D and adding the base pressure contribution. Thus,

$$\frac{T}{2\pi} = \int_T^D [p(\dot{y} - \dot{\delta}') + \tau](y - \delta')dx - (y_D - \delta_D')^2 p_b/2 \tag{A-17}$$

Since $\dot{y}$ is negative along TD, Eq.(A-17) will produce a negative value for thrust. Without loss of generality, the signs are changed so that a positive value of thrust is obtained. The thrust expression becomes

$$\frac{T}{2\pi} = -\int_T^D [p(\dot{y} - \dot{\delta}') + \tau](y - \delta')dx + (y_D - \delta_D')^2 p_b/2 \tag{A-18}$$

APPENDIX B

CALCULUS OF VARIATIONS

Miele (15) has presented the calculus of variations for a functional of the form

$$I = \iint_S F(x,y,z_k,p_k,q_k)dxdy + \oint_B G(x,y,z_k,\dot{y},\dot{z}_k)dx \qquad \text{(B-1)}$$

The current formulation, however, requires the maximization of a functional which has the form

$$I = \iint_S F(x,y,z_k,p_k,q_k)dxdy + \oint_B G(x,y,z_k,\dot{y},\dot{z}_k)dx$$

$$+ \Phi(y_c,x_c,z_{k_c}) \qquad \text{(B-2)}$$

Thus, it is necessary to account for the first variation of the term $\Phi(y_c,x_c,z_{k_c})$ which is to be evaluated at a corner point c. The starting point for this will be the first variation of the functional (B-1) as given by Miele (15).

For purposes of illustration, Miele assumed the presence of only one corner line in the class of admissable surfaces and the presence of only one corner point in the class of boundary lines examined. His expression for the first variation

is given as

$$\delta I = \iint\limits_{S_1} \sum_{k=1}^{n} [F_{z_k} - (F_{p_k})_x - (F_{q_k})_y] \, \tilde{\delta} z_k dxdy$$

$$+ \int\limits_{S_2} \sum_{k=1}^{n} [F_{z_k} - (F_{p_k})_x - (F_{q_k})_y] \, \tilde{\delta} z_k dxdy$$

$$+ \oint\limits_{B} (\xi \delta x + \eta \delta y + \sum_{k=1}^{n} \zeta_k \delta z_k) dx$$

$$- \oint\limits_{C} (\Delta X \delta x + \Delta Y \delta y + \sum_{k=1}^{n} \Delta z_k \delta z_k) dx$$

$$+ [\Delta(G - \dot{y} G_{\dot{y}} - \sum_{k=1}^{n} \dot{z}_k G_{\dot{z}_k}) \delta x + \Delta G_{\dot{y}} \delta y + \sum_{k=1}^{n} \Delta G_{\dot{z}_k} \delta z_k] = 0 \quad \text{(B-3)}$$

where p_k and q_k are the partial derivatives of the generic dependent variable, z_k, with respect to x and y respectively, and

$$\xi = X - \dot{y} E(G,y) - \sum_{k=1}^{n} \dot{z}_k E(G,z_k) \quad \text{(B-4)}$$

$$\eta = Y + E(G,y) \quad \text{(B-5)}$$

$$\zeta_k = z_k + E(G,z_k) \; , \qquad (k = 1,\ldots,n) \quad \text{(B-6)}$$

$$X = \sum_{k=1}^{n} p_k F_{q_k} + \dot{y}(F - \sum_{k=1}^{n} p_k F_{p_k}) \quad \text{(B-7)}$$

$$Y = (F - \sum_{k=1}^{n} q_k F_{q_k}) - \dot{y} \sum_{k=1}^{n} q_k F_{p_k} \tag{B-8}$$

$$Z_k = - F_{q_k} + \dot{y} F_{p_k} , \qquad (k = 1,\ldots,n) \tag{B-9}$$

$$E(G,y) = G_y - dG_{\dot{y}}/dx \tag{B-10}$$

$$E(G,z_k) = G_{z_k} - dG_{\dot{z}_k}/dx , \quad (k = 1,\ldots,n) \tag{B-11}$$

The $\Delta(\ldots)$ under the $\oint$ represents the difference of the quantity $(\ldots)$ evaluated on the outer side of the corner line and the same quantity evaluated on the inner side. The $\Delta(\ldots)$ included within the brackets represents the difference of the quantity $(\ldots)$ evaluated before the corner point and the same quantity evaluated after the corner.

The first variation of Eq.(B-2) can be obtained by adding the first variation of Φ to Eq.(B-3). This variation, given by

$$\delta\Phi = \Phi_{y_c} \delta_{y_c} + \Phi_{x_c} \delta x_c + \sum_{k=1}^{n} \Phi_{z_{k_c}} \delta_{z_{k_c}}$$

can be combined with the bracketed terms of Eq.(B-2) to yield

$$\begin{aligned} &[(G - \dot{y}G_{\dot{y}} - \sum_{k=1}^{n} \dot{z}_k G_{\dot{z}_k})\delta x + G_{\dot{y}}\delta y + \sum_{k=1}^{n} G_{\dot{z}_k} \delta z_k]\Big|_{x_{c^-}} + \Phi_{x_c} \delta x_c \\ &\quad + \Phi_{y_c} \delta y_c + \sum_{k=1}^{n} \Phi_{z_{k_c}} \delta z_{k_c} - [(G - \dot{y}G_{\dot{y}} - \sum_{k=1}^{n} \dot{z}_k G_{\dot{z}_k})\delta x \\ &\quad + G_{\dot{y}}\delta y + \sum_{k=1}^{n} G_{\dot{z}_k} \delta z_k]\Big|_{x_{c+}} \end{aligned} \tag{B-12}$$

where the subscripts c- and c+ denote the conditions immediately before and after the corner point of the boundary line, respectively. Since the variation, $\delta\Phi$, enters only the bracketed term from which the corner condition along the boundary line is obtained, the remaining necessary conditions will be exactly those given by Miele (15).

The Euler equation which must be satisfied on the surface S is given by

$$F_{z_k} - (F_{p_k})_x - (F_{q_k})_y = 0 , \qquad (k = 1,\ldots,n) \qquad \text{(B-13)}$$

When Eq.(B-13) is combined with Eq.(B-3) the transversality condition is obtained,

$$\xi\, \delta x + \eta \delta y + \sum_{k=1}^{n} \zeta_k \delta z_k = 0 \qquad \text{(B-14)}$$

where ξ, η, and δ are defined by Eqs.(B-4) through (B-6). This condition must be satisfied for every set of variations δx, δy and δz_k consistent with the conditions imposed on the boundary line. The Erdmann-Weirstrass corner condition, obtained by combining Eqs.(B-3), (B-13), and (B-14), must be satisfied for every set of variations δx, δy, and δz consistent with the conditions imposed upon the location of the corner line. This condition is given by

$$\Delta X\, \delta x + \Delta Y\, \delta y + \sum_{k=1}^{n} \Delta Z_k\, \delta z_k = 0 \qquad \text{(B-15)}$$

The final condition is obtained by combining Eq.(B-3) with

Eqs.(B-13) through (B-15) and the expression (B-12). This corner condition, given by

$$\left[\left(G - \dot{y}G_{\dot{y}} - \sum_{k=1}^{n} \dot{z}_k G_{\dot{z}_k}\right)\delta x + G_{\dot{y}}\delta y + \sum_{k=1}^{n} G_{\dot{z}_k}\delta z_k\right]\Bigg|_{x_{c-}} + \Phi_{x_c}\delta x_c$$

$$+ \Phi_{y_c}\delta y_c + \sum_{k=1}^{n} \Phi_{z_{k_c}}\delta z_{k_c} - \left[\left(G - \dot{y}G_{\dot{y}} - \sum_{k=1}^{n} \dot{z}_k G_{\dot{z}_k}\right)\delta x + G_{\dot{y}}\delta y\right.$$

$$\left. + \sum_{k=1}^{n} G_{\dot{z}_k}\delta z_k\right]\Bigg|_{x_{c+}} = 0 \qquad \text{(B-16)}$$

must be satisfied for every set of variations δx, δy, and δz_k consistent with the conditions imposed upon the location of the corner point of the boundary line. This last condition is the only one different from those given by Miele. However, in the event that a corner point on the boundary does not have a function Φ to be evaluated at that location then the corner condition reduces to that given by Miele.

When more than one corner point is present an expression of the type given in Eq.(B-16) arises for each corner and the sum of all such expressions is equated to zero. Only when the variations at the corners are independent can Eq.(B-16) be applied to each corner separately.

APPENDIX C

DERIVATION OF THE EULER EQUATIONS

The general form of the Euler equations is given by Eq.(B-13)

$$F_{z_k} - (F_{p_k})_x - (F_{q_k})_y = 0 \qquad \text{(B-13)}$$

This equation must be satisfied for each of the generic dependent variables u,v,p and ρ. The fundamental function, F, given by Eq.(9) is

$$F = \lambda_1(\rho u_x + \rho v_y + u\rho_x + v\rho_y + \rho v/y) + \lambda_2(\rho u u_x + \rho v u_y + p_x) + \lambda_3(\rho u v_x + \rho v v_y + p_y) + \lambda_4(u p_x + v p_y - a^2 u \rho_x - a^2 v \rho_y) \qquad (9)$$

For k = 1: $z_k = u$, $p_k = u_x$, and $q_k = u_y$.

Taking the derivatives indicated in Eq.(B-13) yields

$$F_u = \lambda_1 y\rho_x + \lambda_2 \rho u_x + \lambda_3 \rho v_x + \lambda_4(p_x - a^2\rho_x) \qquad \text{(C-1)}$$

$$F_{u_x} = \lambda_1 \rho y + \lambda_2 \rho u \qquad \text{(C-2)}$$

$$F_{u_y} = \lambda_2 \rho v \qquad \text{(C-3)}$$

When Equations (C-1) through (C-3) are substituted into Eq. (B-13) the following is obtained:

$$\lambda_1 y\rho_x + \lambda_2\rho u_x + \lambda_3\rho v_x + \lambda_4(p_x - a^2\rho_x) - (\lambda_1\rho y + \lambda_2\rho u)_x$$

$$-(\lambda_2\rho v)_y = 0 \qquad \text{(C-4)}$$

Expansion of Eq.(C-4) yields

$$-\lambda_2 u_x - \lambda_3 v_x - \frac{1}{\rho}\lambda_4(p_x - a^2\rho_x) + y\lambda_{1_x} + u\lambda_{2_x} + v\lambda_{2_y}$$

$$= \frac{v}{y}\lambda_2 \qquad \text{(C-5)}$$

Equation (C-5) is the Euler equation for the dependent variable u. The same procedure is followed to obtain the Euler equation for each of the other dependent variables.

For k = 2: $z_k = v$, $p_k = v_x$, and $q_k = v_y$.

$$F_v = \lambda_1 y\rho_y + \lambda_1\rho + \lambda_2\rho u_y + \lambda_3\rho v_y + \lambda_4(p_y - a^2\rho_y) \qquad \text{(C-6)}$$

$$F_{v_x} = \lambda_3\rho u \qquad \text{(C-7)}$$

$$F_{v_y} = \lambda_1\rho y + \lambda_3\rho v \qquad \text{(C-8)}$$

Substitution into Eq.(B-13) yields

$$\lambda_1 y\rho_y + \lambda_1\rho + \lambda_2\rho u_y + \lambda_3\rho v_y + \lambda_4(p_y - a^2\rho_y) - (\lambda_3\rho u)_x$$

$$-(\lambda_1\rho y + \lambda_3\rho v)_y = 0$$

which reduces directly to

$$-\lambda_2 u_y - \lambda_3 v_y - \frac{1}{\rho}\lambda_4(p_y - a^2\rho_y) + y\lambda_{1_y} + u\lambda_{3_x} + v\lambda_{3_y}$$

$$= \frac{v}{y}\lambda_3 \tag{C-9}$$

For $k = 3$: $z_k = p$, $p_k = p_x$, and $q_k = p_y$.

The derivatives with respect to p and ρ are taken using the relation

$$a^2 = \frac{\gamma p}{\rho}$$

such that

$$(a^2)_p = a^2/p, \quad (a^2)_\rho = a^2/\rho$$

Thus,

$$F_p = -\lambda_4 \frac{\gamma}{\rho}(u\rho_x + v\rho_y) \tag{C-10}$$

$$F_{p_x} = \lambda_2 + \lambda_4 u \tag{C-11}$$

$$F_{p_y} = \lambda_3 + \lambda_4 v \tag{C-12}$$

Using the above results, Eq.(B-13) becomes

$$\lambda_4 u_x + \lambda_4 v_y + \lambda_4 \frac{a^2}{p}(u\rho_x + v\rho_y) + \lambda_{2_x} + \lambda_{3_y} + u\lambda_{4_x}$$

$$+ v\lambda_{4_y} = 0 \tag{C-13}$$

For $k = 4$: $z_k = \rho$, $p_k = \rho_x$, and $q_k = \rho_y$.

$$F_\rho = \lambda_1 y u_x + \lambda_1 y v_y + \lambda_1 v + \lambda_2(u u_x + v u_y) + \lambda_3(u v_x + v v_y)$$

$$+ \lambda_4(a^2 u \rho_x/\rho + a^2 v \rho_y/\rho) \qquad \text{(C-14)}$$

$$F_{\rho_x} = \lambda_1 y v - \lambda_4 a^2 v \qquad \text{(C-15)}$$

$$F_{\rho_y} = \lambda_1 y v - \lambda_4 a^2 v \qquad \text{(C-16)}$$

Substitution of Eqs.(C-14) through (C-16) into Eq.(B-13) yields

$$\lambda_1(y u_x + y v_y + v) + \lambda_2(u u_x + v u_y) + \lambda_3(u v_x + v v_y)$$

$$+ \lambda_4(a^2 u \rho_x/\rho + a^2 v \rho_y/\rho) + (\lambda_1 y u - \lambda_4 a^2 u)_x$$

$$- (\lambda_1 y v - \lambda_4 a^2 v)_y = 0 \qquad \text{(C-17)}$$

which can be expanded to

$$\lambda_2(u u_x + v u_y) + \lambda_3(u v_x + v v_y) - y u \lambda_{1_x} + a^2(u\lambda_4)_x$$

$$+ \lambda_4 u(a^2 p_x/p - a^2 \rho_x/\rho) + \lambda_4 v(a^2 p_y/p - a^2 \rho_y/\rho) - y v \lambda_{1_y}$$

$$+ a^2(v\lambda_4)_y - y u \lambda_{1_x} + \lambda_4\, a^2(u \rho_x + v \rho_y)/\rho = 0 \qquad \text{(C-18)}$$

Multiplication of Eq.(C-13) by $-a^2$, addition of the result to Eq.(C-18), and use of the two momentum equations

$$u u_x + v u_y = -\, p_x/\rho$$

$$uv_x + vv_y = -p_y/\rho$$

results in

$$-\lambda_2 p_x/\rho - \lambda_3 p_y/\rho - yu\lambda_{1_x} - yv\lambda_{1_y} - a^2\lambda_{2_x} - a^2\lambda_{3_y}$$

$$+ \lambda_4 a^2(up_x + vp_y - ua^2\rho_x - va^2\rho_y)/p = 0 \qquad \text{(C-19)}$$

The last term in the above equation is identical to Eq.(5). Thus, Eq.(C-19) reduces to

$$\frac{1}{\rho}\lambda_2 p_x + \frac{1}{\rho}\lambda_3 p_y + yu\lambda_{1_x} + yv\lambda_{1_y} + a^2\lambda_{2_x} + a^2\lambda_{3_y} = 0 \qquad \text{(C-20)}$$

Thus, the Euler equations are Eqs.(C-5), (C-9), (C-13), and (C-20).

APPENDIX D

DERIVATION OF THE TRANSVERSALITY CONDITIONS

Since the function G is not the same on all portions of the boundary of the region (R) and different assumptions apply to the variations, it is necessary to consider each portion of the boundary separately. The general transversality condition which must be satisfied is given by Eq.(B-14)

$$\xi\delta x + \eta\delta y + \sum_{k=1}^{n} \zeta_k \delta z_k = 0 \qquad \text{(B-14)}$$

The terms in this equation are defined by Eqs.(B-4) through (B-11) and the function G along each portion of the boundary is given by Eqs.(10) through (12) which are

$$G = -[f + C_1 g + C_2 y\rho(u\dot{y} - v)] \qquad \text{along TD} \qquad (10)$$

$$G = 0 \qquad \text{along DE} \qquad (11)$$

$$G = 0 \qquad \text{along ET} \qquad (12)$$

Since the fundamental function, F, is zero, Eq.(B-14) can be written as

$$\sum_{k=1}^{4} [(F_{q_k} - \dot{y}F_{p_k})(p_k\delta x + q_k\delta y - \delta z_k) + (\delta z_k - \dot{z}_k\delta x)B(G,z_k)]$$
$$+ E(G,y)(\delta y - \dot{y}\delta x) = 0 \qquad \text{(D-1)}$$

1. CONDITIONS ALONG ET

There can be no variations in u, v, p, ρ, x, or y along ET since the flow properties along and the location of this line are determined from the fixed upstream geometry. Therefore, Eq.(B-14) is satisfied identically.

2. CONDITIONS ALONG DE

Since the function G = 0 along this portion of the boundary,

$E(G,z_k) = E(G,y) = 0$

and the transversality condition, Eq.(D-1), becomes

$$\sum_{k=1}^{4} (F_{q_k} - \dot{y}F_{p_k})(p_k\delta x + q_k\delta y - \delta z_k) = 0 \qquad \text{(D-2)}$$

Gas property variations along ED are arbitrary which requires the coefficient of δz_k to be zero. If this is done no requirement need be placed on the variations of δx and δy. Thus, it is required that

$$F_{q_k} - \dot{y}F_{p_k} = 0 \qquad (k = 1,\ldots,4) \qquad \text{(D-3)}$$

For k = 1: $z_k = u$, $p_k = u_x$, and $q_k = u_y$.

The derivations F_{p_k} and F_{q_k}, given by Eqs.(C-2) and (C-3), are substituted into Eq.(D-3) which results in

$$(v - \dot{y}u)\lambda_2 - \lambda_1\dot{y}y = 0 \qquad \text{(D-4)}$$

For k = 2: $z_k = v$, $p_k = v_x$, and $q_k = v_y$.

The derivatives F_{p_k} and F_{q_k}, given by Eqs.(C-7) and (C-8), are

also substituted into Eq.(D-3) to yield

$$(v - \dot{y}u)\lambda_3 + \lambda_1 y = 0 \tag{D-5}$$

For k = 3: $z_k = p$, $p_k = p_x$, and $q_k = p_y$.

In this case the derivatives F_{p_k} and F_{q_k} are given by Eqs.(C-11) and (C-12) and when substituted into Eq.(D-3) yields

$$\lambda_3 + (v - \dot{y}u)\,\lambda_4 - \dot{y}\lambda_2 = 0 \tag{D-6}$$

For k = 4: $z_k = \rho$, $p_k = \rho_x$, and $q_k = \rho_y$.

The derivatives F_{p_k} and F_{q_k}, given by Eqs.(C-15) and (C-16) are substituted into Eq. (D-3) which results in

$$\lambda_1 y - \lambda_4 a^2 = 0 \tag{D-7}$$

Equations (D-4) through (D-7) must be satisfied along ED. However, these four equations can be combined to yield the equation of a right-running characteristic which can be used to replace one of the four. First, eliminating λ_3 from Eqs. (D-5) and (D-6) results in

$$\lambda_1 y - (v - \dot{y}u)^2\lambda_4 + \dot{y}(v - \dot{y}u)\,\lambda_2 = 0 \tag{D-8}$$

An expression for λ_2 can be obtained from Eq.(D-4) and substituted into Eq.(D-8) to yield

$$\lambda_1 y(1 + \dot{y}^2) - (v - \dot{y}u)^2\lambda_4 = 0 \tag{D-9}$$

Using Eq.(D-7) to eliminate λ_1 from Eq.(D-9) results in

$$\lambda_4[(u^2 - a^2)\dot{y}^2 - 2uv\dot{y} + (v^2 - a^2)] = 0 \tag{D-10}$$

Since λ_4 will not in general be zero, the bracketed term in Eq.(D-10) must vanish. Thus,

$$[(u^2 - a^2)\dot{y}^2 - 2uv\dot{y} + (v^2 - a^2)] = 0 \tag{D-11}$$

As shown in Appendix F, Eq.(D-11) is the equation of a right-running characteristic. For convenience, Eq.(D-11) will be used to replace Eq.(D-6). Thus, the equations which must be satisfied along DE are: (D-4), (D-5), (D-7), and (D-11).

3. CONDITIONS ALONG TD

Along this portion of the boundary variations in the gasdynamic properties are arbitrary, thus, their coefficients must vanish. From Eq.(B-14) it is required that

$$\zeta_k = F_{q_k} - \dot{y}F_{p_k} - E(G,z_k) = 0 \qquad (k = 1,\ldots,4) \tag{D-12}$$

For k = 1: $z_k = u$, $p_k = u_x$, and $q_k = u_y$.

$$E(G,z_k) = G_u - dG_{\dot{u}}/dx = -C_2\rho y\dot{y} \tag{D-13}$$

When equations (C-2), (C-3) and (D-13) are substituted into Eq.(D-12) the following is obtained:

$$-\lambda_1\rho y\dot{y} + C_2\rho y\dot{y} = 0$$

or

$$\lambda_1 = C_2 \tag{D-14}$$

For $k = 2$: $z_k = v$, $p_k = v_x$, and $q_k = v_y$.

$$E(G,z_k) = +C_2\rho y \tag{D-15}$$

Substitution of Eqs.(C-7), (C-8) and (D-15) into Eq.(D-12) yields

$$\lambda_1 \rho y - C_2 \rho y = 0$$

or

$$\lambda_1 = C_2 \tag{D-16}$$

For $k = 3$: $z_k = p$, $p_k = p_x$, and $q_k = p_y$.

$$E(G,z_k) = -f_p - C_1 g_p \tag{D-17}$$

Substitution of Eqs.(C-11), (C-12) and (D-17) into Eq.(D-12) yields

$$-\dot{y}\lambda_2 + \lambda_3 + f_p + C_1 g_p = 0$$

or

$$u\lambda_3 - v\lambda_2 + uf_p + ug_p C_1 = 0 \tag{D-18}$$

where $f_p = \dot{y}(y - \delta')$

For $k = 4$: $z_k = \rho$, $p_k = \rho_x$, ρ_x, and $q_k = \rho_y$.

$$E(G,z_k) = -f_\rho - C_1 g_\rho$$

but $f_\rho = 0$, therefore

$$E(G,z_k) = -C_1 g_\rho \tag{D-19}$$

Substitution of Eqs.(C-15), (C-16) and (D-19) into Eq.(D-12) yields only the identity $0 = 0$.

Variations in x and y are also arbitrary along TD. However, it is convenient to rearrange the coefficients of δx and δy in Eq.(B-14) as

$$\xi\delta x + \eta\delta y = (\delta y - \dot{y}\delta x)\{\sum_{k=1}^{4}[q_k E(G,z_k)] + E(G,y)\}$$

Thus, for arbitrary variations in x and y it is required that

$$\sum_{k=1}^{4} q_k E(G,z_k) + E(G,y) = 0 \tag{D-20}$$

The expressions for $E(G,z_k)$ as k takes on the values 1 to 4, are given by Eqs.(D-13), (D-15), (D-17), and (D-19). The function $E(G,y)$ is written as

$$E(G,y) = G_y - dG_{\dot{y}}/dx$$

or

$$E(G,y) = -f_y - C_1 g_y + \frac{d}{dx}(f_{\dot{y}} + C_2 \rho y u + C_1 g_{\dot{y}}) \tag{D-21}$$

Substitution into Eq.(D-20) yields

$$C_2[\rho y \dot{y} u_y - \rho y v_y - \frac{d}{dx}(\rho y u)] - y\rho u \frac{d}{dx} C_2$$

$$+ C_1[p_y g_p + g_y - \frac{d}{dx} g_{\dot{y}}] + f_y - \frac{d}{dx}(f_{\dot{y}}) + f_p p_y = 0 \tag{D-22}$$

Using the continuity equation and the fact that TD is a streamline, it can be shown that

$$-\frac{d}{dx}(y\rho u) = y\rho v_y - \dot{y}\rho y u_y \tag{D-23}$$

Substitution of Eq.(D-23) into Eq.(D-22) shows that the coefficient of C_2 is zero.

Further simplifications to Eq.(D-22) can be obtained by using the following expanded terms

$$f_y - \frac{d}{dx} f_{\dot{y}} = +\tau - (y - \delta')\frac{dp}{dx} \tag{D-24}$$

$$-(y - \delta')\frac{dp}{dx} = -(y - \delta')\, p_x - (y - \delta')\dot{y} p_y \tag{D-25}$$

$$f_p p_y = \dot{y}(y - \delta')p_y - \dot{\delta}'(y - \delta')p_y \tag{D-26}$$

Substitution of Eqs.(D-24) through (D-26) into Eq.(D-22) yields

$$- y\rho u \frac{dC_2}{dx} + C_1\left(p_y g_p + g_y - \frac{d}{dx} g_{\dot{y}}\right) + \tau - (y - \delta')p_x$$
$$- \dot{\delta}'(y - \delta')p_y = 0 \tag{D-27}$$

From Eqs.(3) and (4)

$$p_x = -\rho u u_x - \rho v u_y = -\rho u \frac{du}{dx} \tag{D-28}$$

$$p_y = -\rho u v_x - \rho v v_y = -\rho u \frac{dv}{dx} \tag{D-29}$$

Substitution of these expressions into Eq.(D-27) gives

$$- y\rho u \frac{dC_2}{dx} + C_1(-\rho u g_p \frac{dv}{dx} + g_y - \frac{d}{dx}g_{\dot{y}}) + \tau + (y - \delta')\rho u \frac{du}{dx}$$

$$\dot{\delta}'(y - \delta')\rho u \frac{dv}{dx} = 0 \qquad \text{(D-30)}$$

Equation (D-30) can be rewritten as

$$y\rho u \frac{d}{dx} C_2 = \rho u(y - \delta')(\frac{du}{dx} + \dot{\delta}' \frac{dv}{dx})$$

$$- C_1(\rho u g_p \frac{dv}{dx} - g_y + \frac{d}{dx}g_{\dot{y}}) + \tau \qquad \text{(D-31)}$$

Thus, Eqs.(D-14), (D-16), (D-18), and (D-31) must be satisfied along TD.

APPENDIX E

DERIVATION OF THE CORNER CONDITIONS

Since flows in which corner lines arise are not to be considered, the only corner condition which must be satisfied at points E, T, and D is given by Eq.(B-16)

$$\Big[\Big(G - \dot{y}G_{\dot{y}} - \sum_{k=1}^{n} \dot{z}_k G_{\dot{z}_k}\Big)\delta x + G_{\dot{y}}\delta y + \sum_{k=1}^{n} G_{\dot{z}_k}\delta z_k\Big]\Big|_{x_{c-}}$$

$$+ \Phi_{x_c}\delta x_c + \Phi_{y_c}\delta y_c + \sum_{k=1}^{n} \Phi_{z_{k_c}}\delta z_{k_c} - \Big[\Big(G - \dot{y}G_{\dot{y}}$$

$$- \sum_{k=1}^{n} \dot{z}_k G_{\dot{z}_k}\Big)\delta x + G_{\dot{y}}\delta y + \sum_{k=1}^{n} G_{\dot{z}_k}\delta z_k\Big]\Big|_{x_{c+}} = 0 \qquad \text{(B-16)}$$

where the subscripts c- and c+ denote the conditions immediately before and after the corner point, respectively.

1. CONDITIONS AT POINTS E AND T

These two points are considered to be fixed which implies that $\delta y = \delta x = \delta z_k = 0$. Hence, the corner condition is satisfied identically at these two points.

2. CONDITIONS AT POINT D

The variations in $x, y, u, v, p,$ and ρ can be treated as arbitrary and independent at this point. Thus, the coefficient

of each of these variables must vanish. Since $G_{\dot{z}_k} = 0$ on all portions of the boundary of the region (R), it is required that

$$(G - \dot{y}G_{\dot{y}})_{TD} + \Phi_{x_D} = (G - \dot{y}G_{\dot{y}})_{DE} \qquad \text{(E-1)}$$

$$(G_{\dot{y}})_{TD} + \Phi_{y_D} = (G_{\dot{y}})_{DE} \qquad \text{(E-2)}$$

$$(\Phi_u)_{TD} = 0 \qquad \text{(E-3)}$$

$$(\Phi_v)_{TD} = 0 \qquad \text{(E-4)}$$

$$(\Phi_p)_{TD} = 0 \qquad \text{(E-5)}$$

$$(\Phi_\rho)_{TD} = 0 \qquad \text{(E-6)}$$

The function Φ is independent of $u, v, p,$ and ρ, therefore Eqs.(E-3) through (E-6) are satisfied identically. Also, the function G is 0 along DE which reduces Eqs.(E-1) and (E-2) to

$$(G - \dot{y}G_{\dot{y}})_{TD} + \Phi_{x_D} = 0 \qquad \text{(E-7)}$$

$$(G_{\dot{y}})_{TD} + \Phi_{y_D} = 0 \qquad \text{(E-8)}$$

The derivatives indicated in these two equations are

$$G_{\dot{y}} = -[p(y - \delta') + C_1 g_{\dot{y}} + C_2 \rho y u] \qquad \text{(E-9)}$$

$$\Phi_{x_D} = 0 \qquad \text{(E-10)}$$

$$\Phi_{y_D} = (y_D - \delta'_D)p_b \tag{E-11}$$

Substitution of Eqs.(E-9) and (E-10) into Eq.(E-7) yields

$$[- p(\dot{y} - \dot{\delta}')(y - \delta') - \tau(y - \delta') - C_1 g + \dot{y}p(y - \delta')$$
$$+ C_1 \dot{y} g_{\dot{y}} + C_2 \rho y \dot{y} u]_{TD} = 0$$

or

$$[(y - \delta')(p\dot{\delta}' - \tau) + C_2 \rho u y \dot{y} - C_1(g - \dot{y} g_{\dot{y}})]_{TD} = 0 \tag{E-12}$$

Substitution of Eqs.(E-9) and (E-11) into Eq.(E-8) yields

$$[p(y - \delta') + C_1 g_{\dot{y}} + C_2 \rho u y]_{TD} = (y_D - \delta'_D)p_b \tag{E-13}$$

Thus, Eqs.(E-12) and (E-13) are the corner conditions which must be satisfied at point D.

APPENDIX F

CHARACTERISTIC AND COMPATIBILITY EQUATIONS

In this section the method of characteristics will be used to obtain the characteristic and compatibility equations for the system of partial differential equations consisting of Eqs.(2) through (5) and Eqs.(15) through (18). The method of characteristics as used here is described in such references as (17), (18), and (19).

The system of equations to be considered consists of those mentioned above which are written here for convenience.

$$L_1 = \rho u_x + \rho v_y + u\rho_x + v\rho_y + \frac{\rho v}{y} = 0 \tag{F-1}$$

$$L_2 = \rho u u_x + \rho v u_y + p_x = 0 \tag{F-2}$$

$$L_3 = \rho u v_x + \rho v v_y + p_y = 0 \tag{F-3}$$

$$L_4 = u p_x + v p_y - a^2 u \rho_x - a^2 v \rho_y = 0 \tag{F-4}$$

$$L_5 = -\lambda_2 u_x - \lambda_3 v_x - \frac{1}{\rho}\lambda_4 (p_x - a^2 \rho_x) + y\lambda_{1_x} + u\lambda_{2_x} + v\lambda_{2_y} - \lambda_2 v/y = 0 \tag{F-5}$$

$$L_6 = -\lambda_2 u_y - \lambda_3 v_y - \frac{1}{\rho}\lambda_4(p_y - a^2\rho_y) + y\lambda_{1_y} + u\lambda_{3_x}$$

$$+ v\lambda_{3_y} - \lambda_3 v/y = 0 \qquad \text{(F-6)}$$

$$L_7 = \lambda_4 u_x + \lambda_4 v_y + \frac{a^2}{p}\lambda_4(u\rho_x + v\rho_y) + \lambda_{2_x} + \lambda_{3_y} + u\lambda_{4_x}$$

$$+ v\lambda_{4_y} = 0 \qquad \text{(F-7)}$$

$$L_8 = \frac{1}{\rho}\lambda_2 p_x + \frac{1}{\rho}\lambda_3 p_y + yu\lambda_{1_x} + yv\lambda_{1_y} + a^2\lambda_{2_x}$$

$$+ a^2\lambda_{3_y} = 0 \qquad \text{(F-8)}$$

Equations (F-1) through (F-8) are now multiplied by the arbitrary functions σ_1 through σ_8 to form the differential operator

$$L = \sigma_1 L_1 + \sigma_2 L_2 + \sigma_3 L_3 + \sigma_4 L_4 + \sigma_5 L_5 + \sigma_6 L_6$$

$$+ \sigma_7 L_7 + \sigma_8 L_8 = 0 \qquad \text{(F-9)}$$

Equation (F-9) can be rearranged such that

$$L = A(u_x + \frac{B}{A}u_y) + C(v_x + \frac{D}{C}v_y) + E(p_x + \frac{F}{E}p_y)$$

$$+ G(\rho_x + \frac{H}{G}\rho_y) + I(\lambda_{1_x} + \frac{J}{I}\lambda_{1_y}) + K(\lambda_{2_x} + \frac{L}{K}\lambda_{2_y})$$

$$+ M(\lambda_{3_x} + \frac{N}{M}\lambda_{3_y}) + P(\lambda_{4_x} + \frac{Q}{P}\lambda_{4_y}) + R = 0 \qquad \text{(F-10)}$$

where

$$A = \sigma_1 \rho + \sigma_2 \rho u - \sigma_5 \lambda_2 + \sigma_7 \lambda_4 \qquad \text{(F-11)}$$

$$B = \sigma_2 \rho v - \sigma_6 \lambda_2 \qquad \text{(F-12)}$$

$$C = \sigma_3 \rho u - \sigma_5 \lambda_3 \qquad \text{(F-13)}$$

$$D = \sigma_1 \rho + \sigma_3 \rho v - \sigma_6 \lambda_3 + \sigma_7 \lambda_4 \qquad \text{(F-14)}$$

$$E = \sigma_2 + \sigma_4 u - \frac{1}{\rho} \sigma_5 \lambda_4 + \frac{1}{\rho} \sigma_8 \lambda_2 \qquad \text{(F-15)}$$

$$F = \sigma_3 + \sigma_4 v - \frac{1}{\rho} \sigma_6 \lambda_4 + \frac{1}{\rho} \sigma_8 \lambda_3 \qquad \text{(F-16)}$$

$$G = \sigma_1 u - \sigma_4 a^2 u + \sigma_5 \lambda_4 \frac{a^2}{\rho} + \sigma_7 \lambda_4 \frac{a^2 u}{p} \qquad \text{(F-17)}$$

$$H = \sigma_1 v - \sigma_4 a^2 v + \sigma_6 \lambda_4 \frac{a^2}{\rho} \pm \sigma_7 \lambda_4 \frac{a^2 v}{p} \qquad \text{(F-18)}$$

$$I = \sigma_5 y + \sigma_8 y u \qquad \text{(F-19)}$$

$$J = \sigma_6 y + \sigma_8 y v \qquad \text{(F-20)}$$

$$K = \sigma_5 u + \sigma_7 + \sigma_8 a^2 \qquad \text{(F-21)}$$

$$L = \sigma_5 v \qquad \text{(F-22)}$$

$$M = \sigma_6 u \qquad \text{(F-23)}$$

$$N = \sigma_6 v + \sigma_7 + \sigma_8 a^2 \qquad \text{(F-24)}$$

$$P = \sigma_7 u \qquad \text{(F-25)}$$

$$Q = \sigma_7 v \qquad \text{(F-26)}$$

$$R = \sigma_1 \frac{\rho v}{y} - \sigma_5 K_1 - \sigma_6 K_2 \tag{F-27}$$

Under certain conditions Eq.(F-10) can be written as

$$L = A \frac{du}{dx} + C \frac{dv}{dx} + E \frac{dp}{dx} + G \frac{d\rho}{dx} + I \frac{d\lambda_1}{dx} + K \frac{d\lambda_2}{dx} + M \frac{d\lambda_3}{dx}$$

$$+ P \frac{d\lambda_4}{dx} + R = 0$$

or

$$Adu + Cdv + Edp + Gd\rho + Id\lambda_1 + Kd\lambda_2 + Md\lambda_3 + Pd\lambda_4$$

$$+ Rdx = 0 \tag{F-28}$$

The conditions under which this equation can be written are that the ratios B/A,D/C,F/E,H/G,J/I,L/K,N/M,and Q/P must equal the dy/dx which is designated by λ. If these conditions are to hold then the following eight equations can be written.

$$A\lambda - B = 0 \tag{F-29}$$

$$C\lambda - D = 0 \tag{F-30}$$

$$E\lambda - F = 0 \tag{F-31}$$

$$G\lambda - H = 0 \tag{F-32}$$

$$I\lambda - J = 0 \tag{F-33}$$

$$K\lambda - L = 0 \tag{F-34}$$

$$M\lambda - N = 0 \tag{F-35}$$

$$P\lambda - Q = 0 \tag{F-36}$$

These equations can then be arranged with the multipliers σ_1 through σ_8 as the unknowns. If this system of equations is to have a solution other than the trivial, σ_1 through σ_8 equal to zero, then the coefficient determinant must vanish. This determinant is as follows:

$$\begin{vmatrix}
\rho\lambda & \rho(\lambda u-v) & 0 & 0 & -\lambda_2\lambda & \lambda_2 & \lambda_4\lambda & 0 \\
-\rho & 0 & \rho(\lambda u-v) & 0 & -\lambda_3\lambda & \lambda_3 & -\lambda_4 & 0 \\
0 & \lambda & -1 & (\lambda u-v) & -\lambda_4\dfrac{\lambda}{\rho} & \dfrac{1}{\rho}\lambda_4 & 0 & \dfrac{1}{\rho}(\lambda_2\lambda-\lambda_3) \\
(\lambda u-v) & 0 & 0 & -a^2(\lambda u-v) & \lambda_4\dfrac{a^2\lambda}{\rho} & \dfrac{-\lambda_4 a^2}{\rho} & \dfrac{\lambda_4 a^2(\lambda u-v)}{p} & 0 \\
0 & 0 & 0 & 0 & \lambda y & -y & 0 & y(\lambda u-v) \\
0 & 0 & 0 & 0 & (\lambda u-v) & 0 & \lambda & a^2\lambda \\
0 & 0 & 0 & 0 & 0 & (\lambda u-v) & -1 & -a^2 \\
0 & 0 & 0 & 0 & 0 & 0 & (\lambda u-v) & 0
\end{vmatrix} \tag{F-37}$$

Since the lower left corner of the above determinant is filled with zeros, the expansion of the determinant (F-37) reduces to the following:

$$|X| \times |Y| = 0 \tag{F-38}$$

where X represents the upper left 4 x 4 submatrix and Y represents the lower right 4 x 4 submatrix. Equation (F-38) can be zero by either the determinant of X or Y being zero. Setting these two determinants to zero results in the identical expression

$$(\lambda u - v)^2[\lambda^2(u^2 - a^2) - 2\lambda uv + (v^2 - a^2)] = 0 \qquad \text{(F-39)}$$

The characteristic curves are found by solving this equation for λ. The resulting expressions are

$$\lambda = \frac{dy}{dx} = \frac{v}{u} \qquad \text{(F-40)}$$

$$\lambda = \frac{dy}{dx} = \frac{uv \pm a^2(M^2 - 1)^{1/2}}{u^2 - a^2} \qquad \text{(F-41)}$$

Equation (F-41) can be rewritten in terms of the Mach angle and flow angle as

$$\lambda = \frac{dy}{dx} = \tan(\theta \pm \alpha) \qquad \text{(F-42)}$$

Thus, the characteristic curves are the gas streamlines appearing four times and the Mach lines appearing two times each. The system is then totally hyperbolic since there are a total of eight real characteristic curves.

The corresponding compatibility equations are obtained by substituting Eqs.(F-40) and (F-42) into Eqs.(F-29) through (F-36) which are then solved for the multipliers σ_1 through σ_8. The expressions for σ_1 through σ_8 are then substituted into Eq.(F-28) which is the general compatibility relation.

The compatibility relations along the gas streamlines will be obtained first. Using Eq.(F-40) in Eqs.(F-29) through (F-36) results in four independent relations to determine σ_1 through σ_8. Thus, four of the σ's can be arbitrary and these are chosen to be σ_2, σ_4, σ_5, and σ_8. Expressions for the remaining σ's are;

$$\sigma_7 = -a^2\sigma_8 \qquad \text{(F-43)}$$

$$\sigma_6 = \lambda\sigma_5 \qquad \text{(F-44)}$$

$$\sigma_3 = \lambda\sigma_2 + \frac{1}{\rho}\sigma_8(\lambda\lambda_2 - \lambda_3) \qquad \text{(F-45)}$$

$$\sigma_1 = \frac{a^2}{\rho}\lambda_4\sigma_8 \qquad \text{(F-46)}$$

Equations (F-43) through (F-46) are now substituted into Eq.(F-28). Since the multipliers σ_2, σ_4, σ_5, and σ_8 are arbitrary the resulting equation can be zero only if the coefficient of each of the arbitrary multipliers is zero. Equating to zero the coefficient of each of the arbitrary multipliers results in the following ordinary differential equations.

$$\rho u du + \rho v dv + dp = 0 \qquad \text{(F-47)}$$

$$dp - a^2 d\rho = 0 \qquad \text{(F-48)}$$

$$-\lambda_2 du - \lambda_3 dv + y d\lambda_1 + u d\lambda_2 + v d\lambda_3 = (v/y)(\lambda_2 dx + \lambda_3 dy) \qquad \text{(F-49)}$$

$$(v\lambda_2 - u\lambda_3)dv + \frac{1}{\rho}\lambda_2 dp - \lambda_4 \frac{ua^2}{\rho}(\gamma - 1)d\rho + yud\lambda_1 - a^2 u d\lambda_4 = -\lambda_4 \frac{a^2 v}{y} dx \qquad \text{(F-50)}$$

Proceeding as before, the compatibility relations along the Mach lines can be obtained. Equation (F-41) is used in Eqs.(F-29) through (F-36) which results in six independent relations to determine the eight multipliers σ_1 through σ_8. Thus, only two of the σ's are arbitrary in this case and are chosen to be σ_4 and σ_8. The expressions for the remaining σ's

are

$$\sigma_7 = 0 \tag{F-51}$$

$$\sigma_6 = \frac{a^2}{\lambda u - v}\,\sigma_8 \tag{F-52}$$

$$\sigma_5 = \frac{-a^2\lambda}{\lambda u - v}\,\sigma_8 \tag{F-53}$$

$$\sigma_3 = \frac{a^2}{\lambda u - v}\,\sigma_4 + \frac{1}{\rho}\,\sigma_8\left[\frac{a^2}{\lambda u - v}\,\lambda_4 - \lambda_3\right] \tag{F-54}$$

$$\sigma_2 = \frac{-a^2\lambda}{\lambda u - v}\,\sigma_4 - \frac{1}{\rho}\,\sigma_8\left[\frac{a^2\lambda}{\lambda u - v}\,\lambda_4 + \lambda_2\right] \tag{F-55}$$

$$\sigma_1 = a^2\sigma_4 + \frac{a^2}{\rho}\,\lambda_4\sigma_8 \tag{F-56}$$

Equations (F-51) through (F-56) are then substituted into Eq.(F-28) and the coefficients of σ_4 and σ_8 are collected. These coefficients are then equated to zero, which results in the following:

$$\lambda_2 du + \lambda_3 dv - \frac{1}{\rho}\,\lambda_4(dp + a^2 d\rho) - y d\lambda_1 \pm \tan\alpha(v d\lambda_2 - u d\lambda_3)$$

$$= \mp \tan\alpha(\lambda_3\,dx - \lambda_2 dy)(v/y) \tag{F-57}$$

$$a^2(vdu - udv) \pm \frac{a^2}{\rho}\,\mathrm{ctn}\,\alpha\;dp = \frac{a^2 v}{y}\,(udy - vdx) \tag{F-58}$$

The upper signs in Eqs.(F-57) and (F-58) apply to the left-running Mach lines and the lower signs to the right-running Mach lines.

Thus, the system of partial differential equations given by Eqs. (F-1) through (F-8) can be replaced by the equivalent system of characteristic and compatibility equations developed in this section. A total of eight characteristic equations were found, of which three, the two Mach lines and the gas

streamline, were distinct. A total of eight compatibility equations, each valid along one of the characteristic curves, were found.

APPENDIX G

BASE PRESSURE MODEL

The optimization of plug nozzles, as carried out in this report, requires that the base pressure be recalculated each time the plug contour is modified. It is therefore desirable to have a rapid method of calculating the base pressure. The purpose here is to review the fluid mechanics of the base pressure problem in which the flow ahead of the base is supersonic and remains so through the wake. The expression used to calculate the base pressure will be discussed briefly even though the program is not restricted to any particular model. The model can be changed in the program simply by changing subprogram BASE.

Base pressures of various types have been under study both theoretically and experimentally for several years so that one can find an abundance of information in the literature. The early work was concerned with predicting the base pressure on axisymmetric bodies of revolution traveling at supersonic speeds, the blunt trailing edges of wings, rearward facing steps, and the internal flow situation of an abrupt increase in cross-section. These are shown schematically in Figures G-1a through G-1d.

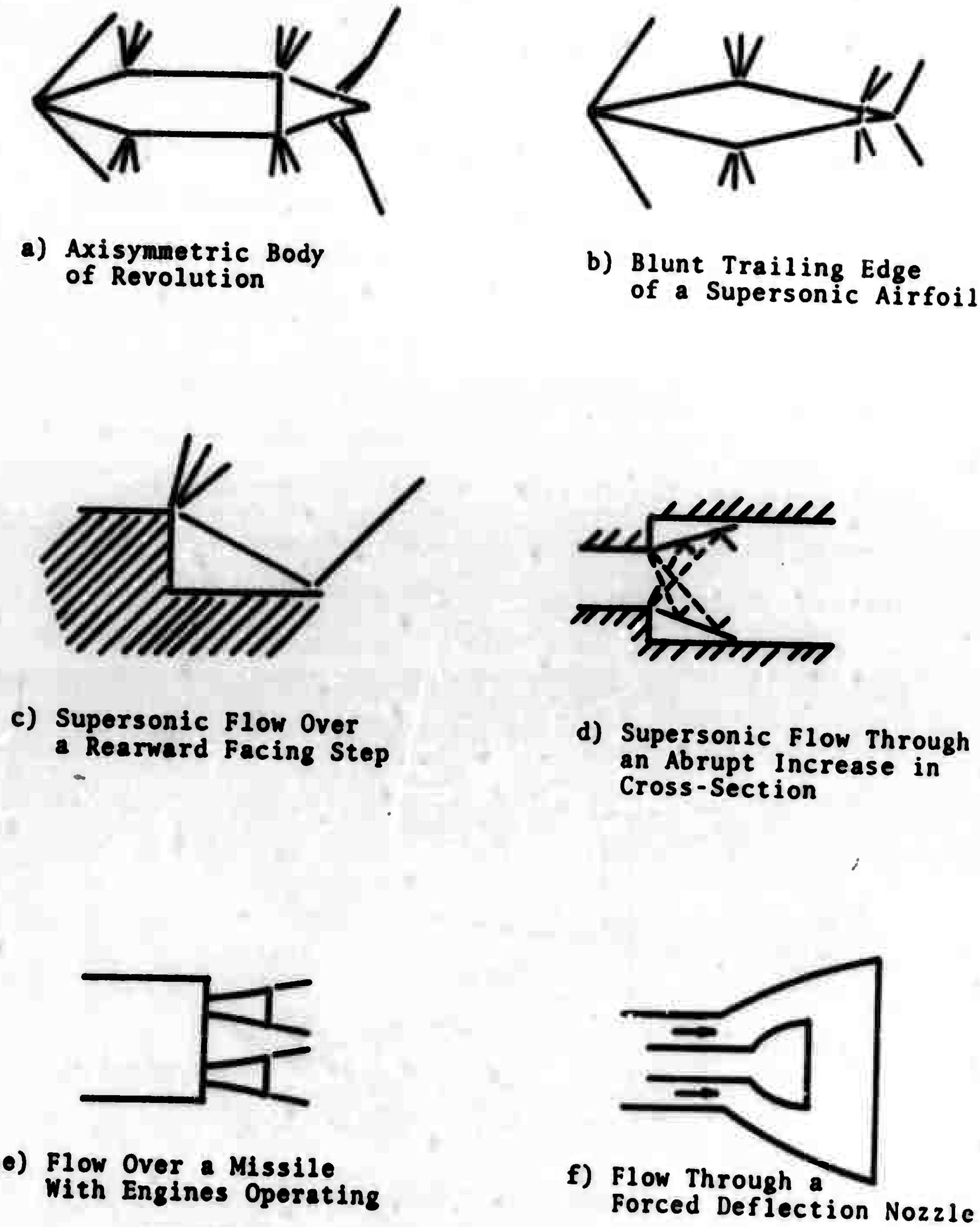

FIGURE G-1. TYPICAL FLOW CONFIGURATIONS FOR BASE PRESSURE PROBLEMS

In more recent years other base pressure problems such as those depicted in Figure G-1e and G-1f have received attention.

The next few paragraphs will be devoted to a discussion of two-dimensional flow. The conceptual model used here can be applied to the axisymmetric case.

1. FLOW DESCRIPTION

a. Two-Dimensional Flow. As in any problem of this nature it is necessary to have a model which accurately represents the actual flow. Figure G-2 depicts the Chapman-Korst model which is frequently used to describe the flow in the base region. The general features of the flow were first described by Chapman(20) and extended

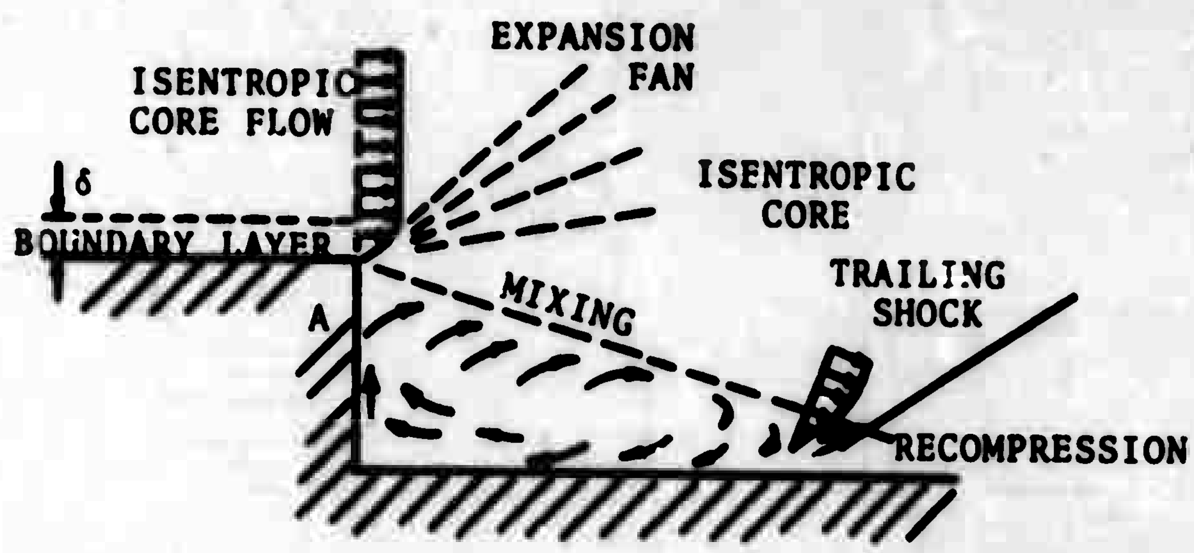

FIGURE G-2. CHAPMAN-KORST MODEL OF SEPARATED FLOW

by Korst(21) in order to formulate an energetic criterion for penetration into the high pressure region of the

wake throat.

The flow, with boundary layer thickness δ, expands around the corner A and separates from the surface at that point. The interaction of the external inviscid flow and the internal dissipative region produces a circular motion of the fluid in the base region and an inherent decrease of base pressure. The flow is deflected towards the surface of the afterbody due to the lower pressure in this region and then must be recompressed as the afterbody surface is reached. The recompression produces waves, as shown in Figure G-2, which coalesce to form the trailing edge shock just downstream of the wake throat. The fluid entrained by the internal flow near the base is returned to the separated flow region near the wake throat. This flow characteristic satisfies the conservation of mass requirement in the base region and helps to define the dividing streamline which is considered to originate at the corner and stagnate at a point near the wake throat. The pressure across the base is considered to be constant. Experimental studies indicate that the pressure downstream of the base region is nearly constant and equal to that on the base for distances up to one half the length of the separated flow region (21).

Each of the characteristics of this model warrant individual attention and discussion in light of the experimental evidence. However, since it is not intended to

solve the base pressure problem here it suffices to say that certain aspects of this model have recently been subject to criticism (22,23).

The flow in plug nozzles is axisymmetric, and there are some significant differences between two-dimensional and axisymmetric flows which should be noted.

b. Axisymmetric Flow. As mentioned earlier the conceptual model used for two-dimensional flow can be applied to the axisymmetric case; i.e., a meridian section of an axisymmetric body would appear exactly as depicted in Figure G-2 for the two-dimensional case. Since plug nozzles do not have an afterbody or sting as shown in Figure G-2, the discussion here will be directed to the no sting situation. Thus, recompression begins to occur as the fluid from opposite sides of the body converge instead of approaching an afterbody surface.

The expansion about the corner at the base of an axisymmetric body is not expected to be the same as for the two-dimensional case. This expansion in two-dimensional flow is frequently taken to be the Prandtl-Meyer expansion-even though there are indications that this is incorrect (22).

The wake flow also has some differences as one might expect. The converging wake in axisymmetric flow is essentially conical and must experience a pressure increase along the cone's surface. This is not the case for

two-dimensional flow where flow along the converging portion of the wake produces no change in pressure. As mentioned by Mueller (24) the pressure increase measured along the axis of the separated flow region is greater behind axisymmetric bodies.

In addition to being axisymmetric, plug nozzle flow is also expected to be turbulent and any adequate theory must give this consideration.

c. Turbulent Flow. It has been shown that the boundary layer profile at separation has a considerable influence upon the wake evolution (25). Thus, a turbulent profile at separation could be expected to influence the base pressure. Crocco and Lees (26) state that one of the major differences between laminar and turbulent flows is the mixing rate. Turbulent mixing rates are from five to ten times larger than laminar mixing rates. The survey article by Lykoudis (27) contains further discussion and references on this topic.

2. BASE PRESSURE DETERMINATION

A review of the literature reveals that methods are available for predicting the base pressure in a turbulent axisymmetric flow. The survey article by Sedney (28) contains a large collection of the references on the base pressure problem. The more recent paper by Mueller (24) enumerates seven methods of calculating the base pressure in this type of flow and adds his own method to bring the

total to eight. None of these methods have direct application to plug nozzles since they assume a uniform axial flow upstream of the plug base. Mueller applies his method to an ideal forced-deflection nozzle by selecting the proper reference conditions but it is unlikely that this could be done in the case of a plug nozzle.

It is also known that methods which are probably more directly applicable have been developed by the industry but have not as yet appeared in the unclassified literature. Work of this nature has been and is being conducted at Rocketdyne (29). Personal conversations with Mr. Grant A. Hosack of that company reveal that all of the details of their methods may not be available even in a classified form since part of the work was done on independent research and development funds. Pratt and Whitney along with General Electric (30) has also been active in this field. A program is in existence at Pratt and Whitney for base pressure calculations in plug nozzles (31).

Even though methods are available for base pressure determination, it is desirable, in the thrust optimization of plug nozzles, to have an analytical expression for base pressure in terms of the upstream flow properties. An expression of this type lends itself to the rapid interaction techniques necessary to this optimization method. Rom (32) has reported empirical expressions for the base pressure in two-dimensional laminar and turbulent flows for backward facing steps and base flows. He points out

that axisymmetric base flows cannot be treated by a simple modification of the two-dimensional analysis because of the difference in the interaction between the external inviscid flow and the viscous mixing region. Rom's attempt to obtain an analytical expression for base pressure is apparently the first to meet with any degree of success and appear in the literature.

3. EQUATION FOR BASE PRESSURE

It is not intended to investigate the validity of the various methods used to compute p_b, but rather to be able to calculate a representative value of base pressure in order that its effect upon the optimization can be demonstrated. It was found that a curve fit of experimental data would serve this purpose. Reference (32) contains a plot which shows the effect of the local Mach number at separation on the base pressure. This experimental data can be represented by the empirical equation

$$p_b = 0.846\ p/M^{1.3} \qquad \text{(G-1)}$$

where p and M are the local values of pressure and Mach number at separation. Equation (G-1) has been incorporated into the computer program for base pressure calculations. In order to determine the importance of accurate base pressure calculations in plug nozzle optimization, an alternate empirical equation for base pressure was obtained from Reference (33). This equation is

$$p_b = p_\infty[1 - .715\gamma(M_\infty^{2.3} - 0.92M_\infty^2 - 0.03)/M_\infty^{2.7}] \quad \text{(G-2)}$$

where p_∞ and M_∞ are free stream values of pressure and Mach number. Since Eq.(G-2) is based upon free stream conditions rather local conditions at separation, it is not expected that base pressures calculated from this equation will accurately represent those occurring in plug nozzles. However, as shown in Section V, it illustrates the importance of calculating the base pressure accurately. Equations (G-1) and (G-2) are plotted as a function of Mach number in Figure G-3.

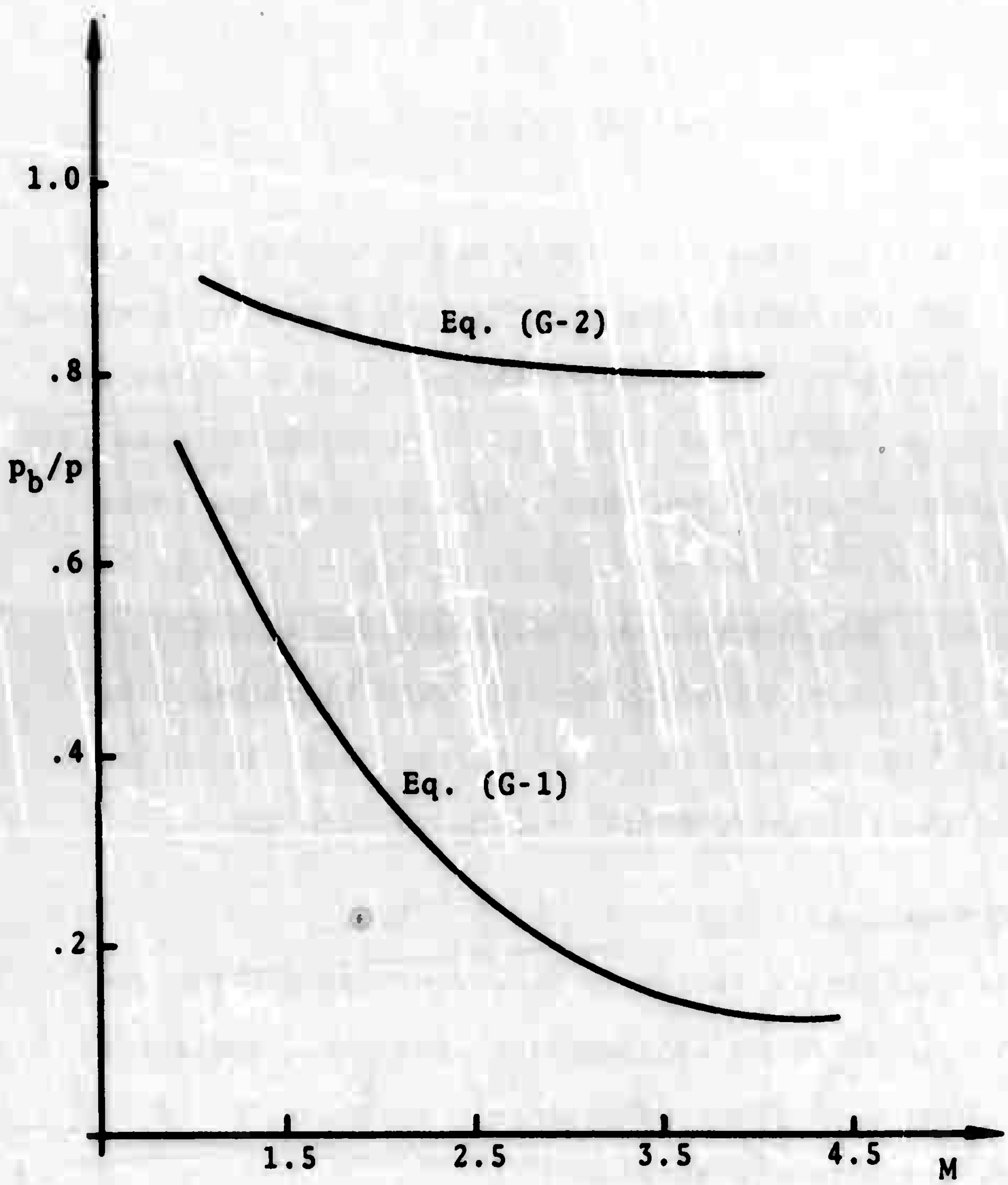

FIGURE G-3. BASE PRESSURE AS A FUNCTION OF MACH NUMBER

APPENDIX H

TRANSONIC FLOW ANALYSIS

An initial-value line, along which the velocity components and thermodynamic properties are known, is required in order to start the method of characteristics solution for the flow field. The start line can either be read into the computer program from data cards or generated internally if the nozzle being analyzed is for a subsonic burning engine. The internally generated start line is obtained from a modified Moore-Hall (16) transonic flow analysis. The results of their analysis will be outlined here and the necessary modifications pointed out.

1. MOORE-HALL ANALYSIS

The coordinate system is shown in Figure H-1. The flow is assumed to be axisymmetric, inviscid, and irrotational. The applicable equations in terms of the (X,Y) coordinate system are given as

$$\frac{\partial V}{\partial x} - \frac{\partial U}{\partial y} = 0 \tag{H-1}$$

$$\frac{1}{\rho}\frac{\partial(\rho U)}{\partial x} + \frac{1}{\rho}\frac{\partial(\rho V)}{\partial y} + \frac{V}{y} = 0 \tag{H-2}$$

$$a^2 = \frac{\gamma + 1}{2} a^{*2} - \frac{\gamma - 1}{2}(U^2 + V^2) \tag{H-3}$$

where a* is the critical speed of sound. Since the boundary conditions are complicated in the (X,Y) coordinate system the problem is transformed to the (x,y) system and the solution is then given in terms of the (x,y) system.

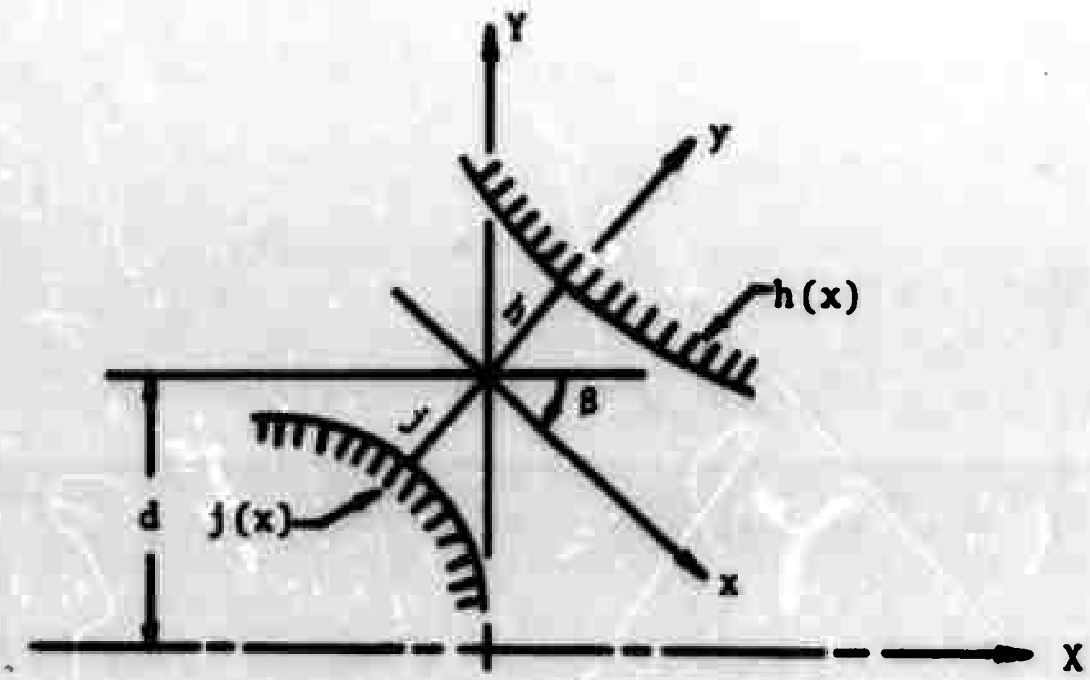

FIGURE H-1. COORDINATE SYSTEM FOR TRANSONIC FLOW ANALYSIS

The velocity components are given as u and v but are written in a non-dimensional form as

$$\frac{u}{a^*} = 1 + u'$$

$$\frac{v}{a^*} = v' \tag{H-4}$$

Without loss of generality the origin is taken to be at the minimum cross-sectional area (throat) and the throat half-height to be unity. The axis is oriented so that the wall slopes at x = 0 are equal in magnitude but opposite in sign. The equations which describe the upper and lower

nozzle walls are written in terms of a MacLaurin's series. These equations are

$$h(x) = 1 - m' x + \frac{1 + \eta}{2} m'' x^2 + \cdots$$

$$j(x) = 1 + m' x + \frac{1 - \eta}{2} m'' x^2 + \cdots \qquad \text{(H-5)}$$

where

$$\frac{dh(o)}{dx} = - m'$$

$$\frac{dj(o)}{dx} = m'$$

$$(1 + \eta)m'' = d^2h(o)/dx^2$$

$$(1 - \eta)m'' = d^2j(o)/dx^2$$

with η representing the asymmetry of the nozzle profile and m" a mean radius of curvature. As a boundary condition, the flow is required to be parallel to the walls. This condition at the outer and inner walls can be written as

$$v' (x,h) = [1 + u'(x,h)]dh/dx$$

$$-v'(x,h) = [1 + u'(x, - j)]dj/dx$$

The quantities x and m' are replaced by εz and εm where $\varepsilon = R^{-1/2}$, m is a quantity of order unity, and R is a non-dimensional radius of curvature of a meridian section at the throat. The velocity components are then sought as series expansions in powers of ε. Thus,

$$u' = u_1\varepsilon^2 + u_2\varepsilon^3 + \cdots$$

$$v' = my\varepsilon + m^2\varepsilon^2(y^2 - 1)\text{ctn }\beta + v_1\varepsilon^3 + v_2\varepsilon^4 + \cdots$$

These equations are substituted into the flow equations and the boundary conditions are required to hold. This results in an infinite sequence of pairs of differential equations, the first of which is solved. The solution can be written in the form

$$v_1 = A_0'(y) + zA_1'(y)$$

$$u_1 = A_1(y) + B_0 + B_1 z \qquad \text{(II-6)}$$

where

$$B_1^2 = (1 - \psi)(1/2 - m^2)$$

$$B_0 = (1 - \psi)m/4B_1 - (1 - \psi)m^3/6B_1 - 1/6$$

$$A_1(y) = (1 - mB_1 - m^2)y^2/2 + \eta y$$

$$A_0'(y) = K_0 + K_1 y + K_2 y^2/2 + K_3 y^3/3$$

$$K_0 = m\eta/2 - B_1\eta/(1 - \psi)$$

$$K_1 = 2B_0B_1/(1 - \psi) - mB_0 + m^3 \mathrm{ctn}^3\beta$$

$$K_2 = 2B_1\eta/(1 - \psi) - 3m\eta$$

$$K_3 = B_1/(1 - \psi) + 3m^2B_1/2 - 3m + 5m^3/2 - 3m^3 \mathrm{ctn}^2\beta$$

$$A_1'(y) = \partial A_1(y)/\partial y$$

The equation for the sonic line is obtained by using the following equation for total velocity

$$q^2 = u^2 + v^2$$

and

$$M^{*2} = q^2/a^{*2} = (1 + u')^2 + (v')^2$$

$$M^{*2} = 1 + 2u' + (u')^2 + (v')^2$$

Since

$$u' = u_1\varepsilon^2 + \cdots \qquad \text{(H-7)}$$

and

$$v' = -my\varepsilon + m^2\varepsilon^2(y^2 - 1)\text{ctn } \beta + v_1\varepsilon^3 + \cdots \qquad \text{(H-8)}$$

this equation becomes

$$M^{*2} = 1 + (u_1 + m^2y^2/2)\varepsilon^2 + O(\varepsilon^3) \qquad \text{(H-9)}$$

When the Mach number is one, $M^* = 1$, and the remaining terms must vanish. Thus

$$Q = u_1 + m^2y^2/2 = 0 \qquad \text{(H-10)}$$

and the equation for u_1 provides sufficient information to locate the sonic line.

$$z = (Q - A_1 - B_0 - m^2y^2/2)/B_1 + O(\varepsilon) \qquad \text{(H-11)}$$

When $Q = 0$ the above equation locates the sonic line and when Q is greater than zero it locates lines of constant Mach number.

The flow direction relative to the x-axis is θ, where

$$\theta = \tan^{-1} \frac{v'}{1 + u'}$$

2. MODIFICATIONS TO THE MOORE-HALL ANALYSIS

It was found upon programming that the equation given for the sonic line did not yield a local Mach number of unity at all points. This was due to the terms of order ε^3 and higher which were dropped from Eq. (H-9). Once

the definitions of u' and v' have been established all of the terms must be retained. Thus, Eq. (H-9) should be written as

$$M^{*2} = 1 + 2(u_1 + m^2y^2/2)\varepsilon^2 - 2[m^3y(y^2 - 1)\text{ctn}\ \beta]\varepsilon^3$$
$$+ 2[u_1^2/2 - v_1my + m^4(y^2 - 1)^2\text{ctn}^2\beta/2]\varepsilon^4$$
$$+ 2[v_1m^2(y^2 - 1)\text{ctn}\ \beta]\varepsilon^5 + v_1^2\varepsilon^6 \qquad \text{(H-12)}$$

and Eq. (H-10) as

$$Q = u_1 + m^2y^2/2 - [m^3y(y^2 - 1)\text{ctn}\ \beta]\varepsilon$$
$$+ [u_1^2/2 - v_1my + m^4(y^2 - 1)^2\text{ctn}^2\beta/2]\varepsilon^2$$
$$+ [v_1m^2(y^2 - 1)\text{ctn}\ \beta]\varepsilon^3 + v_1^2\varepsilon^4/2 \qquad \text{(H-13)}$$

Again when $Q = 0$, $M^* = 1$. Thus, when Eqs. (H-6) are substituted into (H-13) the equation of the sonic line results. It was found that this procedure resulted in the local Mach number, M, being unity at every point along the sonic line. Values of Q greater than zero yield the equations of lines of constant Mach number.

A second problem was encountered when an attempt was made to initiate a method of characteristics solution from a line of constant Mach number which passed through the wall points h(1) and j(-1). This particular line was chosen since the flow matches the wall at only these two points. It was found that this line was not a space-like curve, or some of the points on this line lie within the zone of influence of neighboring points. That is, some

points lie within the Mach cone of neighboring points. This is shown schematically in Figure H-2 where point 2 lies in the zone of influence of point 1. Two things were done to minimize this problem. It was found that the

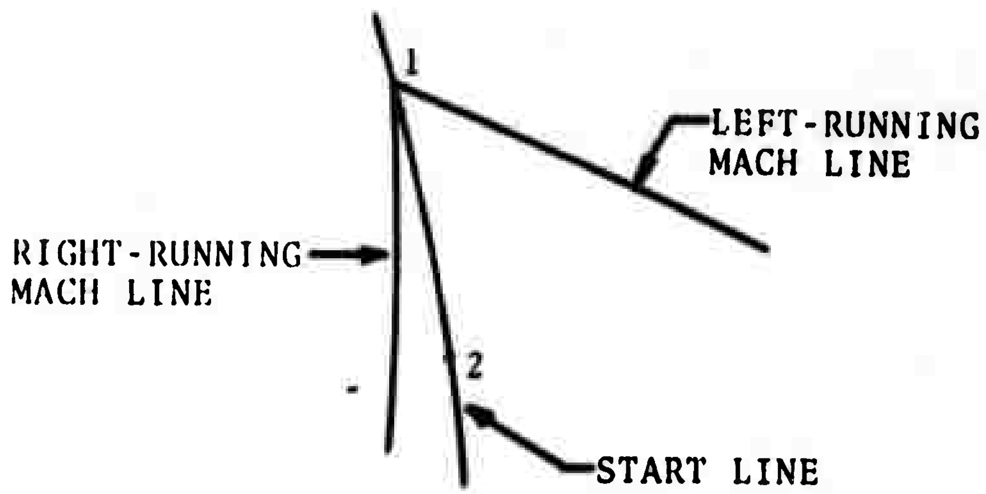

FIGURE H-2. ZONE OF INFLUENCE IN SUPERSONIC FLOW

flow properties could be evaluated along two straight lines passing through h(1) and j(-1) and intersecting at a chosen place on the x-axis. Thus, it was possible to vary the slopes of these two lines and in so doing minimize the number of points lying in the zone of influence of another point. Also, right characteristics were not started from those points which had other points in their zone of influence. This produced very little error since the right characteristics normally pass very close to the neighboring points in this region.

APPENDIX I

WALL SHEAR MODEL

The optimization problem formulated in Section III requires the calculation of the boundary layer thickness and the wall shear. However, the computer program which solves the resulting design equations only accounts for the wall shear. The correction for boundary layer thickness can be made to the optimized contour by using the boundary layer thickness to adjust the wall coordinates. The purpose here is to discuss briefly the wall shear model which has been incorporated into the computer program to evaluate the wall shear.

The shearing stress at the wall is given by Newton's law of friction as

$$\tau = \mu(\partial u/\partial y)_{y=0} \tag{I-1}$$

which requires the evaluation of the velocity gradient normal to the wall. This can be a very difficult task in the case of plug nozzles since 1) the boundary layer is expected to be turbulent, 2) compressibility effects are important, 3) heat transfer to the wall must be considered, and 4) the favorable free stream pressure gradient must be taken into

account. Numerous methods can be found in the literature for evaluating the wall shear stress. Since it was not intended to investigate the validity of the many boundary layer methods used to compute the shear stress, an alternate approach was taken for calculation purposes. The shear stress was written as

$$\tau = c_f \rho V^2/2 \tag{I-2}$$

where c_f, ρ, and V are the local values of the skin friction coefficient, density, and velocity. It then remains to find an expression for c_f which can be used in the optimization analysis and which gives reasonably accurate values for the local skin friction coefficient expected in plug nozzles. An expression obtained by Liepman and Goddard (35) for compressible, turbulent flow over a flat plate was selected for this purpose. This expression is

$$c_f = c_{f_i}/[1 + r(\gamma - 1)M^2/2] \tag{I-3}$$

where c_{f_i} is the incompressible skin friction coefficient and r is the recovery factor. A representative value of the recovery factor was chosen as 0.72 and c_{f_i} is an input parameter to the computer program. It should be emphasized that the optimization process is not restricted to this or any other wall shear model. Any desired model can be incorporated into subprogram SKIN which is described in Appendix J.

APPENDIX J

COMPUTER PROGRAM DESCRIPTION

The program was written in the Fortran IV language and has been run on the CDC 6500 and IBM 7094 computers at Purdue University and the Burroughs 5500 computer at the United States Air Force Academy. The program fits entirely in the core of these machines without an overlay scheme. It is composed of a main program and fifteen subprograms whose functions are described here. The input and output parameters are discussed in Appendix K with a complete program listing in Appendix L.

1. MAIN PROGRAM

The primary purpose of the main program is to control the program logic even though it contains some calculations. The key functions of the main program are shown in Figure J-1 with the subprograms involved being indicated at the bottom of each block. These subprograms may in turn call upon other subprograms which are not indicated. The main program also reads in all the input data which are discussed in a later section.

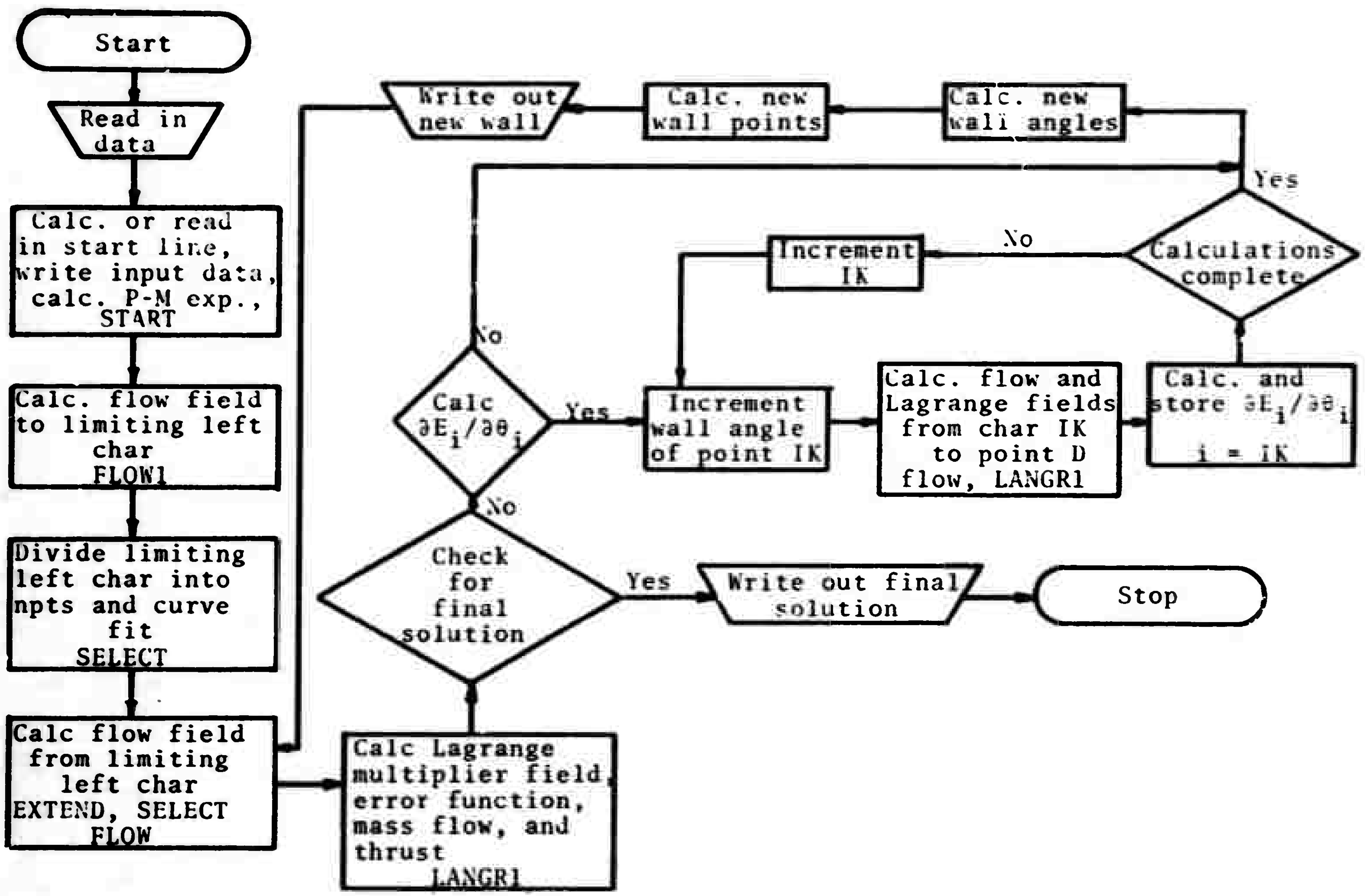

FIGURE J-1. MAIN PROGRAM FLOW CHART

2. SUBPROGRAMS

a. Subprogram START. Subprogram START performs several functions. It first calculates the start line by either a modified Moore-Hall analysis or a simple isentropic analysis along a straight line of constant Mach number. At the same time it calculates the thrust and mass flow rate along the initial-value line. If the start line data are read in, the thrust and mass flow rate along this line will also be calculated. If the mass flow rate is not the specified value, FLRTC, and the start line is generated internally, an option can be selected which modifies the throat half-height to obtain the correct mass flow rate. Then the start line solution is written out. Once the start line is complete the Prandtl-Meyer expansion at point E' (Figure 3) is calculated and written out. The expansion is allowed to continue until either the ambient pressure is reached or the last right characteristic generated from E' has a direction parallel to the center line at that point. Finally, the first guess for the optimum contour, which may be read in or generated internally, is written out.

b. Subprogram FLOW1. This subprogram performs one basic function. It calculates the flow field in the region between the start line and exit characteristic DE down to the left characteristic which originates at point A (Figure 3). It makes use of Subprogram QUAD to determine

whether or not points on the start line lie within the zone of influence of each other. Right characteristics are not initiated from those points which have other points in their zone of influence. The output from this subprogram is written out along the right characteristics as the calculations proceed from left to right starting at point A.

c. Subprogram SELECT. Subprogram SELECT divides the left-characteristic which originates at point T (Figure 3) into (NPTS-1) points and curve fits the flow data along this line. This process may involve all or a portion of the data points along the characteristic. Any portion of the (NPTS-1) points designated by (NS-1) can have a reduced spacing determined by dividing the spacing the points would have if all (NPTS-1) points were spaced equally by the factor CS. The remaining (NPTS-NS) points have equal spacing.

d. Subprogram EXTEND. This subprogram extends the flow field calculations from the left characteristic originating at point A down to the left characteristic originating at point T. It also calculates the thrust contribution due to that portion of the plug surface between points A and T. The output from this subprogram is written out along the left characteristics as the calculations proceed downward from point A to point T.

e. Subprogram FLOW. This subprogram calculates the flow field in the region (R). Calculations begin on and are carried out down the right characteristic designated by the subprogram variable NZ. NZ = 1 corresponds to point T and NZ = NPTS corresponds to the exit characteristic DE. The output from this subprogram is written out along the right characteristics as the calculations proceed from left to right starting at the point designated by NZ.

f. Subprogram LANGR1. This subprogram calculates the Lagrange multipliers in the region (R), calculates the thrust developed by the plug surface between points T and D and the total thrust, and evaluates the error function along the right characteristic DE. The Lagrange multipliers calculated by this subprogram are written out along the right characteristics as the calculations proceed from left to right starting from the same point as in FLOW.

g. Subprogram CHAR1. This subprogram is an iteration procedure which solves the flow field characteristic and compatibility equations which, in finite difference form, are

$$y_3 - y_1 = (x_3 - x_1)\tan(\theta_{13} - \alpha_{13}) \tag{J-1}$$

$$y_3 - y_2 = (x_3 - x_2)\tan(\theta_{23} + \alpha_{23}) \tag{J-2}$$

$$(\theta_3 - \theta_1) + Q_{13}(V_3 - V_1) - G_{13}(y_3 - y_1)/y_{13} = 0 \tag{J-3}$$

$$(\theta_3 - \theta_2) - Q_{23}(V_3 - V_2) + F_{23}(y_3 - y_2)/y_{23} = 0 \tag{J-4}$$

The double subscript indicates the average value of the

parameter between the two points and

$$Q_{13} = \text{ctn}\ \alpha_{13}/V_{13}$$

$$Q_{23} = \text{ctn}\ \alpha_{23}/V_{23}$$

$$G_{13} = \sin\theta_{13}\sin\alpha_{13}/\sin(\theta_{13} - \alpha_{13})$$

$$F_{23} = \sin\theta_{23}\sin\alpha_{23}/\sin(\theta_{23} + \alpha_{23})$$

The points 1 and 2 are assumed to be known and the procedure solves for the location and flow properties at point 3. This is shown schematically in Figure J-2.

h. Subprogram SURF. This subprogram finds the point where a right characteristic intersects the plug surface TD. Since the wall location and slope are known it is only necessary to satisfy Eqs. (J-1) and (J-3). The location and flow properties at point 1, shown in Figure J-3, are assumed to be known and the location and velocity at point 3 are found.

i. Subprogram LOCAT. This subprogram performs a similar function to that of subprogram SURF. Here it is desired to start from a point on the plug surface where the location and flow angle are known and extend a right characteristic to a known left characteristic. Thus, it is desired to find the velocity at point 1 shown in Figure J-4 and the location and flow properties at point 3. In general, interpolation along the known left characteristic is required.

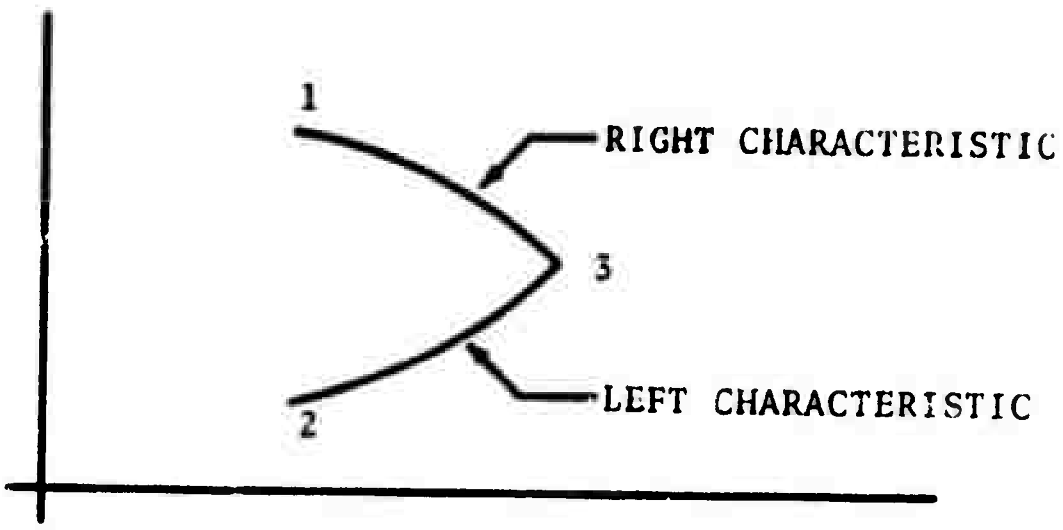

FIGURE J-2. CHARACTERISTIC NET LABELING
FOR SUBPROGRAM CHAR1

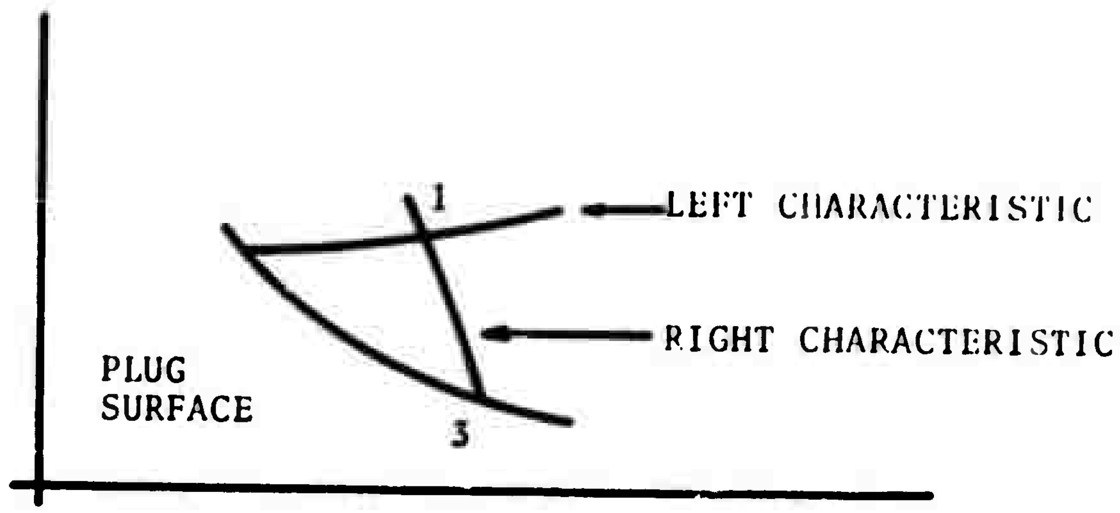

FIGURE J-3. WALL POINT LABELING
FOR SUBPROGRAM SURF

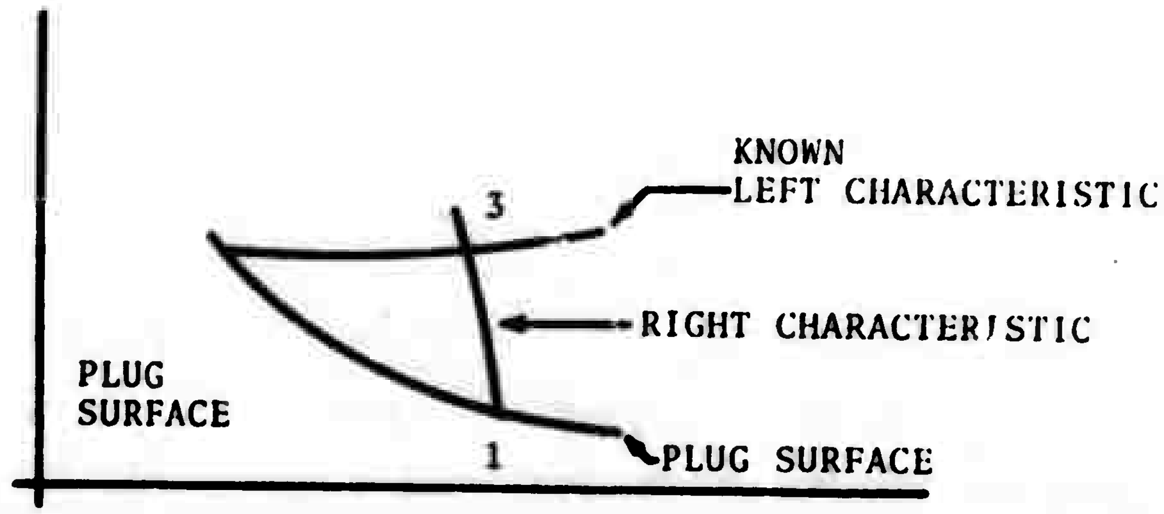

FIGURE J-4. WALL POINT LABELING
FOR SUBPROGRAM LOCAT

j. Subprogram SKIN. This subprogram calculates the wall shear stress at a given point on the plug surface using the equation

$$\tau = \frac{1}{2} C_f \rho V^2 \tag{J-5}$$

where

$$C_f = C_{f_i} / [1 + .72(\gamma - 1)M^2/2]^{.578}$$

The incompressible coefficient of friction, C_{f_i}, is constant and is an input parameter to the program. The input arguments to SKIN are the local Mach number and velocity and the incompressible coefficient of friction. The output argument is the value of τ. This subprogram could be easily modified to incorporate any desired wall shear model.

k. Subprogram BASE. Subprogram BASE calculates the base pressure using the empirical equation

$$p_b = Ap/M^B \tag{J-6}$$

where the constants A and B are program input parameters. The input arguments to BASE are the x and y coordinates and the local Mach number and velocity. The output arguments are p_b and $y\, p_b$. This subprogram could also be modified to incorporate any desired base pressure model.

l. Subprogram REST. This subprogram evaluates the general isoperimetric constraint g and its derivatives g_p, g_y, $g_{\dot{y}}$, and $d(g_{\dot{y}})/dx$. Since this constraint was taken

to be one which requires the nozzle to have a fixed length, $g = 1$, and all the derivatives are zero. Currently there are no required input arguments to BASE and the output arguments are g, g_p, g_y, $g_{\dot{y}}$, and $dg_{\dot{y}}/dx$. This subprogram could be changed to include other constraints such as constant wetted area by setting

$$g = y\ (1 + \dot{y}^2) \tag{J-7}$$

$$g_p = 0 \tag{J-8}$$

$$g_y = 1 + \dot{y}^2 \tag{J-9}$$

$$g_{\dot{y}} = 2y\dot{y} \tag{J-10}$$

$$\frac{d}{dx}\, g_{\dot{y}} = 2(y\ddot{y} + y^2) \tag{J-11}$$

m. Subprogram QUAD. This subprogram simply determines the angular location of one point with respect to another. It is used in subprogram FLOW1 to help determine if a point on the start line lies within the zone of influence of another.

n. Subprogram LSQUARE. This subprogram determines the constants A and B for a least squares fit of data to a straight line whose equation is

$y = Ax + B$

o. Subprogram AITKEN. This is an interplating subprogram which uses Aitken's method of interpolation. The maximum degree of the interpolating polynomial is 10.

APPENDIX K

COMPUTER PROGRAM OPERATION

The program input-output parameters are discussed in this Appendix and are illustrated by means of two sample cases. The program failure modes and flags are also discussed.

1. PROGRAM INPUT

The program input parameters are read in from data cards by the main program. All of the input parameters are identified here in the order in which they appear in the data deck and are discussed as necessary.

Card 1 FORMAT (12A6)

This card contains 72 characters of identifying information which is written out on the first page of the computer output.

Card 2 FORMAT (9F8.0)

This card contains the engine operating conditions and information for the first guess of the plug surface.

PA Atmospheric pressure (lbf/in^2).

PO Chamber pressure (lbf/in^2).

TO Chamber temperature (°R).

R Gas constant (ft - lbf/lbm - °R).

G Ratio of specific heats (non-dimensional).

FLRTC Desired mass flow rate (lbm/sec).

XLENG Desired length of the plug surface (in).

YLAST The estimate for y_D (in) when the first guess of the plug surface is generated internally.

TLAST The estimate for the wall slope (degrees) at point D when the first guess of the plug surface is generated internally.

Card 3 FORMAT (7F10.0)

These data are concerned with the specification of the throat geometry and start line. Appendix G contains a detailed discussion of these parameters.

HO Throat half-height (in).

RE Cowl lip radius (in).

BD Mean flow angle at the throat (degrees).

RRE The mean radius of curvature of the nozzle walls at the throat (in).

EPS Velocity component expansion parameter = $R^{-1/2}$ (nondimensional).

CENTM Desired Mach number along the start line at the throat center-line or the Mach number along the linear, internally generated start line.

RHOD The downstream radius of curvature of the plug surface (in).

Card 4 FORMAT (14I5)

This card contains integer parameters for controlling the numerical algorithm.

NPTSL	Desired number of points on the start line or the number of points on the start line to be read in (maximum = 100). Typically 31.
NPTS	Number of points on the portion of the plug surface to be optimized (maximum = 50). Typically 50.
NDEGR1	Degree of the interpolating polyromial used for interpolation of the data along the left characteristic originating at point T in subprograms SELECT and EXTEND (maximum = 10). Typically 1.
NDEGR2	Degree of the interpolating polynomial used in subprogram SURF (maximum = 10). Typically 1.
NDERMX	Number of iterations before recalculating the partial derivatives, $\partial E/\partial \theta$. Typically 5.
NPTSS	One plus the number of wall points to be read in as the first guess for the optimum surface (maximum = 200). Should be at least 15.
NS	Number of points which are to have reduced spacing along the left characteristic originating at point T. NS = 1 if all points are to have equal spacing. Generally less than 10.

NWRITE Controls the output. NWRITE = 1: all calculations are written out; NWRITE = 0: limited output as described in the next section.

NCNT The desired number of points of the internally generated first guess for the optimum surface which are to be on the arc of a circle of radius RHOD. Typically 5.

NREAD1 0: Read in 2 through NPTSS data points as the first guess for the optimum surface. The first point corresponds to the lowest point on the start line and need not be read in.
1: Generate the first guess for the optimum surface internally.

NREAD2 0: If other than a Moore-Hall start line is desired. 1: If a Moore-Hall start line is desired.

OPT1 0: To analyze a given plug contour. 1: To obtain the optimum contour.

OPT2 0: Read in NPTSL data point for the start line.
1: Generate a linear start line internally.

OPT3 0: HO is fixed at the value read in. 1: Change HO to obtain the desired mass flow rate.

Card 5 FORMAT (9F8.0)

This card contains more information for the control of the numerical algorithm.

DELTPM The Mach number increment for the Prandtl-Meyer expansion at point E'. Typically .05.

CFI Incompressible flow coefficient of friction. Typically .003 to .008. CFI = 0.0 if wall shear is to be zero.

ERR The acceptable error along the exit characteristic. Typically 0.001.

WEIGHT The weighting factor applied to changes in the wall angle. Typically 0.85.

DELTAT Wall angle increment from point A to T. Used in generating the first guess for the optimum surface and also in the optimization process. Typically 0.5 degrees.

CS The factor used to reduce the spacing of the points along the left characteristic originating at point T. The discussion of subprogram SELECT contains additional information about CS. CS = 1 if all points are to have equal spacing.

AA Constant coefficient used to calculate the base pressure in subprogram BASE. Typically 0.846.

AB The exponent of the Mach number used to calculate the base pressure in subprogram base. Typically 1.3.

THETAC The decrease in the flow angle (degrees) across the throat. Used when the linear start line is generated internally. Typically 6.0.

Cards 6 FORMAT (3F10.0)

These are (NPTSS-1) cards containing the data for the first estimate of the optimum plug contour. I = 1 corresponds to point A shown in Figure 3 and this data point is not read in since it is included in the start line data.

XS(I) Ith value of the x-coordinate (in).

RS(I) Ith value of the y-coordinate (in).

TS(I) Ith value of the wall angle (degrees).

Cards 7 FORMAT (5F10.0)

These are NPTSL cards containing the data for the start line if it is to be read in. I = 1 corresponds to point A shown in Figure 3.

XL (I) Ith value of the x-coordinate (in).

RL (I) Ith value of the y-coordinate (in).

ML (I) Ith value of the Mach number.

VL (I) Ith value of the velocity (ft/sec).

TL (I) Ith value of the flow angle (degrees).

2. PROGRAM OUTPUT

The only program output control is the input parameter NWRITE. The value of NWRITE determines whether or not the flow properties and Lagrange multipliers at each point in the flow field will be written out. These are written out as the calculations are made in subprograms FLOW1, EXTEND, FLOW, and LANGR1. The order in which the output appears is explained in the descriptions of the

subprograms in Appendix I.

Portions of the output are printed independent of the value of NWRITE. These data include all input data, the start line, throat half-height, Prandtl-Meyer expansion, first guess for the optimum surface, Lagrange multipliers along the wall, error along the exit characteristic, calculated and adjusted partial derivatives ($\partial E/\partial \theta$), new wall contour, final wall contour, thrust (lbf), mass flow rate (lbm/sec), specific impulse (lbf-sec/lbm), flow injection angle (degrees), and the ambient pressure (lbf/in^2).

3. SAMPLE CASES

In this section the input data and selected program output sheets are presented for two sample cases.

a. Sample Case Number One. For this case, it is desired to obtain the optimum plug contour for a nozzle which has a fixed length XLENG = 12.0 in., a cowl lip radius RE = 8.34612 in., an injection angle BD = -45.0°, a downstream radius of curvature RHOD = 0.5 in., a mean radius of curvature RRE = 0.705 in., and no asymmetry which implies that ETA = 0.0. The engine is assumed to operate with a chamber pressure PO = 500. psia and a chamber temperature TO = 6000°R. The exhaust products are assumed to have a gas constant of R = 56.0 (ft - lbf)/(lbm - °R) and a ratio of specific heats G = 1.23. The nozzle is to be designed for an ambient pressure PA = 14.7 psia

and to have a mass flow FLRTC = 148.077 lbm/sec. The throat half-height which will pass this mass flow rate is estimated to be HO = 0.4155 in. The y coordinate of point D and the wall slope at that point are estimated to be YLAST = 1.75 in. and TLAST = -13.00°.

The Moore-Hall start line analysis is to be used and the throat half-height is to be modified to obtain the desired mass flow rate. This requires that OPT2 = 1, NREAD2 = 1, and OPT3 = 1. The Mach number at the throat center line is chosen as CENTM = 1.1. A total of 15 data points are to be generated along the start line so that NPTSL = 15. It is desired to have the maximum number of points on the plug surface which is to be optimized so that NPTS = 50. NDEGR1 and NDEGR2 are both set equal to 1. Ten points along the left characteristic originating at point T are to have their spacing reduced by a factor of two, thus NS = 10 and CS = 2.0. It is desired to have the partial derivatives, $\partial E/\partial \theta$, recalculated after every six iterations so that NDERMX = 6. The first guess for the optimum surface is to be generated internally with a total of 17 data points. Five of these points are to be located on the circular arc whose radius is RHOD. Consequently, NPTSS = 17, NCNT = 5, and NREAD1 = 1. Since the optimization analysis is to be carried out OPT1 = 1. NWRITE is set equal to 0 so that the flow field and Lagrange multiplier fields will be written out in limited form.

The Mach number increment for the Prandtl-Meyer expansion at point E', the flow angle increment along the circular arc of radius RHOD, and the incompressible skin friction coefficient are selected as DELTPM = 0.05, DELTAT = 0.5, and CFI = 0.002. Values for ERR and WEIGHT are selected as 0.001 and 0.85, respectively. The constants for the base pressure model are AA = 0.846 and AB = 1.3. Finally, the decrease in the flow angle along the linear start line, THETAC, is arbitrarily set equal to zero since it is not used.

The input data sheet for this case is shown in Figure K-1 and typical program output is shown in Figure K-2.

b. Sample Case Number Two. This sample case is similar to the first but will illustrate the use of the linear start line. Only those input parameters which are different or not used will be pointed out.

Since the start line is to be linear, ETA and RRE will not be used but for convenience left at the same values as the previous case. CENTM now becomes the value of the Mach number along the entire start line and is given a value of 1.08. The linear start line option also requires that NREAD2 = 0. The flow angle decrease across the throat THETAC = 6.0°. The nozzle length, cowl lip radius, and injection angle are selected as XLENG = 10.0 in., RE = 9.5 in., and BD = - 50.0° The nozzle is to be

designed for an ambient pressure PA = 0.0. Limited program out is desired so that NWRITE = 0.

The input data sheet for this case is shown in Figure K-3 and typical program output is shown in Figure K-4.

4. FAILURE MODES

Only one primary failure mode has been observed in the program. If the first guess for the optimum surface is not smooth and compatible with the upstream geometry, the flow in the throat region may become subsonic and negative square roots will cause the program to stop. The program contains several other error checks and if a specific error is encountered an appropriate message is printed out. Since the program was found to have few error modes, the output control NWRITE was normally set equal to 0.

Card														
CARD 1	HEADER													
	SAMPLE CASE NO. 1													
CARD 2	PA	PØ	TØ	R	G	FLRTC	XLENG	YLAST	TLAST					
	14.7	500.0	6000.0	56.00	1.23	148.077	12.00	1.75	-13.00					
CARD 3	HØ	RE	BD	ETA	RRE	CENTM	RHØD							
	.4155	8.34612	-45.00	0.0	.705	1.1	0.5							
CARD 4	NPTSL	NPTS	NDEGR1	NDEGR2	NDERMX	NPTSS	NS	NWRITE	NCNT	NREAD1	NREAD2	ØPT1	ØPT2	ØPT3
	15	50	1	1	6	17	10	Ø	5	1	1	1	1	1
CARD 5	DELTPM	CFI	ERR	WEIGHT	DELTAT	CS	AA	AB	THETAC					
	0.05	0.002	0.002	0.85	0.5	2.0	0.846	1.3	0.0					

FIGURE K-1. INPUT DATA SHEET FOR SAMPLE CASE NO. 1

```
                         SAMPLE CASE NC. 1

                           INPUT DATA

       PA =    14.700  PC =   50C.00C  TC =  6CC0.COC  R =    56.000  G =     1.230
         FLRTC =    148.077  XLENG =    12.C00  YLAST =     1.750  TLAST =   -13.000

  MO = 0.41550  RE = 8.34612  BD =-45.0C00  ETA =0.      RRE =0.7050  CENTM =   1.10000  RHOD =   0.50C00

         NPTSL =  15  NPTS =  50  NDEGR1 =   1  NDEGR2 =   1  NDERMX =   6  NPTSS =  17  NS =  10
NWRITE =   0     NCNT =    5     NREAC1 =    1     NREAD2 =    1     CPT1 =    1     CPT2 =    1     OPT3 =    1

    DELTPM =  0.0500  CFI =  0.0020  ERR =  0.C010  WEIGHT =  0.8500  DELTAT =  0.5000  CS =  2.0000
                    AA =   0.8460     AB =   1.3000     THETAC =   0.
```

FIGURE K-2. SELECTED OUTPUT FOR SAMPLE CASE NO. 1

DATA FOR THE START LINE

XC (IN)	RC (IN)	MACH NUMBER	VELOCITY (FPS)	FLOW ANGLE (DEGREES)
-0.00000	8.34612	1.01918	3512.53018	-42.79400
-0.01429	8.27196	1.02682	3536.03900	-42.90326
-0.02859	8.19781	1.03573	3563.37405	-43.07355
-0.04288	8.12365	1.04593	3594.56052	-43.30770
-0.05718	8.04950	1.05745	3629.64050	-43.60805
-0.07147	7.97534	1.07031	3668.67572	-43.97642
-0.08577	7.90119	1.08456	3711.74924	-44.41411
-0.10006	7.82703	1.10027	3758.96758	-44.92189
-0.17422	7.81274	1.08453	3711.66019	-45.43092
-0.24837	7.79844	1.07026	3668.51959	-45.87660
-0.32253	7.78415	1.05738	3629.44690	-46.25991
-0.39668	7.76985	1.04587	3594.36331	-46.58232
-0.47084	7.75556	1.03568	3563.20886	-46.84578
-0.54500	7.74126	1.02679	3535.94055	-47.05271
-0.61915	7.72697	1.01918	3512.53018	-47.20600

MASS FLOW RATE = 148.07654 LBM/SEC

HO = 0.43781 INCHES

FIGURE K-2 (Continued)

DATA FOR PRANDTL-MEYER EXPANSION AT E

XC (IN)	RC (IN)	MACH NUMBER	VELOCITY (FPS)	FLOW ANGLE (DEGREES)
-0.00000	8.34612	1.06918	3665.24677	-42.07338
-0.00000	8.34612	1.11918	3815.49463	-41.05527
-0.00000	8.34612	1.16918	3963.22870	-39.84744
-0.00000	8.34612	1.21918	4108.41064	-38.50356
-0.00000	8.34612	1.26918	4251.00873	-37.05764
-0.00000	8.34612	1.31918	4390.99725	-35.53356
-0.00000	8.34612	1.36918	4528.35681	-33.94911
-0.00000	8.34612	1.41918	4663.07367	-32.31807
-0.00000	8.34612	1.46918	4795.13953	-30.65140
-0.00000	8.34612	1.51918	4924.55133	-28.95795
-0.00000	8.34612	1.56918	5051.31091	-27.24505
-0.00000	8.34612	1.61918	5175.42493	-25.51877
-0.00000	8.34612	1.66918	5296.90393	-23.78424
-0.00000	8.34612	1.71918	5415.76288	-22.04577
-0.00000	8.34612	1.76918	5532.02026	-20.30705
-0.00000	8.34612	1.81918	5645.69812	-18.57123
-0.00000	8.34612	1.86918	5756.82135	-16.84102
-0.00000	8.34612	1.91918	5865.41803	-15.11874
-0.00000	8.34612	1.96918	5971.51855	-13.40639
-0.00000	8.34612	2.01918	6075.15570	-11.70569
-0.00000	8.34612	2.06918	6176.36450	-10.01813
-0.00000	8.34612	2.11918	6275.18146	-8.34497
-0.00000	8.34612	2.16918	6371.54508	-6.68730
-0.00000	8.34612	2.21918	6465.79474	-5.04606
-0.00000	8.34612	2.26918	6557.67153	-3.42205
-0.00000	8.34612	2.31918	6647.31732	-1.81591
-0.00000	8.34612	2.36918	6734.77441	-0.22823
-0.00000	8.34612	2.41918	6820.08636	1.34055
-0.00000	8.34612	2.46918	6903.29659	2.89006
-0.00000	8.34612	2.51917	6984.46952	4.41998
-0.00000	8.34612	2.56917	7063.58917	5.93009
-0.00000	8.34612	2.61917	7140.76007	7.42023
-0.00000	8.34612	2.66917	7216.00623	8.89027
-0.00000	8.34612	2.71917	7289.37213	10.34015
-0.00000	8.34612	2.76917	7360.90157	11.76983
-0.00000	8.34612	2.81917	7430.63837	13.17934
-0.00000	8.34612	2.84953	7472.11627	14.02517

PFINAL = 14.70000 PSIA

FIGURE K-2 (Continued)

FIRST GUESS FOR THE OPTIMUM SURFACE

XS (IN)	RS (IN)	THETA (DEGREES)
-0.61915	7.72697	-47.20600
-0.61620	7.72375	-47.70600
-0.61328	7.72051	-48.20600
-0.61039	7.71725	-48.70600
-0.60752	7.71396	-49.20600
0.39151	6.69466	-42.12827
1.39054	5.87625	-36.66502
2.38957	5.19169	-32.28801
3.38860	4.60454	-28.68724
4.38763	4.09241	-25.66403
5.38666	3.64037	-23.08370
6.38570	3.23786	-20.85124
7.38473	2.87710	-18.89746
8.38376	2.55214	-17.17070
9.38279	2.25834	-15.63155
10.38182	1.99197	-14.24937
11.38085	1.75000	-13.00000

FIGURE K-2 (Continued)

LAM4 = 85.86692

LAGRANGE MULTIPLIERS ALONG WALL

POINT	LAMBDA1	LAMBDA2
1	-217.75	-5186.75
3	-219.63	-5082.05
6	-220.54	-5038.20
10	-220.02	-5031.56
15	-219.48	-5024.78
21	-218.93	-5017.77
28	-218.36	-5010.55
36	-217.79	-5003.14
45	-217.20	-4995.57
55	-216.60	-4987.84
66	-215.24	-4959.99
78	-213.82	-4951.74
91	-212.35	-4933.00
105	-210.84	-4913.83
120	-209.27	-4894.28
136	-207.67	-4874.39
153	-206.02	-4854.18
171	-204.33	-4833.72
190	-202.60	-4813.01
210	-200.83	-4792.08
231	-199.03	-4770.94
253	-197.18	-4749.62
276	-195.31	-4728.13
300	-193.39	-4705.50
325	-187.88	-4609.07
351	-178.31	-4442.90
378	-166.33	-4249.48
406	-152.19	-4032.33
435	-136.35	-3793.86
465	-119.78	-3538.15
496	-103.27	-3271.62
528	-87.51	-2999.71
561	-73.03	-2727.03
595	-60.13	-2455.69
630	-48.91	-2193.37
666	-39.24	-1940.70
703	-31.03	-1703.24
741	-24.07	-1483.67
780	-18.23	-1282.73
820	-13.39	-1100.15
861	-9.40	-934.20
903	-6.70	-780.34
946	-4.27	-671.73

THRUST = 32473.44067 LBF

FIGURE K-2 (Continued)

ERROR ALONG EXIT CHAR

POINT	ERROR
1	26.75906
2	21.60920
3	17.78381
4	17.76507
5	17.74876
6	17.72935
7	17.70725
8	17.68304
9	17.65718
10	17.63000
11	17.55747
12	17.49206
13	17.42726
14	17.36442
15	17.30502
16	17.25029
17	17.19978
18	17.15779
19	17.12318
20	17.09709
21	17.08020
22	17.07330
23	17.07709
24	17.09224
25	15.62179
26	12.91686
27	9.98359
28	7.10332
29	4.53761
30	2.05996
31	-0.06379
32	-1.48215
33	-2.14844
34	-2.64489
35	-2.70101
36	-2.53269
37	-2.11817
38	-1.55723
39	-0.98753
40	-0.47862
41	-0.07773
42	0.08246
43	0.00073

FIGURE K-2 (Continued)

CALCULATED PARTIAL DERIVATIVES

POINT	DTHETA	DE/DT
43	0.10694	0.32544
39	0.11276	0.74828
35	0.11361	0.89441
31	0.11439	1.53692
27	0.11438	2.80143
23	0.11424	3.55861
19	0.11419	3.60956
15	0.11412	3.67076
11	0.11403	3.73761
7	0.11453	3.77930

FIGURE K-2 (Continued)

ADJUSTED PARTIAL DERIVATIVES

POINT	DE/DT
1	5.88877
2	5.77836
3	5.66796
4	5.55755
5	5.44715
6	5.33674
7	5.22634
8	5.11594
9	5.00553
10	4.89513
11	4.78472
12	4.67432
13	4.56391
14	4.45351
15	4.34311
16	4.23270
17	4.12230
18	4.01189
19	3.90149
20	3.79108
21	3.68068
22	3.57028
23	3.45987
24	3.34947
25	3.23906
26	3.12866
27	3.01825
28	2.90785
29	2.79744
30	2.68704
31	2.57664
32	2.46623
33	2.35583
34	2.24542
35	2.13502
36	2.02461
37	1.91421
38	1.80381
39	1.69340
40	1.58300
41	1.47259
42	1.36219
43	1.25178

FIGURE K-2 (Continued)

NEW WALL COMPUTED,   ITERATION = 0

XS (IN)	RS (IN)	THETA (DEGREES)
-0.61915	7.72697	-47.20600
-0.61620	7.72375	-47.70600
-0.61328	7.72051	-48.20600
-0.61039	7.71725	-48.70600
-0.60752	7.71396	-49.20600
-0.60468	7.71064	-49.70600
-0.60188	7.70730	-50.20600
-0.59910	7.70394	-50.70600
-0.59753	7.70201	-50.99053
-0.59129	7.69425	-51.38405
-0.58375	7.68474	-51.80391
-0.57575	7.67458	-51.79632
-0.56741	7.66398	-51.78869
-0.55892	7.65320	-51.78165
-0.55029	7.64224	-51.77543
-0.54151	7.63110	-51.77021
-0.53259	7.61977	-51.76621
-0.52353	7.60827	-51.76362
-0.50314	7.58243	-51.67561
-0.48169	7.55534	-51.58413
-0.45947	7.52736	-51.49025
-0.43648	7.49852	-51.39445
-0.41271	7.46881	-51.29722
-0.38816	7.43822	-51.19906
-0.36281	7.40675	-51.10048
-0.33666	7.37439	-51.00207
-0.30969	7.34115	-50.90446
-0.28190	7.30701	-50.80831
-0.25328	7.27196	-50.71437
-0.22381	7.23600	-50.62350
-0.19349	7.19910	-50.53664
-0.16229	7.16126	-50.45486
-0.10832	7.09661	-49.83930
-0.02802	7.00334	-48.69214
0.07103	6.89330	-47.30678
0.19265	6.76502	-45.72471
0.34327	6.61512	-43.97405
0.53059	6.44005	-42.12433
0.75616	6.24264	-40.23166
1.02693	6.02129	-38.27101
1.36150	5.76696	-36.18232
1.78222	5.47088	-34.06242
2.27106	5.15380	-31.84796
2.87886	4.79266	-29.56016
3.59466	4.40568	-27.20710
4.46347	3.98160	-24.80448
5.49529	3.53049	-22.40295
6.71150	3.05844	-20.00369
8.15566	2.56711	-17.55712
9.87923	2.06312	-15.02504
11.40247	1.68285	-13.00049

FIGURE K-2 (Continued)

NEW WALL COMPUTED, ITERATION = 12

XS (IN)	RS (IN)	THETA (DEGREES)
-0.61915	7.72697	-47.20600
-0.61620	7.72375	-47.70600
-0.61328	7.72051	-48.20600
-0.61039	7.71725	-48.70600
-0.60752	7.71396	-49.20600
-0.60468	7.71064	-49.70600
-0.60188	7.70730	-50.20600
-0.59910	7.70394	-50.70600
-0.59635	7.70055	-51.20600
-0.59363	7.69713	-51.70600
-0.59094	7.69370	-52.20600
-0.58828	7.69024	-52.70600
-0.58565	7.68676	-53.20600
-0.58306	7.68325	-53.70600
-0.58049	7.67972	-54.20600
-0.57795	7.67617	-54.70600
-0.57622	7.67371	-55.05119
-0.55909	7.64925	-54.95100
-0.54177	7.62460	-54.84952
-0.52424	7.59976	-54.74796
-0.50651	7.57471	-54.64535
-0.48858	7.54948	-54.54468
-0.47043	7.52405	-54.44293
-0.45208	7.49843	-54.34126
-0.43353	7.47261	-54.23951
-0.41476	7.44660	-54.13775
-0.37224	7.38802	-53.91120
-0.32866	7.32448	-53.68476
-0.28400	7.26797	-53.45843
-0.23825	7.20649	-53.23226
-0.19139	7.14403	-53.00574
-0.13791	7.07372	-52.48025
-0.07029	6.98732	-51.43378
0.00672	6.89293	-50.17740
0.09442	6.79018	-48.82454
0.19384	6.67934	-47.37741
0.30606	6.56052	-45.85896
0.43222	6.43391	-44.31513
0.57338	6.29977	-42.74145
0.73061	6.15839	-41.15232
0.90492	6.01011	-39.57282
1.09737	5.85523	-38.04383
1.30900	5.69406	-35.52344
1.54092	5.52687	-35.03724
1.79431	5.35390	-33.58877
2.07043	5.17533	-32.17981
2.37073	4.99131	-30.81070
2.69680	4.80191	-29.48134
3.04888	4.60[illegible]9	-28.19834
3.42492	4.40964	-26.95951
3.83805	4.20629	-25.75514
4.28279	3.99768	-24.59448
4.76129	3.78446	-23.44577
5.27326	3.56819	-22.35077
5.82713	3.34649	-21.27471
6.42758	3.11906	-20.21186
7.06667	2.89025	-19.18197
7.76028	2.65593	-18.14719
8.51360	2.41666	-17.09216
9.31728	2.17776	-16.01453
10.19580	1.93535	-14.83366
11.14108	1.69674	-13.49567
11.42378	1.62998	-13.07836

FIGURE K-2 (Continued)

LAM4 = 85.71503

LAGRANGE MULTIPLIERS ALONG WALL

POINT	LAMBDA1	LAMBDA2
1	-218.99	-4947.75
3	-217.64	-4935.95
6	-216.29	-4924.17
10	-214.94	-4912.28
15	-213.58	-4900.43
21	-212.23	-4888.56
28	-210.87	-4876.69
36	-209.51	-4864.81
45	-208.14	-4852.92
55	-206.77	-4841.02
66	-203.72	-4814.52
78	-200.67	-4787.99
91	-197.60	-4761.44
105	-194.52	-4734.87
120	-191.44	-4708.28
136	-186.41	-4647.48
153	-177.78	-4523.59
171	-168.21	-4382.39
190	-157.93	-4226.53
210	-147.21	-4059.72
231	-136.31	-3885.80
253	-125.45	-3707.02
276	-114.81	-3526.15
300	-104.55	-3345.46
325	-94.79	-3166.79
351	-85.59	-2991.64
378	-77.01	-2821.10
406	-69.05	-2655.97
435	-61.73	-2496.77
465	-55.02	-2343.77
496	-48.89	-2197.10
528	-43.31	-2056.72
561	-38.27	-1923.39
595	-33.73	-1796.86
630	-29.61	-1676.20
666	-25.90	-1561.06
703	-22.56	-1451.72
741	-19.58	-1348.98
780	-16.89	-1250.87
820	-14.46	-1157.06
861	-12.33	-1069.76
903	-10.40	-986.36
946	-8.66	-906.90
990	-7.13	-833.36
1035	-5.75	-763.37
1081	-4.51	-698.76
1128	-4.19	-692.03

THRUST = 32648.37720 LBF

FIGURE K-2 (Continued)

ERROR ALONG EXIT CHAR

POINT	ERROR
1	0.00334
2	0.00321
3	0.00295
4	0.00286
5	0.00274
6	0.00268
7	0.00261
8	0.00256
9	0.00252
10	0.00248
11	0.00223
12	0.00219
13	0.00213
14	0.00215
15	0.00326
16	0.00432
17	0.00222
18	0.00189
19	0.00174
20	0.00151
21	0.00133
22	0.00133
23	0.00129
24	0.00123
25	0.00120
26	0.00116
27	0.00115
28	0.00112
29	0.00106
30	0.00101
31	0.00085
32	0.00065
33	0.00046
34	0.00029
35	0.00009
36	-0.00020
37	-0.00054
38	-0.00072
39	-0.00103
40	-0.00153
41	-0.00170
42	-0.00175
43	-0.00148
44	0.00021
45	0.00304
46	0.00317
47	0.00127

FIGURE K-2 (Continued)

FINAL SOLUTION

XS (IN)	RS (IN)	THETA (DEGREES)
-0.61915	7.72697	-47.20600
-0.61620	7.72375	-47.70600
-0.61328	7.72051	-48.20600
-0.61039	7.71725	-48.70600
-0.60752	7.71396	-49.20600
-0.60468	7.71064	-49.70600
-0.60188	7.70730	-50.20600
-0.59910	7.70394	-50.70600
-0.59635	7.70055	-51.20600
-0.59363	7.69713	-51.70600
-0.59094	7.69370	-52.20600
-0.58828	7.69024	-52.70600
-0.58565	7.68676	-53.20600
-0.58306	7.68325	-53.70600
-0.58049	7.67972	-54.20600
-0.57795	7.67617	-54.70600
-0.57622	7.67371	-55.05119
-0.55909	7.64923	-54.95090
-0.54177	7.62458	-54.84941
-0.52424	7.59973	-54.74783
-0.50650	7.57468	-54.64622
-0.48857	7.54944	-54.54454
-0.47042	7.52401	-54.44283
-0.45207	7.49838	-54.34109
-0.43351	7.47256	-54.23933
-0.41474	7.44655	-54.13756
-0.37222	7.38799	-53.91107
-0.32863	7.32844	-53.68462
-0.28396	7.26792	-53.45827
-0.23821	7.20644	-53.23207
-0.19134	7.14397	-53.00551
-0.13784	7.07363	-52.47917
-0.07020	6.98722	-51.40267
0.00682	6.89279	-50.17588
0.09454	6.79006	-48.82289
0.19397	6.67920	-47.37762
0.30622	6.56036	-45.86707
0.43240	6.43374	-44.31414
0.57358	6.29959	-42.73942
0.73083	6.15870	-41.16029
0.90517	6.00991	-39.59087
1.09764	5.85502	-38.04189
1.30929	5.69385	-36.52157
1.54123	5.52666	-35.03545
1.79463	5.35368	-33.58708
2.07077	5.17512	-32.17822
2.37108	4.99110	-30.80942
2.69716	4.80170	-29.47998
3.04926	4.60179	-28.19706
3.42889	4.40940	-26.95846
3.83931	4.20610	-25.75511
4.28314	3.99752	-24.58359
4.76163	3.78430	-23.44597
5.27356	3.56805	-22.35010
5.82738	3.34638	-21.27417
6.42778	3.11897	-20.21145
7.06680	2.89018	-19.18166
7.76033	2.65589	-18.14790
8.51357	2.41663	-17.07204
9.31719	2.17774	-16.01446
10.19572	1.93532	-14.83347
11.14108	1.69668	-13.49528
11.42378	1.62798	-13.07836

THRUST = 32648.37720 LBF

MASS FLOW RATE = 148.07654 LBM/SEC

ISP = 220.48297 LBF-SEC/LBM

BETA = -45.000 DEGREES   PA = 14.70 PSIA

FIGURE K-2 (Continued)

CARD 1

HEADER
SAMPLE CASE NO. 2

CARD 2

PA	PØ	TØ	R	G	FLRTC	XLENG	YLAST	TLAST
0.0	500.0	6000.0	56.0	1.23	148.077	10.00	1.75	-13.00

CARD 3

HØ	RE	BD	ETA	RRE	CENTM	RHØD
.4155	9.5	-50.00	0.0	.705	1.08	0.5

CARD 4

NPTSL	NPTS	NDEGR1	NDEGR2	NDERMX	NPTSS	NS	NWRITE	NCNT	NREAD1	NREAD2	ØPT1	ØPT2	ØPT3
15	50	-1	-1	6	17	10	0	5	-1	0	-1	-1	-1

CARD 5

DELTPM	CFI	ERR	WEIGHT	DELTAT	CS	AA	A3	THETAC
0.05	0.002	0.001	0.85	0.5	2.0	0.846	1.3	6.0

FIGURE K-3. INPUT DATA SHEET FOR SAMPLE CASE NO. 2

```
                         SAMPLE CASE NO. 2

                            INPUT DATA

      PA =      0.     PD =   500.000  TO =  6000.000  R =    56.000  G =     1.230
      FLRTC =   148.077  XLENG =    10.000  YLAST =     1.750  TLAST =   -13.000

HO = 0.41550  RE = 9.50000  BD =-50.0000  ETA =0.     RRE =0.7050  CENTM =   1.08000  RHOD =   0.50000

        NPTSL =  15  NPTS =  50  NDEGR1 =   1  NDEGR2 =   1  NDERMX =   6  NPTSS =  17  NS =  10
NWRITE =   0     NCNT =    5     NREAD1 =    1     NREAD2 =    0     OPT1 =    1     OPT2 =    1     OPT3 =    1

   DELTPM =  0.0500  CFI =  0.0020  ERR =  0.0010  WEIGHT =  0.8500  DELTAT =  0.5000  CS =  2.0000
                AA =   0.8460     AB =   1.3000     THETAC =   6.0000
```

FIGURE K-4: SELECTED OUTPUT FOR SAMPLE CASE NO. 2

DATA FOR THE START LINE

XC (IN)	RC (IN)	MACH NUMBER	VELOCITY (FPS)	FLOW ANGLE (DEGREES)
0.	9.50000	1.08000	3697.98572	-47.00000
-0.04064	9.46590	1.08000	3697.98572	-47.42857
-0.08128	9.43179	1.08000	3697.98572	-47.85714
-0.12193	9.39769	1.08000	3697.98572	-48.28571
-0.16257	9.36359	1.08000	3697.98572	-48.71428
-0.20321	9.32948	1.08000	3697.98572	-49.14285
-0.24385	9.29538	1.08000	3697.98572	-49.57143
-0.28450	9.26128	1.08000	3697.98572	-50.00000
-0.32514	9.22717	1.08000	3697.98572	-50.42857
-0.36578	9.19307	1.08000	3697.98572	-50.85714
-0.40642	9.15897	1.08000	3697.98572	-51.28571
-0.44707	9.12487	1.08000	3697.98572	-51.71428
-0.48771	9.09076	1.08000	3697.98572	-52.14286
-0.52835	9.05666	1.08000	3697.98572	-52.57143
-0.56899	9.02256	1.08000	3697.98572	-53.00000

MASS FLOW RATE = 148.07702 LBM/SEC

HO = 0.37138 INCHES

FIGURE K-4 (Continued)

DATA FOR PRANDTL-MEYER EXPANSION AT E

XC (IN)	RC (IN)	MACH NUMBER	VELOCITY (FPS)	FLOW ANGLE (DEGREES)
0.	9.50000	1.13000	3847.69293	-45.93457
0.	9.50000	1.18000	3994.87750	-44.69364
0.	9.50000	1.23000	4139.50255	-43.32523
0.	9.50000	1.28000	4281.53760	-41.86061
0.	9.50000	1.33000	4420.95844	-40.32211
0.	9.50000	1.38000	4557.74689	-38.72652
0.	9.50000	1.43000	4691.89032	-37.08692
0.	9.50000	1.48000	4823.38165	-35.41376
0.	9.50000	1.53000	4952.21893	-33.71553
0.	9.50000	1.58000	5078.40509	-31.99925
0.	9.50000	1.63000	5201.94751	-30.27078
0.	9.50000	1.68000	5322.85797	-28.53505
0.	9.50000	1.73000	5441.15198	-26.79623
0.	9.50000	1.78000	5556.84894	-25.05789
0.	9.50000	1.83000	5669.97150	-23.32308
0.	9.50000	1.88000	5780.54523	-21.59440
0.	9.50000	1.93000	5888.59888	-19.87411
0.	9.50000	1.98000	5994.16327	-18.16414
0.	9.50000	2.03000	6097.27167	-16.45617
0.	9.50000	2.08000	6197.95947	-14.78162
0.	9.50000	2.13000	6296.26361	-13.11172
0.	9.50000	2.18000	6392.22290	-11.45754
0.	9.50000	2.23000	6485.87708	-9.81997
0.	9.50000	2.28000	6577.26727	-8.19977
0.	9.50000	2.33000	6666.43549	-6.59759
0.	9.50000	2.38000	6753.42450	-5.01396
0.	9.50000	2.43000	6838.27771	-3.44932
0.	9.50000	2.48000	6921.03887	-1.90404
0.	9.50000	2.53000	7001.75214	-0.37838
0.	9.50000	2.58000	7080.46179	1.12742
0.	9.50000	2.63000	7157.21216	2.61321
0.	9.50000	2.68000	7232.04755	4.07889
0.	9.50000	2.73000	7305.01215	5.52439
0.	9.50000	2.78000	7376.14990	6.94971
0.	9.50000	2.83000	7445.50415	8.35486
0.	9.50000	2.88000	7513.11823	9.73989
0.	9.50000	2.93000	7579.03491	11.10489
0.	9.50000	2.98000	7643.29626	12.44996
0.	9.50000	3.03000	7705.94385	13.77525
0.	9.50000	3.08000	7767.01886	15.08089
0.	9.50000	3.13000	7826.56146	16.36705
0.	9.50000	3.18000	7884.61151	17.63394
0.	9.50000	3.20067	7908.18787	18.19502

PFINAL = 7.78023 PSIA

FIGURE K-4 (Continued)

FIRST GUESS FOR THE OPTIMUM SURFACE

XS (IN)	RS (IN)	THETA (DEGREES)
-0.56899	9.02256	-53.00000
-0.56638	9.01906	-53.50000
-0.56380	9.01554	-54.00000
-0.56125	9.01200	-54.50000
-0.55874	9.00844	-55.00000
0.27374	7.88769	-51.73091
1.10622	6.89303	-48.35806
1.93870	6.01113	-44.89351
2.77118	5.23086	-41.35328
3.60366	4.54280	-37.75689
4.43613	3.93891	-34.12676
5.26861	3.41226	-30.48725
6.10109	2.95680	-26.86361
6.93357	2.56725	-23.28078
7.76605	2.23896	-19.76230
8.59853	1.96777	-16.32934
9.43101	1.75000	-13.00000

FIGURE K-4 (Continued)

LAM4 = 164.97913

LAGRANGE MULTIPLIERS ALONG WALL

POINT	LAMBDA1	LAMBDA2
1	-275.28	-4752.82
3	-276.40	-4702.85
6	-275.92	-4692.23
10	-275.23	-4685.90
15	-274.53	-4679.76
21	-273.83	-4673.69
28	-273.12	-4667.73
36	-272.42	-4661.88
45	-271.71	-4656.06
55	-271.01	-4650.40
66	-269.43	-4637.92
78	-267.85	-4625.88
91	-266.27	-4614.20
105	-264.68	-4602.81
120	-263.08	-4591.69
136	-261.49	-4580.82
153	-259.89	-4570.22
171	-254.16	-4494.79
190	-244.95	-4380.28
210	-232.11	-4236.02
231	-215.31	-4063.82
253	-194.65	-3865.38
276	-171.29	-3647.21
300	-146.82	-3413.57
325	-123.09	-3166.07
351	-101.24	-2910.39
378	-82.13	-2648.27
406	-66.25	-2371.98
435	-53.21	-2090.78
465	-42.76	-1804.40
496	-34.24	-1521.86
528	-27.11	-1254.22
561	-20.76	-1052.77
595	-14.92	-908.59
630	-9.56	-824.06
666	-6.96	-785.48

THRUST = 35892.77539 LBF

FIGURE K-4 (Continued)

ERROR ALONG EXIT CHAR

POINT	ERROR
1	-6.04158
2	-10.79777
3	-11.86355
4	-11.89563
5	-11.92187
6	-11.94587
7	-11.96653
8	-11.98405
9	-11.99976
10	-12.01137
11	-12.03304
12	-12.03968
13	-12.03462
14	-12.01949
15	-11.99474
16	-11.96166
17	-11.91884
18	-12.94987
19	-14.52193
20	-16.30766
21	-18.03127
22	-19.38413
23	-20.08290
24	-20.03929
25	-19.38645
26	-18.23950
27	-16.80228
28	-15.38812
29	-13.98865
30	-12.65011
31	-11.24749
32	-9.54065
33	-7.20379
34	-4.16381
35	-0.96856
36	0.34578

FIGURE K-4 (Continued)

CALCULATED PARTIAL DERIVATIVES

POINT	DTHETA	DE/DT
36	0.10705	0.51604
32	0.11279	0.02277
28	0.11447	-0.41638
24	0.11475	0.09701
20	0.11463	1.53350
16	0.11440	2.30957
12	0.11437	2.36282
8	0.11450	2.42157
4	0.11451	2.45974
2	0.11923	2.54819

FIGURE K-4 (Continued)

ADJUSTED PARTIAL DERIVATIVES

POINT	DE/DT
1	4.12026
2	4.03236
3	3.94447
4	3.85657
5	3.76867
6	3.68078
7	3.59288
8	3.50499
9	3.41709
10	3.32919
11	3.24130
12	3.15340
13	3.06551
14	2.97761
15	2.88971
16	2.80182
17	2.71392
18	2.62603
19	2.53813
20	2.45023
21	2.36234
22	2.27444
23	2.18655
24	2.09865
25	2.01075
26	1.92286
27	1.83496
28	1.74707
29	1.65917
30	1.57127
31	1.48338
32	1.39548
33	1.30759
34	1.21969
35	1.13179
36	1.04390

FIGURE K-4 (Continued)

NEW WALL COMPUTED, ITERATION = 0

XS (IN)	RS (IN)	THETA (DEGREES)
-0.56899	9.02256	-53.00000
-0.56077	9.01169	-53.41534
-0.55193	8.99973	-53.64747
-0.54277	8.98730	-53.57762
-0.53341	8.97463	-53.50608
-0.52393	8.96183	-53.43266
-0.51432	8.94889	-53.35740
-0.50459	8.93583	-53.28018
-0.49476	8.92267	-53.20076
-0.48480	8.90938	-53.11926
-0.46248	8.87969	-52.98544
-0.43943	8.84921	-52.84839
-0.41590	8.81822	-52.70842
-0.39189	8.78678	-52.56529
-0.36743	8.75492	-52.41890
-0.34254	8.72266	-52.26911
-0.31722	8.69003	-52.11568
-0.27880	8.64099	-51.[illegible]2692
-0.22826	8.57755	-51.18012
-0.16449	8.49921	-50.51792
-0.08478	8.40312	-49.77222
0.01726	8.28475	-48.98129
0.14557	8.13927	-48.18552
0.30893	7.95921	-47.37916
0.51752	7.73599	-46.49313
0.77872	7.46548	-45.50348
1.11348	7.13184	-44.29124
1.54871	6.71921	-42.63359
2.08263	6.24491	-40.55438
2.76240	5.68993	-37.84100
3.60098	5.07685	-34.42510
4.59672	4.44342	-30.40973
5.75859	3.82006	-25.92433
7.07806	3.24396	-21.15350
8.56497	2.74170	-16.08883
9.43101	2.51568	-13.14601

FIGURE K-4 (Continued)

FINAL SOLUTION

XS (IN)	RS (IN)	THETA (DEGREES)
-0.56899	9.02256	-53.00000
-0.56638	9.01906	-53.50000
-0.56380	9.01554	-54.00000
-0.56125	9.01200	-54.50000
-0.55874	9.00844	-55.00000
-0.55625	9.00485	-55.50000
-0.55379	9.00125	-56.00000
-0.55137	8.99762	-56.50000
-0.54898	8.99397	-57.00000
-0.54662	9.99030	-57.50000
-0.54429	8.98661	-58.00000
-0.54199	8.98290	-58.50000
-0.54033	8.98017	-58.85530
-0.52735	8.95869	-58.80886
-0.51427	8.93711	-58.75064
-0.50109	8.91542	-58.69405
-0.48782	8.89361	-58.63898
-0.47445	8.87170	-58.58525
-0.46099	8.84969	-58.53307
-0.44745	8.82758	-58.48229
-0.43381	8.80537	-58.43259
-0.42009	8.78306	-58.38390
-0.38928	8.73311	-58.28029
-0.35805	8.68269	-58.18127
-0.32645	8.63185	-58.08564
-0.27069	8.57460	-57.64344
-0.24723	8.50741	-56.77254
-0.19733	8.43269	-55.72022
-0.13946	8.34972	-54.65018
-0.07231	8.25919	-53.01979
0.00539	8.15801	-51.43573
0.05605	8.04930	-49.75015
0.18661	7.94230	-48.01575
0.31260	7.80731	-46.24202
0.44360	7.67472	-44.43250
0.59065	7.53496	-42.61769
0.75474	7.38842	-40.85245
0.93694	7.23562	-39.11848
1.13788	7.07698	-37.41402
1.35879	6.91297	-35.75424
1.60050	6.74400	-34.14720
1.86398	6.57048	-32.57853
2.15028	6.39278	-31.05303
2.46052	6.21125	-29.59397
2.79596	6.02613	-28.15838
3.15799	5.83789	-26.78245
3.54733	5.64705	-25.43515
3.96314	5.45507	-24.13461
4.40959	5.26092	-22.85151
4.88855	5.06505	-21.61110
5.40271	4.86771	-20.37710
5.94556	4.67250	-19.17756
6.52666	4.47713	-17.98345
7.14957	4.28209	-16.78553
7.80718	4.09112	-15.59712
8.50668	3.90370	-14.39727
9.25644	3.71978	-13.15528
9.45967	3.67283	-12.84692

THRUST = 36249.59814 LBF

MASS FLOW RATE = 148.07702 LBM/SEC

ISP = 244.79557 LBF-SEC/LBM

BETA = -50.000 DEGREES PA = 0. PSIA

FIGURE K-4 (Continued)

APPENDIX L

COMPUTER PROGRAM LISTING

This appendix is a complete listing of the computer program.

```
$IBFTC MAIN
C       PLUG NOZZLE PROGRAM WITH FIXED INLET
C
      DIMENSION REG(1275,7), XL(75), RL(75), ML(75), VL(75), TL(75), XS(
     1125), RS(125), TS(125), NPOINT(51), ERROR(50), FX(50), TY(50), HXS
     2(50), HRS(50), HTS(50), COEF(50), ED(50), XA(75), YA(75), MA(75),
     3VA(75), TA(75), HEADER(12)
      REAL M,ML,MA
      INTEGER OPT1,OPT2,OPT3
      COMMON /B2/ XL,RL,ML,VL,TL
      COMMON /B3/ PA,PO,TO,RHOO,G,R,GO
      COMMON /B4/ HO,RE,BD,ETA,RRE,RHOD,DELTAT,AA,AB,VCNT,THETAC
      COMMON /B5/ REG
      COMMON /B6/ NPOINT
      COMMON /B7/ ERROR
      COMMON /B8/ NWRITE
      COMMON /B9/ RAD,FOOT
      COMMON /B10/ XA,YA,MA,VA,TA
      COMMON /B11/ CF1,CF2,CF3,CFI,FLRT,THRUST,FLRTC
      COMMON /B12/ NREAD1,NREAD2,OPT1,OPT2,OPT3
      COMMON /B13/ XS,RS,TS
C
10    WRITE (6,390)
      READ (5,640) HEADER
      READ (5,450) PA,PO,TO,R,G,FLRTC,XLENG,YLAST,TLAST
      READ (5,460) HO,RE,BD,ETA,RRE,CENTM,RHOD
      READ (5,470) NPTSL,NPTS,NDEGR1,NDEGR2,NDERMX,NPTSS,NS,NWRITE,NCNT,
     1NREAD1,NREAD2,OPT1,OPT2,OPT3
      READ (5,480) DELTPM,CFI,ERR,WEIGHT,DELTAT,CS,AA,AB,THETAC
      IF (NREAD1.EQ.1) GO TO 20
      READ (5,490) (XS(I),RS(I),TS(I),I=2,NPTSS)
20    CONTINUE
      RAD=3.14159/180.
      FOOT=12.0
      GO=32.1739
      IF (OPT2.EQ.1) GO TO 40
      READ (5,500) (XL(I),RL(I),ML(I),VL(I),TL(I),I=1,NPTSL)
      DO 30 I=1,NPTSL
      XL(I)=XL(I)/FOOT
      RL(I)=RL(I)/FOOT
30    CONTINUE
40    CONTINUE
C
C     WRITE THE INPUT DATA
C
      WRITE (6,650) HEADER
      WRITE (6,400) PA,PO,TO,R,G,FLRTC,XLENG,YLAST,TLAST
      WRITE (6,410) HO,RE,BD,ETA,RRE,CENTM,RHOD
      WRITE (6,420) NPTSL,NPTS,NDEGR1,NDEGR2,NDERMX,NPTSS,NS,NWRITE,NCNT
     1,NREAD1,NREAD2,OPT1,OPT2,OPT3
      WRITE (6,430) DELTPM,CFI,ERR,WEIGHT,DELTAT,CS,AA,AB,THETAC
C
      RE=RE/FOOT
      XLENG=XLENG/FOOT
      YLAST=YLAST/FOOT
```

```
      HO=HO/FOOT
      DO 50 I=2,NPTSS
      XS(I)=XS(I)/FOOT
      RS(I)=RS(I)/FOOT
50    CONTINUE
      PA=PA*144.0
      PO=PO*144.0
      RHOO=PO/(R*TO)
      RHOO=RHOO/FOOT
      NPTSN=0
      IDERIV=0
      ISCIL=0
      ITER=0
      NRECDS=0
      NTIP=0
      N1=2
      N2=0
      NZ=2
      PSTOP=PA
C
C     CALCULATE THE START LINE AND THE P-M EXPANSION
C
      CALL START (CENTM,NPTSL,PSTOP,J,NPTSS,DELTPM,XLENG,YLAST,TLAST)
C
C     CALCULATE THE FLOW IN REGION R1
C
      CALL FLOW1 (NPTSL,J,NTOT)
      XHOLD=XL(1)
      RHOLD=RL(1)
      THOLD=TL(1)/RAD
C
C     DIVIDE THE LIMITING LEFT CHARACTERISTIC INTO NPTS AND CURVE FIT
C
      CALL SELECT (NPTS,NTOT,NDEGR1,NS,CS,XL,RL,ML,VL,TL)
      CF2=0.0
      GO TO 70
C
60    CALL EXTEND (NTOT,NDEGR1,NPTSN,ITOT,NWRITE,NSAVE,XFINAL,ITER)
      NEWS=ITOT
      IF (ITER.GE.2) NEWS=NSAVE
      IF (NTIP.EQ.1) NEWS=NSAVE
      CALL SELECT (NPTS,NEWS,NDEGR1,NS,CS,XA,YA,MA,VA,TA)
70    CONTINUE
C
C     CALCULATE THE MAIN FLOW FIELD
C
      NCHECK=0
      CALL FLOW (NZ,NPTS,NPTSS,NDEGR2,NCHECK,XLENG,NRECRD,XFINAL)
C
C     CALCULATE THE LAGRANGIAN MULTIPLIER FIELD
C
      CALL LANGR1 (NRECRD,N1,N2,LAN4,OPT1)
      IF (OPT1.EQ.0) GO TO 380
C
C     SUBSTITUTE WALL POINTS
C
```

```
      DO 80 K=1,NRECRD
      J=NPOINT(K)+K
      I=NPTSN+K
      XS(I)=REG(J,1)
      RS(I)=REG(J,2)
      TS(I)=REG(J,5)/RAD
      EU(K)=ERROR(K)
      HXS(K)=XS(I)
      HRS(K)=RS(I)
      HTS(K)=TS(I)
80    CONTINUE
C
C     CHECK FOR FINAL SOLUTION
C
      IFIN=0
      IZ=NPOINT(NRECRD)
      DO 90 I=1,NRECRD
      IZ=IZ+1
      IF (ABS(ERROR(I)/REG(IZ,6)).GE.ERR) GO TO 100
90    CONTINUE
      IFIN=1
      GO TO 320
C
100   IF (ITER.EQ.0) GO TO 110
      IF (IDERIV.EQ.NDERMX) GO TO 110
      IF (NRECRD.GT.NRECDS) GO TO 140
      GO TO 210
C
C     BEGIN ADJUSTING SLOPES TO DETERMINE PARTIAL DERIVATIVES
C
110   DT=.002
      NCAL=10
      IF (NCAL.GT.NRECRD) NCAL=NRECRD
      IDADJ=(NRECRD+5)/NCAL
      WRITE (6,570)
      WRITE (6,560)
      NADJ=1-IDADJ
      NCHECK=1
      DO 120 I=1,NCAL
      NADJ=NADJ+IDADJ
      IK=NRECRD-NADJ+1
      IF (IK.LT.2) IK=2
      IJ=NPTSN+IK
      TS(IJ)=HTS(IK)+DT*180./3.14159
C
C     DETERMINE THE FLOW FIELD FROM IK TO NRECRD AND THE LANGR FIELD
C
      LMXY=NPTSN+NRECRD
      CALL FLOW (IK,NRECRD,LMXY,NDEGR2,NCHECK,XLENG,NRECRD,XFINAL)
      N2=1
      CALL LANGR1 (NRECRD,IK,N2,LAM4,OPT1)
C
C     CALCULATE AND STORE THE PARTIAL DERIVATIVES
C
      K=NPOINT(IK)+IK
      DS=REG(K,5)*180./3.14159-HTS(IK)
```

```
      COEF(I)=(ERROR(IK)-EO(IK))/DS
      WRITE (6,580) IK,DS,COEF(I)
      TS(IJ)=HTS(IK)
120   CONTINUE
      K=1-IDADJ
      DO 130 I=1,NCAL
      K=K+IDADJ
      I1=NPTS-K+1
      IF (I1.LT.2) I1=2
      TX(I)=I1
      TY(I)=COEF(I)
130   CONTINUE
      CALL LSQARE (NCAL,TX,TY,A,B)
      GO TO 150
C
140   CONTINUE
      Y1=COEF(1)*RAD
      Y2=COEF(NRECDS)*RAD
      X1=1.0
      X2=NRECRD
      A=(Y2-Y1)/(X2-X1)
      B=Y1-A*X1
150   WRITE (6,590)
      WRITE (6,560)
      CSML=0.01*12.*RE
      DO 200 I=1,NRECRD
      ZI=I
      COEF(I)=A*ZI+B
      IF (COEF(I)) 160,170,180
160   IF (COEF(I).GT.-CSML) COEF(I)=-CSML
      GO TO 190
C
170   COEF(I)=-CSML
      GO TO 190
C
180   IF (COEF(I).LT.CSML) COEF(I)=CSML
190   WRITE (6,600) I,COEF(I)
      COEF(I)=COEF(I)*180./3.14159
200   CONTINUE
C
C     CALCULATE CORRECTIONS TO NOZZLE WALL ANGLES
C
210   AMAX2=5.*RAD
      AMAX=5.*RAD
      DO 220 I=1,NRECRD
      TS(I)=-EO(I)/COEF(I)
      IF (ABS(TS(I)).LT.AMAX) GO TO 220
      AMAX=ABS(TS(I))
220   CONTINUE
      WF=WEIGHT*AMAX2/AMAX
      DO 230 I=1,NRECRD
      HTS(I)=HTS(I)+TS(I)*WF*180./3.14159
C
230   CONTINUE
C
C     CALCULATE NEW WALL POINTS
```

```
C
      TN=(90.+THOLD)*RAD
      XC=XHOLD-RHOD*COS(TN)
      YC=RHOLD-RHOD*SIN(TN)
      TS(1)=THOLD
      XS(1)=XHOLD
      RS(1)=RHOLD
      TN=(90.+HTS(1))*RAD
      XSTAR=XC+RHOD*COS(TN)
      RSTAR=YC+RHOD*SIN(TN)
      DX=XSTAR-HXS(1)
      DO 240 I=2,200
      TS(I)=TS(I-1)-DELTAT
      TN=(90.+TS(I))*RAD
      XS(I)=RHOD*COS(TN)+XC
      RS(I)=YC+RHOD*SIN(TN)
      IH=I
      IF (TS(I).LE.HTS(1)) GO TO 250
240   CONTINUE
250   CONTINUE
      IF (IH.EQ.2) GO TO 270
260   NEWPTS=IH+NRECRD-1
      NPTSN=IH-1
      TS(I)=HTS(1)
      XS(I)=XSTAR
      RS(I)=RSTAR
      GO TO 300
C
270   CONTINUE
      IF (TS(I).LE.HTS(1).AND.ITER.GT.8) GO TO 290
      IF (TS(I).LE.HTS(1)) GO TO 280
      GO TO 260
C
280   NEWPTS=NRECRD
      IH=1
      NPTSN=IH-1
      DX=0.0
      GO TO 300
C
290   WRITE (6,510)
      GO TO 380
C
300   CONTINUE
      DO 310 I=2,NRECRD
      K=NPTSN+I
      TS(K)=HTS(I)
      XS(K)=HXS(I)+DX
      T1=HTS(I)*3.14159/180.
      T2=HTS(I-1)*3.14159/180.
      TB=(TAN(T1)+TAN(T2))/2.
      HRS(I)=RS(K-1)+(XS(K)-XS(K-1))*TB
      RS(K)=HRS(I)
      IF (RS(K).LT.0.0) MESAG=1
310   CONTINUE
320   CONTINUE
      IF (IFIN.EQ.0) GO TO 340
```

```
      IF (IFIN.EQ.1.AND.NEWS.NE.NSAVE) GO TO 330
      IF (IFIN.EQ.1) WRITE (6,620)
      GO TO 350
C
330   NTIP=1
      GO TO 60
C
340   WRITE (6,610) ITER
350   WRITE (6,630)
      WRITE (6,560)
      DO 360 I=1,NTWPTS
      XD=XS(I)*FCOT
      RD=RS(I)*FCOT
      WRITE (6,550) XD,RD,TS(I)
360   CONTINUE
      IF (IFIN.EQ.1) GO TO 380
      IF (MESAG.EQ.1) GO TO 370
      ISCIL=ISCIL+1
      IF (ISCIL.GE.4) ISCIL=0
      ITER=ITER+1
      IF (IDERIV.EQ.NDERMX) IDERIV=0
      IDERIV=IDERIV+1
      IF (ITER.GE.25) NWRITE=1
      K2=0
      NPTSS=NTWPTS
      NREAD2=1
      NRECDS=NRECRP
      GO TO 60
C
370   WRITE (6,660)
380   CONTINUE
      XISP=THRUST/FLRT
      WRITE (6,520) THRUST
      WRITE (6,530) FLRT
      WRITE (6,540) XISP
      PA=PA/144.0
      WRITE (6,440) BD,PA
      GO TO 10
C
C
390   FORMAT (1H1)
400   FORMAT (1H0,55X,10HINPUT DATA//22X,4HPA =,F10.3,2X,4HPO =,F10.3,2X
     1,4HTO =,F10.3,2X,3HR =,F10.3,2X,3HG =,F10.3,/23X,7HFLRTC =,F10.3,2
     2X,7HXLENG =,F10.3,2X,7HYLAST =,F10.3,2X,7HTLAST =,F10.3)
410   FORMAT (1H0,9X,4HHO =,F8.5,2X,4HRE =,F8.5,2X,4H3D =,F8.4,2X,5HETA
     1=,F6.4,2X,5HRRE =,F6.4,2X,7HCENTM =,F10.5,2X,6HRHOD =,F10.5)
420   FORMAT (1H0,16X,7HNPTSL =,I4,2X,6HNPTS =,I4,2X,8HNDEGR1 =,I4,2X,8H
     1NDEGR2 =,I4,2X,8HNDERMX =,I4,2X,7HNPTSS =,I4,2X,4HNS =,I4/2X,8HNWR
     2ITE =,I4,5X,6HNCNT =,I5,5X,8HNREAD1 =,I5,5X,8HNREAD2 =,I5,5X,6HOPT
     31 =,I5,5X,6HOPT2 =,I5,5X,6HOPT3 =,I5)
430   FORMAT (1H0,12X,8HDELTPM =,F8.4,2X,5HCFI =,F8.4,2X,5HERR =,F8.4,2X
     1,8HWEIGHT =,F8.4,2X,8HDELTAT =,F8.4,2X,4HCS =,F8.4/36X,5HAA = ,F8.
     24,5X,5HAB = ,F8.4,5X,9HTHETAC = ,F8.4)
440   FORMAT (1H0,46X,7HBETA = ,F8.3,8H DEGREES,5X,5HPA = ,F5.2,5H PSIA)
450   FORMAT (9F8.0)
460   FORMAT (7F10.0)
```

```
470   FORMAT (14I5)
480   FORMAT (9F8.0)
490   FORMAT (3F10.0)
500   FORMAT (5F10.0)
510   FORMAT (1H0,35X,49HWALL ANGLE LARGER THAN SELECTED UPSTREAM GEOMET
     1RY)
520   FORMAT (1H0,46X,9HTHRUST = ,F15.5,4H LBF)
530   FORMAT (1H0,46X,17HMASS FLOW RATE = ,F15.5,8H LBM/SEC)
540   FORMAT (1H0,46X,6HISP = ,F10.5,12H LBF-SEC/LBM)
550   FORMAT (46X,2F10.5,F15.5)
560   FORMAT (1H0)
570   FORMAT (1H1,50X,30HCALCULATED PARTIAL DERIVATIVES//48X,5HPOINT,7X,
     16HDTHETA,10X,5HDE/DT)
580   FORMAT (1H ,48X,I3,2F15.5)
590   FORMAT (1H1,50X,28HADJUSTED PARTIAL DERIVATIVES//54X,5HPOINT,10X,5
     1HDE/DT)
600   FORMAT (1H ,54X,I3,2X,F15.5)
610   FORMAT (1H1,45X,18HNEW WALL COMPUTED,5X,12HITERATION = ,I2)
620   FORMAT (1H1,57X,14HFINAL SOLUTION)
630   FORMAT (1H0,51X,2HXS,9X,2HRS,8X,5HTHETA/50X,4H(IN),8X,4H(IN),8X,9H
     1(DEGREES))
640   FORMAT (12A6)
650   FORMAT (1H0,51X,12A6)
660   FORMAT (1H0,43X,34HPLUG SURFACE HAS NEGATIVE Y VALUES)
      END
```

```
$IBFTC LANG
      SUBROUTINE LANGR1 (N,N1,NX,LAM4,OPTION)
      COMMON /B3/ PA,PO,TO,RHOO,G,R,GO
      COMMON /B4/ HO,RE,BD,ETA,RRE,RHOD,DELTAT,AA,AB,NCNT,THETAC
      COMMON /B5/ REG
      COMMON /B6/ NLOC
      COMMON /B7/ ERROR
      COMMON /B8/ NWRITE
      COMMON /B11/ CF1,CF2,CF3,CFI,FLRT,THRUST,FLRIC
      REAL LAM4,MOT
      DIMENSION REG(1275,7), NLOC(51), ERROR(50)
      INTEGER OPTION
      J1=NLOC(N)+N
      J2=NLOC(N-1)+N-1
      CALL SKIN (REG(J1,4),REG(J1,3),CFI,TAU,TAURD,TAUR,TAURHO,TAUVD,TAU
     1PD,RTAUDX)
      CALL BASE (REG(J1,1),REG(J1,2),REG(J1,4),REG(J1,3),PB,PPHIPY,PPHIP
     1X,AA,AB)
      FUNCT=1.+(G-1.)*REG(J1,3)**2/2.
      TE3A=TO/FUNCT
      P3A=PO/FUNCT**(G/(G-1.))
      DYDX=TAN(REG(J1,5))
      RHOA=RHOO/FUNCT**(1./(G-1.))
      U3A=REG(J1,4)*COS(REG(J1,5))
      CALL REST (REG(J1,1),H,HP,HR,HRD,DDX)
      LAM4=(REG(J1,2)*TAU+P3A*REG(J1,2)*DYDX-DYDX*PPHIPY+PPHIPX)/(-H)
      UU=U3A
      IF(NX.NE.1.AND.OPTION.NE.0) WRITE (6,120) LAM4
      REG(J1,7)=(REG(J1,2)*(TAU-DYDX*TAURD)+LAM4*(H-DYDX*HRD)+PPHIPX)*GO
     1/(+REG(J1,2)*RHOA*U3A*DYDX)
      AL2U=REG(J1,7)
      REG(J1,6)=+REG(J1,2)*RHOA*REG(J1,4)*SIN(REG(J1,5))-REG(J1,2)*U3A*(
     1TAUVD/REG(J1,4)-RHOA*TAUPD-RHOA*TAURHO/(G*GO*R*TE3A))+LAM4*RHOA*U3
     2A*HP
      C5=0.0
      CFI=0.0
      JO=N-1
      IF (NX.EQ.1) JO=N+1-N1
      J4=NLOC(N)+N
      DO 10 I=1,JO
      JT=N-I
      J1=NLOC(JT+1)+JT+1
      J2=NLOC(JT)+JT
      DX=REG(J2,1)-REG(J1,1)
      DY=REG(J2,2)-REG(J1,2)
      DV=REG(J2,4)*SIN(REG(J2,5))-REG(J1,4)*SIN(REG(J1,5))
      DVDX=DV/DX
      HP1=HP
      HR1=HR
      HRD1=HRD
      TAU1=TAU
      TAURD1=TAURD
      TAUR1=TAUR
      TAURH1=TAURHO
      TAUVD1=TAUVD
```

```
      TAUPD1=TAUPD
      RTAUX1=RTAUDX
      CALL SKIN (REG(J2,4),REG(J2,3),CF1,TAU,TAURD,TAUR,TAURHO,TAUVD,TAU
     1PD,RTAUDX)
      CALL REST (REG(J2,1),H,HP,HR,HRD,DDX)
      XE1=(REG(J1,1)+REG(J2,1))/2.
      YE1=(REG(J1,2)+REG(J2,2))/2.
      FE1=(REG(J1,3)+REG(J2,3))/2.
      VE1=(REG(J1,4)+REG(J2,4))/2.
      UE1=(REG(J1,4)*COS(REG(J1,5))+REG(J2,4)*COS(REG(J2,5)))/2.
      TE1=(REG(J1,5)+REG(J2,5))/2.
      FUNCT=1.+(G-1.)*FE1**2/2.
      RHOE1=RHOO/FUNCT**(1./(G-1.))
      TEE1=TO/FUNCT
      PE1=PO/FUNCT**(G/(G-1.))
      DYDX1=(TAN(REG(J1,5))+TAN(REG(J2,5)))/2.
      ASOE1=G*GO*R*TEE1
      HPE1=(HP1+HP)/2.
      HRE1=(HR1+HR)/2.
      HRDE1=(HRD-HRD1)/DX
      TAUE1=(TAU1+TAU)/2.
      TAURE1=(TAUR1+TAUR)/2.
      TAUDE1=(TAURD1+TAURD)/2.
      TAUVE1=(TAUVD1+TAUVD)/2.
      TAUPE1=(TAUPD1+TAURD)/2.
      TARHE1=(TAURHO+TAURH1)/2.
      RTAXE1=(RTAUX1+RTAUDX)/2.
      C1=(HPE1*DVDX-(HRE1-HRDE1)*GO/(RHOE1*UE1))*LAN4/YE1
      C2=(TAUE1+YE1*TAURE1-RTAXE1)*GO/(YE1*RHOE1*UE1)
      C3=Q1-C2
      C4=(TAUVE1*DVDX/(VE1*RHOE1)-TAUPE1*DVDX-TARHE1*DVDX/ASOE1)
      C5=Q1-C4
      UDOT=(REG(J2,4)*COS(REG(J2,5))-REG(J1,4)*COS(REG(J1,5)))/DX
      CF1=CF1+(PE1*DYDX1+TAUE1)*YE1*DX
      TE=TO/FUNCT
      FUNCT=1.+(G-1.)*REG(J2,3)**2/2.
      RHO=RHOO/FUNCT**(1./(G-1.))
      ASQ=G*GO*R*TE
      ALM2DX=UDOT-Q5
      REG(J2,7)=REG(J1,7)+ALM2DX*DX
      REG(J2,6)=+REG(J2,2)*RHO*REG(J2,4)*SIN(REG(J2,5))-REG(J2,2)*REG(J2
     1,4)*COS(REG(J2,5))*(TAUVD/REG(J2,4)-RHO*TAUPD-RHO*TAURHO/ASQ)+LAN4
     2*RHO*REG(J2,4)*COS(REG(J2,5))*HP
   10 CONTINUE
      IF (OPTION.EQ.0) GO TO 30
      IF (NX.EQ.1) GO TO 40
      WRITE (6,140)
      DO 20 I=1,N
      J1=NLOC(I)+1
      WRITE (6,150) J1,REG(J1,6),REG(J1,7)
   20 CONTINUE
   30 THRUST=2.*3.14159*(CF1+CF2+CF3-RE**2*PA/2.+REG(J4,2)**2*PR/2.)
      IF(OPTION.NE.0) WRITE (6,160) THRUST
      IF(OPTION.EQ.0) GO TO 100
C
C     CALCULATE THE LAGRANGIAN MULTIPLIERS IN R
```

```
C
      IF (NWRITE.NE.0) WRITE (6,110)
      IOB=1
      JOB=1
      IF (NWRITE.NE.0) WRITE (6,120) IOB,JOB,REG(1,6),REG(1,7)
      IF (NWRITE.NE.0) WRITE (6,130)
40    DO 60 I=N1,N
      I1=I-1
      I2=I+1
      IS=I+1-N1
      JOB=NLOC(I)+1
      IF (NWRITE.NE.0) WRITE (6,120) I,I,REG(JOB,6),REG(JOB,7)
      DO 50 M=1,IS
      M1=I-M
      M2=I2-M
      J1=NLOC(I)+M2
      J2=NLOC(I1)+M1
      J3=J1-1
      E13=(REG(J1,3)+REG(J3,3))/2.
      E23=(REG(J2,3)+REG(J3,3))/2.
      Y13=(REG(J1,2)+REG(J3,2))/2.
      Y23=(REG(J2,2)+REG(J3,2))/2.
      RHO13=RHO0/(1.+(G-1.)*E13**2/2.)**(1./(G-1.))
      RHO23=RHO0/(1.+(G-1.)*E23**2/2.)**(1./(G-1.))
      F1=Y13*RHO13*SQRT(E13**2-1.)
      F2=Y23*RHO23*SQRT(E23**2-1.)
      REG(J3,7)=(REG(J1,6)-REG(J2,6)+REG(J1,7)*F1+REG(J2,7)*F2)/(F1+F2)
      REG(J3,6)=REG(J1,6)-F1*(REG(J3,7)-REG(J1,7))
      JOB=M2-1
      IF (NWRITE.NE.0) WRITE (6,120) I,JOB,REG(J3,6),REG(J3,7)
      IF (I.LT.N) GO TO 50
      ME=N+1-M
      RHO=RHO0/(1.+(G-1.)*REG(J1,3)**2/2.)**(1./(G-1.))
      ERROR(ME)=REG(J1,6)-REG(J1,7)*REG(J1,2)*RHO*SQRT(REG(J1,3)**2-1.)
50    CONTINUE
      IF (NWRITE.NE.0) WRITE (6,130)
60    CONTINUE
      IF (ME.NE.2) GO TO 70
      RHO=RHO0/(1.+(G-1.)*REG(J3,3)**2/2.)**(1./(G-1.))
      ERROR(1)=REG(J3,6)-REG(J3,7)*REG(J3,2)*RHO*SQRT(REG(J3,3)**2-1.)
70    CONTINUE
      IF (NK.NE.1) GO TO 80
      GO TO 100
C
80    WRITE (6,140)
      DO 90 I=1,N
      WRITE (6,150) I,ERROR(I)
90    CONTINUE
100   CONTINUE
      RETURN
C
C
C
110   FORMAT (1H1,46X,1HI,4X,1HJ,5X,7HLAMBDA1,4X,7HLAMBDA2/1H0)
120   FORMAT (1H1,50X,7HLAM4 = ,F12.5)
130   FORMAT (1H0)
```

```
140   FORMAT (1H0,48X,31HLAGRANGE MULTIPLIERS ALONG WALL//1H0,48X,5HPOINLAN 167
     1T,7X,7HLAMBDA1,6X,7HLAMBDA2)                                      LAN 168
150   FORMAT (50X,I4,4X,F10.2,4X,F10.2)                                 LAN 169
160   FORMAT (1H0,46X,9HTHRUST = ,F15.5,4H LBF)                         LAN 170
170   FORMAT (43X,2I5,F10.2,4X,F10.2)                                   LAN 171
180   FORMAT (1H1,50X,21HERROR ALONG EXIT CHAR//53X,5HPOINT,8X,5HERROR//LAN 172
     1)                                                                 LAN 173
190   FORMAT (54X,I3,3X,F12.5)                                          LAN 174
      END                                                               LAN 175-
```

```
$IBFTC STARTI
      SUBROUTINE START (F1,N2,PNO,J,NPTSS,DELTPP,XLENS,YLAST,TLAST)
      REAL M,K0,K1,K2,K3,ML,M1,M2,M3,M4,MR,L,NR,KK
      INTEGER OPT1,OPT2,OPT3
      COMMON /B2/ XL,RL,ML,VL,TL
      COMMON /B3/ PA,PO,TO,RHOO,G,R,GO
      COMMON /B4/ HO,RE,BD,ETA,RKE,RHOD,DELTAT,AA,AB,NCNT,THETAC
      COMMON /B8/ NWRITE
      COMMON /B9/ RAD,FOOT
      COMMON /B11/ CF1,CF2,CF3,CFI,FLRT,THRUST,FLRTC
      COMMON /B12/ NREAD1,NREAD2,OPT1,OPT2,OPT3
      COMMON /B13/ XS,RS,TS
      DIMENSION XL(75), RL(75), ML(75), VL(75), TL(75), XS(125), RS(125)
     1,TS(125), A9(4,5)
      WRITE (6,490)
      THETAC=THETAC*RAD
      PN=0
10    CF3=0.0
      FLRT=0.0
      IF (NREAD2.EQ.0) GO TO 140
      AS=SQRT((2.0*G*GO*R*TO)/(G+1.0))
      RX=RKE/MI
      EPS=1.0/SQRT(RX)
      FI=(G-1.0)/(G+1.0)
      BR=BD*3.14159/180.0
      D=RL-HO*COS(BR)
      P=HO*SIN(BR)/(D*EPS)
      XO=HO*SIN(BR)
      B1=SQRT((1.0-FI)*(0.5-M**2))
      B0=(1.0-FI)*M/(4.0*B1)-(1.0-FI)*M*M*M/(6.0*B1)-1.0/6.0
      K0=M*ETA/2.-B1*ETA/(1.0-FI)
      K1=2.0*B0*B1/(1.0-FI)-M*B0+M*M*M*(COS(BR)/SIN(BR))**2
      K2=2.0*ETA*B1/(1.0-FI)-3.0*ETA*M
      K3=B1/(1.0-FI)+1.5*M**2*B1-3.0*M+2.5*M*M*M-3.0*M*P*M*(COS(BR)/SIN(
     1BR))**2
      Y=0.0
      Z=0.0
      A1=(1.0-M*B1-M**2)*Y**2/2.0+1.0*ETA*Y
      A1P=(1.0-M*B1-M**2)*Y+2.0*ETA
      A0=K0+K1*Y+0.5*K2*Y**2+K3*Y*Y*Y/3.0
20    Z=Z+0.025
      U1=A1+B0+B1*Z
      V1=A0+Z*A1P
      UP=U1*EPS**2
      VP=-M*Y*EPS+(M*EPS)**2*(Y**2-1.0)*COS(BR)/SIN(BR)+V1*EPS**3.0
      UY=(1.0+UP)*AS
      VY=VP*AS
      VEL=SQRT(VY**2+UY**2)
      TEM=TO-VEL**2*(G-1.0)/(2.0*G*GO*R)
      A=SQRT(G*GO*R*TEM)
      EM=VEL/A
      IF (EM.LE.E1) GO TO 20
      Z0=Z
      N=0
      N1=N2+1
```

```
      N3=N2-1
      DELY=N3
      Y=(DELY+2.)/DELY
      DO 90 I=1,N2
      N=N+1
      N3=N1-1
      Y=(Y*DELY-2.)/DELY
      IF (Y) 40,40,30
30    Z=ZO*(1.0-Y)
      GO TO 50
C
40    Z=ZO*(1.0+Y)
50    A1=(1.0-M*B1-M**2)*Y**2/2.0+2.0*ETA*Y
      A1P=(1.0-M*B1-M**2)*Y+2.0*ETA
      A0=K0+K1*Y+0.5*K2*Y**2+K3*Y*Y*Y/3.0
      U1=A1+A0*B1*Z
      V1=A0+Z*A1P
      YP=H0*Y
      XP=H0*EPS*Z
      UP=U1*EPS**2
      VP=-H*Y*EPS+(H*EPS)**2*(Y**2-1.0)*COS(BR)/SIN(BR)+V1*EPS**3.0
      TR=ATAN(VP/(1.0+UP))
      TL(N3)=TR+BR
      VY=VP*AS
      UY=(1.0+UP)*AS
      VL(N3)=SQRT(VY**2+UY**2)
      XL(N3)=XP*COS(BR)-YP*SIN(BR)+XO
      RL(N3)=D+XP*SIN(BR)+YP*COS(BR)
      TE=TO-VL(N3)**2*(G-1.)/(2.*GO*R*G)
      A=SQRT(G*GO*R*TE)
      ML(N3)=VL(N3)/A
      IF (Y.GT.0.0) GO TO 60
      PHIN=ATAN(1./(EPS*ZO))+BR
      GO TO 70
C
60    PHIN=3.14159+ATAN(-1./(EPS*ZO))+BR
70    CONTINUE
      IF (I.EQ.1) GO TO 80
      T1=(TL(N3)+TL(N3+1))/2.
      PHIA=(PHIN+PHIO)/2.
      EE1=(ML(N3)+ML(N3+1))/2.
      VE1=(VL(N3)+VL(N3+1))/2.
      FUNCT=1.+(G-1.)*EE1**2/2.
      PE1=PO/FUNCT**(G/(G-1.))
      RHOE1=RHOO/FUNCT**(1./(G-1.))
      YE1=(RL(N3)+RL(N3+1))/2.
      DY=RL(N3)-RL(N3+1)
      FLRT=FLRT-(RHOE1*VE1*SIN(PHIA-T1)*YE1*DY/(SIN(PHIA)))
      CF3=CF3-(PE1+RHOE1*VE1**2*SIN(PHIA-T1)*COS(T1)/(GO*SIN(PHIA)))*YE1
     1*UY
80    PHIO=PHIN
90    CONTINUE
      FLRT=FLRT*2.*3.14159
      IF (OPT3.EQ.0) GO TO 110
      IF (MN.GT.0) GO TO 100
      IF (ABS(FLRTC-FLRT).LT..001) GO TO 110
```

```
      FLRTS=FLRT
      WRITE (6,460) FLRT
      HO=HO*FOOT
      WRITE (6,470) HO
      DHO=HO*0.01
      HO=HO+DHO
      MN=MN+1
      GO TO 10
C
100   PHDOT=(FLRT-FLRTS)/DHO
      HO=HO-DHO
      DHO=(FLRTC-FLRTS)/PHDOT
      HO=HO+0.75*DHO
      MN=0
      GO TO 10
C
110   WRITE (6,500) EPS,ZO
120   WRITE (6,510)
      WRITE (6,530)
      N1=N2+1
      DO 130 I=1,N2
      N3=N1-I
      TO=TL(N3)*180./3.14159
      XO=XL(N3)*FOOT
      RO=RL(N3)*FOOT
      WRITE (6,520) XO,RO,ML(N3),VL(N3),TO
130   CONTINUE
      WRITE (6,460) FLRT
      HO=HO*FOOT
      WRITE (6,470) HO
      WRITE (6,530)
      GO TO 250
C
140   CONTINUE
      IF (OPT2.EQ.1) GO TO 170
      WRITE (6,510)
      WRITE (6,530)
      N1=N2+1
      N=0
      DO 160 I=1,N2
      N3=N1-I
      N=N+1
      IF (I.EQ.1) GO TO 150
      T1=(TL(N3)+TL(N3+1))/2.
      PHIA=ATAN((RL(N3+1)-RL(N3))/(XL(N3+1)-XL(N3)))
      EE1=(ML(N3)+ML(N3+1))/2.
      VE1=(VL(N3)+VL(N3+1))/2.
      FUNCT=1.+(G-1.)*EE1**2/2.
      PE1=PO/FUNCT**(G/(G-1.))
      RHOE1=RHOO/FUNCT**(1./(G-1.))
      YE1=(RL(N3)+RL(N3+1))/2.
      DY=RL(N3)-RL(N3+1)
      FLRT=FLRT-(RHOE1*VE1*SIN(PHIA-T1)*YE1*DY/(SIN(PHIA)))
      CF3=CF3-(PE1+RHOE1*VE1**2*SIN(PHIA-T1)*COS(T1)/(GO*SIN(PHIA)))*YE1
     1*DY
150   TO=TL(N3)/RAD
```

```
      XD=XL(N3)*FOOT
      RD=RL(N3)*FOOT
      WRITE (6,520) XD,RD,ML(N3),VL(N3),TD
160   CONTINUE
      FLRT=FLRT*2.*3.14159
      WRITE (6,530)
      GO TO 250
C
170   CONTINUE
180   T1=BD*RAD
      X2=0.0
      CF3=0.0
      N=0
      FLRT=0.0
      Y2=RE
      X1=X2+2.*HO*SIN(T1)
      Y1=Y2-2.*HO*COS(T1)
      IF (T1.EQ.0.0) GO TO 190
      B1=(Y2-Y1)/(X2-X1)
      B2=Y1-(Y2-Y1)*X1/(X2-X1)
      XN=N2-1
      DX=(X2-X1)/XN
      X=X1-DX
      DTHETA=THETAC/XN
      T1=T1-DTHETA-THETAC/2.0
      GO TO 200
C
190   DX=0.0
      XN=N2-1
      DY=(Y2-Y1)/XN
      Y=Y1-DY
      DTHETA=THETAC/XN
      T1=T1-DTHETA-THETAC/2.0
200   PHIA=90.0*RAD+T1
      FUNCT=1.+(G-1.)*E1**2/2.
      TE=TO/FUNCT
      A1=SQRT(G*GO*R*TE)
      VE1=E1*A1
      PE1=PO/FUNCT**(G/(G-1.))
      RHOE1=RHOO/FUNCT**(1./(G-1.))
      DO 230 I=1,N2
      N=N+1
      IF (T1.EQ.0.0) GO TO 210
      X=X+DX
      XL(I)=X
      RL(I)=B1*X+B2
      GO TO 220
C
210   XL(I)=X2
      Y=Y+DY
      RL(I)=Y
220   ML(I)=E1
      VL(I)=VE1
      T1=T1+DTHETA
      TL(I)=T1
      IF (I.EQ.1) GO TO 230
```

```
      N3=I-1
      VE1=(RL(I)+RL(N3))/2.
      DY=RL(I)-RL(N3)
      FLRT=FLRT+(RHOE1*VE1*SIN(PHIA-T1)*VE1*DY/(SIN(PHIA)))
      CF3=CF3+(PE1+RHOE1*VE1**2*SIN(PHIA-T1)*COS(T1)/(GO*SIN(PHIA)))*VE1
     1*DY
  230 CONTINUE
      FLRT=FLRT*2.*3.14159
      IF (OPT3.EQ.0) GO TO 120
      IF (MN.GT.0) GO TO 240
      IF (ABS(FLRTC-FLRT).LT..001) GO TO 120
      FLRTS=FLRT
      DHO=HO*0.01
      HO=HO+DHO
      MN=MN+1
      GO TO 180
C
  240 PMDOT=(FLRT-FLRTS)/DHO
      HO=HO-DHO
      DHO=(FLRTC-FLRTS)/PMDOT
      HO=HO+DHO
      MN=0
      GO TO 180
C
C      CALCULATE THE PRANDTL-MEYER EXPANSION AT E
C
  250 DM=DELTPM
  260 NSTOP=0
      J=N
      J=J+1
      E1=ML(N)
      T1=TL(N)
      ALFA=ATAN(1.0/SQRT(E1**2-1.0))
      TCHKS=T1-ALFA+0.00044
      SN2=E1**2/(1.+(G-1.)*E1**2/2.)
      SN4=SN2*(1.-G**2)/2.+G
      SNA=SN4/SQRT(1.0-SN4**2)
      SN6=G-2./SN2
      SNB=SN6/SQRT(1.0-SN6**2)
      PM1=-SQRT((G+1.0)/(G-1.0))*(ATAN(SNA)-3.14159/2.0)/2.0-(ATAN(SNB)+
     13.14159/2.0)/2.0
      WRITE (6,540)
      WRITE (6,510)
      WRITE (6,530)
  270 E1=E1+DM
  280 SN2=E1**2/(1.+(G-1.)*E1**2/2.)
      SN4=SN2*(1.-G**2)/2.+G
      SNA=SN4/SQRT(1.0-SN4**2)
      SN6=G-2./SN2
      SNB=SN6/SQRT(1.0-SN6**2)
      PM2=-SQRT((G+1.0)/(G-1.0))*(ATAN(SNA)-3.14159/2.0)/2.0-(ATAN(SNB)+
     13.14159/2.0)/2.0
      DT=PM2-PM1
      T1=T1+DT
      XL(J)=XL(N)
      RL(J)=RL(N)
```

```
      ML(J)=E1
      TL(J)=T1
      FUNCT=1.0+(G-1.0)*E1**2/2.0
      PRES=PO/FUNCT**(G/(G-1.0))
      TEA=TO/FUNCT
      SPA=SQRT(G*GO*R*TEA)
      VL(J)=ML(J)*SPA
      PNEW=PRES-PNO
      IF (NSTOP.EQ.1) GO TO 340
      ALFA=ATAN(1.0/SQRT(E1**2-1.0))
      TCHK=T1-ALFA+.00044
      DTCPM=(TCHK-TCHKS)/DM
      IF (TCHK.GT.0.0) GO TO 310
      TCHKS=TCHK
      IF (PNEW) 330,340,290
290   CONTINUE
      TD=T1*180./3.14159
      XD=XL(J)*FOOT
      RD=RL(J)*FOOT
      WRITE (6,520) XD,RD,ML(J),VL(J),TD
      J=J+1
      IF (J.GT.75) GO TO 300
      PM1=PM2
      GO TO 270
C
300   DM=DM+.01
      GO TO 260
C
310   CONTINUE
      TCHK=TCHKS
      NSTOP=1
      T1=T1-DT
      E1=E1-DM
320   DMM=-TCHK/DTCPM
      DMM=DMM*0.65
      E1=E1+DMM
      SN2=E1**2/(1.+(G-1.)*E1**2/2.)
      SN4=SN2*(1.-G**2)/2.+G
      SNA=SN4/SQRT(1.0-SN4**2)
      SN6=G-2./SN2
      SNB=SN6/SQRT(1.0-SN6**2)
      PM2=-SQRT((G+1.0)/(G-1.0))*(ATAN(SNA)-3.14159/2.0)/2.0-(ATAN(SNB)+
     13.14159/2.0)/2.0
      DT=PM2-PM1
      T1=T1+DT
      ALFA=ATAN(1.0/SQRT(E1**2-1.0))
      TCHK=T1-ALFA+.00044
      IF (TCHK.GT.-0.00087.AND.TCHK.LT.0.0) GO TO 280
      DTCPM=(TCHK-TCHKS)/DMM
      TCHKS=TCHK
      PM1=PM2
      GO TO 320
C
330   CONTINUE
      NSTOP=1
      T1=T1-DT
```

```
      E1=E1-DM
      E1=SQRT(2.0*((PO/PNO)**((G-1.0)/G)-1.0)/(G-1.0))
      GO TO 280
C
340   CONTINUE
      TD=T1*180./3.14159
      XD=XL(J)*FOOT
      RD=RL(J)*FOOT
      WRITE (6,520) XD,RD,ML(J),VL(J),TD
      PFINAL=PO/(1.0+(G-1.0)*E1**2/2.0)**(G/(G-1.0))
      PFINAL=PFINAL/144.0
      WRITE (6,480) PFINAL
C
C     WRITE OUT THE FIRST GUESS OF THE OPTIMUM SURFACE
C
      IF (NREAD1.EQ.0) GO TO 440
      THOLD=TL(1)/RAD
      XHOLD=XL(1)
      RHOLD=RL(1)
      TN=(90.+THOLD)*RAD
      XC=XHOLD-RHOD*COS(TN)
      YC=RHOLD-RHOD*SIN(TN)
      TS(1)=THOLD
      XS(1)=XHOLD
      RS(1)=RHOLD
      DO 350 I=2,NCNT
      TS(I)=TS(I-1)-DELTAT
      TN=(90.+TS(I))*RAD
      XS(I)=RHOD*COS(TN)+XC
      RS(I)=YC+RHOD*SIN(TN)
      IH=I
350   CONTINUE
      X1=XS(IH)
      Y1=RS(IH)
      T1=TS(IH)*RAD
      X2=XLENG+XL(1)
      Y2=YLAST
      T2=TLAST*RAD
      IF (T1.GT.T2) GO TO 360
      E1=-1.
      E3=0.0
      E4=0.0
      E2=-1.
      A9(1,1)=X1**2
      A9(1,2)=Y1**2
      A9(1,3)=X1
      A9(1,4)=Y1
      A9(2,1)=X2**2
      A9(2,2)=Y2**2
      A9(2,3)=X2
      A9(2,4)=Y2
      A9(3,1)=2.0*X1
      A9(3,2)=2.0*Y1*TAN(T1)
      A9(3,3)=1.0
      A9(3,4)=TAN(T1)
      A9(4,1)=2.0*X2
```

```
      A9(4,2)=2.*Y2*TAN(T2)
      A9(4,3)=1.0
      A9(4,4)=TAN(T2)
      GO TO 370
C
360   E1=Y1
      E2=Y2
      E3=TAN(T1)
      E4=TAN(T2)
      A9(1,1)=X1**3.
      A9(1,2)=X1**2
      A9(1,3)=X1
      A9(1,4)=1.
      A9(2,1)=X2**3.
      A9(2,2)=X2**2
      A9(2,3)=X2
      A9(2,4)=1.
      A9(3,1)=3.*X1**2
      A9(3,2)=2.*X1
      A9(3,3)=1.
      A9(3,4)=0.0
      A9(4,1)=3.*X2**2
      A9(4,2)=2.*X2
      A9(4,3)=1.
      A9(4,4)=0.0
370   CONTINUE
      ADET1=(A9(1,1)*A9(2,2)*A9(3,3)+A9(2,1)*A9(3,2)*A9(1,3)+A9(3,1)*A9(
     12,3)*A9(1,2))-(A9(1,3)*A9(2,2)*A9(3,1)+A9(2,3)*A9(3,2)*A9(1,1)+A9(
     23,3)*A9(2,1)*A9(1,2))
      ADET2=(A9(1,1)*A9(2,2)*A9(3,4)+A9(2,1)*A9(3,2)*A9(1,4)+A9(3,1)*A9(
     12,4)*A9(1,2))-(A9(1,4)*A9(2,2)*A9(3,1)+A9(2,4)*A9(3,2)*A9(1,1)+A9(
     23,4)*A9(2,1)*A9(1,2))
      ADET3=(A9(1,1)*A9(2,2)*A9(4,3)+A9(2,1)*A9(4,2)*A9(1,3)+A9(4,1)*A9(
     12,3)*A9(1,2))-(A9(1,3)*A9(2,2)*A9(4,1)+A9(2,3)*A9(4,2)*A9(1,1)+A9(
     24,3)*A9(2,1)*A9(1,2))
      ADET4=(A9(1,1)*A9(2,2)*A9(4,4)+A9(2,1)*A9(4,2)*A9(1,4)+A9(4,1)*A9(
     12,4)*A9(1,2))-(A9(1,4)*A9(2,2)*A9(4,1)+A9(2,4)*A9(4,2)*A9(1,1)+A9(
     24,4)*A9(2,1)*A9(1,2))
      ADET5=A9(1,1)*A9(2,2)-A9(1,2)*A9(2,1)
      ADET=(ADET1*ADET4)-(ADET2*ADET3)
      ADET=ADET/ADET5
      ADETS=ADET
      DO 380 I=1,4
      A1S=A9(1,I)
      A2S=A9(2,I)
      A3S=A9(3,I)
      A4S=A9(4,I)
      A9(1,I)=E1
      A9(2,I)=E2
      A9(3,I)=E3
      A9(4,I)=E4
      ADET1=(A9(1,1)*A9(2,2)*A9(3,3)+A9(2,1)*A9(3,2)*A9(1,3)+A9(3,1)*A9(
     12,3)*A9(1,2))-(A9(1,3)*A9(2,2)*A9(3,1)+A9(2,3)*A9(3,2)*A9(1,1)+A9(
     23,3)*A9(2,1)*A9(1,2))
      ADET2=(A9(1,1)*A9(2,2)*A9(3,4)+A9(2,1)*A9(3,2)*A9(1,4)+A9(3,1)*A9(
     12,4)*A9(1,2))-(A9(1,4)*A9(2,2)*A9(3,1)+A9(2,4)*A9(3,2)*A9(1,1)+A9(
```

```
23,4)*A9(2,1)*A9(1,2))
 ADET3=(A9(1,1)*A9(2,2)*A9(4,3)+A9(2,1)*A9(4,2)*A9(1,3)+A9(4,1)*A9(
12,3)*A9(1,2))-(A9(1,3)*A9(2,2)*A9(4,1)+A9(2,3)*A9(4,2)*A9(1,1)+A9(
24,3)*A9(2,1)*A9(1,2))
 ADET4=(A9(1,1)*A9(2,2)*A9(4,4)+A9(2,1)*A9(4,2)*A9(1,4)+A9(4,1)*A9(
12,4)*A9(1,2))-(A9(1,4)*A9(2,2)*A9(4,1)+A9(2,4)*A9(4,2)*A9(1,1)+A9(
24,4)*A9(2,1)*A9(1,2))
 ADET5=A9(1,1)*A9(2,2)-A9(1,2)*A9(2,1)
 ADET=(ADET1*ADET4)-(ADET2*ADET3)
 ADET=ADET/ADET5
 A9(1,5)=ADET/ADETS
 A9(1,I)=A1S
 A9(2,I)=A2S
 A9(3,I)=A3S
 A9(4,I)=A4S
380  CONTINUE
     IF (T1.GT.T2) GO TO 390
     M3=(Y2-Y1)/(X2-X1)
     C3=Y1-M3*X1
     KK=-A9(1,5)*A9(2,5)/(A9(2,5)*M3**2+A9(1,5))
     A=A9(1,5)+KK*M3**2
     B=-2.*KK*M3
     C=A9(2,5)+KK
     D=A9(3,5)+2.*KK*C3*M3
     E=A9(4,5)-2.*KK*C3
     F=1.+KK*C3**2
     GU TO 400
C
390  A=A9(1,5)
     B=A9(2,5)
     C=A9(3,5)
     D=A9(4,5)
400  CONTINUE
     CNPTS=NPTSS-NCNT
     DX=(X2-X1)/CNPTS
     X=X1
     NNN=NCNT+1
     DO 430 I=NNN,NPTSS
     X=X+DX
     V=B*X+E
     W=A*X**2+D*X+F
     IF (T1.GT.T2) GO TO 410
     RS(I)=(-V-SQRT(V**2-4.*C*W))/(2.*C)
     TS(I)=ATAN((-2.*A*X-B*RS(I)-D)/(B*X+2.*C*RS(I)+E))/RAD
     GO TO 420
C
410  RS(I)=A*X**3.+B*X**2+C*X+D
     TS(I)=ATAN(3.*A*X**2+2.*B*X+C)/RAD
420  XS(I)=X
430  CONTINUE
440  XS(1)=XL(1)
     RS(1)=RL(1)
     TS(1)=TL(1)/RAD
     WRITE (6,550)
     WRITE (6,530)
     WRITE (6,560)
```

```
      WRITE (6,530)                                                     STA 503
      DO 450 I=1,NPTSS                                                  STA 504
      XO=XS(I)*FOUT                                                     STA 505
      RO=RS(I)*FCOT                                                     STA 506
      WRITE (6,570) XO,RO,TS(I)                                         STA 507
450   CONTINUE                                                          STA 508
      RETURN                                                            STA 509
C                                                                       STA 510
C                                                                       STA 511
C                                                                       STA 512
460   FORMAT (1H0,46X,17HMASS FLOW RATE = ,F15.5,8H LBM/SEC)            STA 513
470   FORMAT (1H0,46X,5HRO = ,F15.5,7H INCHES)                          STA 514
480   FORMAT (1H0,42X,9HPFINAL = ,F10.5,5H PSIA)                        STA 515
490   FORMAT (1H1,48X,23HDATA FOR THE START LINE///)                    STA 516
500   FORMAT (44X,7H LPS = ,F6.3,5X,6H ZO = ,F7.5)                      STA 517
510   FORMAT (1H0,54X,4HMACH,22X,4HFLOW/35X,2HXC,8X,2HRC,5X,6HNUMBER,7X,STA 518
     1HHVELOCITY,7X,5HANGLE/34X,4H(IN),6X,4H(IN),18X,5H(FPS),7X,9H(DEGRESTA 519
     2ES))                                                              STA 520
520   FORMAT (31X,3F10.5,F15.5,F12.5)                                   STA 521
530   FORMAT (1H0)                                                      STA 522
540   FORMAT (1H1,42X,37HDATA FOR PRANDTL-MEYER EXPANSION AT E)         STA 523
550   FORMAT (1H1,42X,35HFIRST GUESS FOR THE OPTIMUM SURFACE)           STA 524
560   FORMAT (1H0,46X,2HXS,8X,2HRS,9X,5HTHETA/45X,4H(IN),8X,4H(IN),6X,9HSTA 525
     1(DEGREES))                                                        STA 526
570   FORMAT (42X,2F10.5,F15.5)                                         STA 527
      END                                                               STA 528-
```

```
$IBFTC EXT
      SUBROUTINE EXTEND (NTOT,NDEGR1,NPTSN,ITOT,NWRITE,NSAVE,XFINAL,ITER
     1)
      REAL ML,MA,MB
      COMMON /B3/ PA,PO,TO,RHOO,G,R,GO
      COMMON /B2/ XL,RL,ML,VL,TL
      COMMON /B5/ REG
      COMMON /B6/ NPOINT
      COMMON /B9/ RAD,FOOT
      COMMON /B10/ XA,YA,MA,VA,TA
      COMMON /B11/ CF1,CF2,CF3,CFI,FLRT,THRUST,FLRTC
      COMMON /B13/ XS,RS,TS
      DIMENSION REG(1275,7), XL(75), RL(75), ML(75), VL(75), TL(75), NPO
     1INT(51), XS(125), RS(125), TS(125), XA(75), YA(75), MA(75), VA(75)
     2, TA(75), XB(100), YB(100), MB(100), VB(100), TB(100)
      IF (NWRITE.NE.0) WRITE (6,70)
      IF (NWRITE.NE.0) WRITE (6,80)
      DO 10 I=1,NTOT
      XA(I)=XL(I)
      YA(I)=RL(I)
      MA(I)=ML(I)
      VA(I)=VL(I)
   10 TA(I)=TL(I)
      ITOT=NTOT
      CF2=0.0
      CALL SKIN (VA(1),MA(1),CFI,TAU,TAURD,TAUR,TAURH),TAUVD,TAUPD,RTAUD
     1X)
      TAU1=TAU
      IF (NPTSN.EQ.0) GO TO 40
      NJOIN=NPTSN+1
      DO 30 J=2,NJOIN
      XB(1)=XS(J)
      YB(1)=RS(J)
      TB(1)=TS(J)*RAD
      CALL LOCAT (ITOT,XB(1),YB(1),TB(1),NDEGR1,V1,E1A,X3A,Y3A,E3A,V3A,T
     13A,NSTRT,J)
      MB(1)=E1A
      VB(1)=V1
      KOB=0
      IOB=1
      JOB=J-1
      TD=TB(1)/RAD
      XD=XB(1)*FOOT
      RD=YB(1)*FOOT
      IF (NWRITE.NE.0) WRITE (6,90) IOB,JOB,XD,RD,MB(1),VB(1),TD,KOB
      EE1=(MA(1)+MB(1))/2.
      VE1=(VA(1)+VB(1))/2.
      DY1=YB(1)-YA(1)
      CALL SKIN (VB(1),MB(1),CFI,TAU,TAURD,TAUR,TAURH),TAUVD,TAUPD,RAUDX
     1)
      TAUE1=(TAU1+TAU)/2.
      DYDX=(TAN(TA(1))+TAN(TB(1)))/2.
      PE1=PO/(1.+(G-1.)*EE1**2/2.)**(G/(G-1.))
      DX=XB(1)-XA(1)
      CF2=CF2-(PE1*DYDX+TAUE1)*VE1*DX
```

```
      TAU1=TAU
      L=0
      NSTOP=ITOT
      DO 20 K=NSTRT,NSTOP
      L=L+1
      CALL CHAR1 (XA(K),XB(L),YA(K),YB(L),VA(K),VB(L),TA(K),TB(L),MA(K),
     1MB(L),TO,G,GO,R,X3A,Y3A,V3A,T3A,E3A,I)
      XB(L+1)=X3A
      YB(L+1)=Y3A
      MB(L+1)=E3A
      VB(L+1)=V3A
      TD=T3A/RAD
      IOB=IOB+1
      XD=X3A*FOOT
      RD=Y3A*FOOT
      IF (NWRITE.NE.0) WRITE (6,90) IOB,JOB,XD,RD,E3A,V3A,TD,I
      TB(L+1)=T3A
      XA(L)=XB(L)
      YA(L)=YB(L)
      MA(L)=MB(L)
      VA(L)=VB(L)
      TA(L)=TB(L)
   20 ITOT=L+1
      XA(ITOT)=XB(ITOT)
      YA(ITOT)=YB(ITOT)
      IF (NWRITE.NE.0) WRITE (6,100)
      MA(ITOT)=MB(ITOT)
      VA(ITOT)=VB(ITOT)
   30 TA(ITOT)=TB(ITOT)
   40 CONTINUE
      DO 50 I=1,NTOT
      ISV=I
      XCK=XFINAL-XA(I)
      IF (XCK) 60,60,50
   50 CONTINUE
   60 NSUB=ISV+2
      NSAVE=ISV+12-ITER
      IF (NSAVE.LT.NSUB) NSAVE=NSUB
      IF (NSAVE.GT.ITOT) NSAVE=ITOT
      RETURN
C
C
C
   70 FORMAT (1H1,39X,32HFLOW FIELD EXTENSION FROM A TO T)
   80 FORMAT (1H0,54X,4HMACH,22X,4HFLOW/25X,1HI,4X,1HJ,4X,2HXC,8X,2HRC,6
     1X,6HNUMBER,6X,8HVELOCITY,7X,5HANGLE,6X,4HITER/34X,4H(IN),6X,4H(IN)
     2,18X,5H(FPS),7X,9H(DEGREES))
   90 FORMAT (21X,2I5,3F10.5,F15.5,F12.5,I7)
  100 FORMAT (1H0)
      END
```

```
$IBFTC LOCAT
      SUBROUTINE LOCAT (ITOT,X1,Y1,T1,ND,V1,E1A,X3A,Y3A,E3A,V3A,T3A,NSTR
     1T,J)
      REAL MA
      COMMON /B13/ XS,RS,TS
      COMMON /B10/ XA,YA,MA,VA,TA
      COMMON /B3/ PA,PO,TO,RHOC,G,R,GO
      DIMENSION  XA(75), YA(75), MA(75), VA(75), TA(75), XS(125), RS(125
     1), TS(125)
      KP=J-1
      I=0
      X3A=(X1+XS(KP))/2.0
      GO TO 20
C
10    ADIV=I
      X3A=XS(KP)+(X1-XS(KP))/ADIV
20    I=I+1
      CALL AITKEN (XA,YA,ITOT,ND,X3A,YB)
      Y3A=YB
      CALL AITKEN (XA,MA,ITOT,ND,X3A,YB)
      E3A=YB
      CALL AITKEN (XA,VA,ITOT,ND,X3A,YB)
      V3A=YB
      CALL AITKEN (XA,TA,ITOT,ND,X3A,YB)
      T3A=YB
      A3A=ATAN(1./SQRT(E3A**2-1.))
      Y13=(Y1+Y3A)/2.
      T13=(T1+T3A)/2.
      IF (I.NE.1) GO TO 30
      C3=COS(A3A)/(SIN(A3A)*V3A)
      G3=SIN(T3A)*SIN(A3A)/SIN(T3A-A3A)
      A13=A3A
      C13=C3
      G13=G3
      GO TO 40
C
30    A13=(A1+A3A)/2.
      V13=(V1+V3A)/2.
      C13=COS(A13)/(SIN(A13)*V13)
      G13=SIN(T13)*SIN(A13)/SIN(T13-A13)
40    C=TAN(T13-A13)
      D=Y1-C*X1
      KP=1
      KX=2
      IF (X3A.GT.XA(KX)) GO TO 70
      IF(I.GE.50) GO TO 140
50    XX1=XA(KP)
      YY1=YA(KP)
      XX2=X3A
      YY2=Y3A
      KY=KP+1
      IF (XX1.EQ.XX2) GO TO 60
      GO TO 90
C
60    XX1=XA(KY)
```

```
      YY1=YA(KY)
      GO TO 90
C
70    DO 80 KQ=3,ITOT
      KX=KQ
      KP=KX-1
      IF (X3A.LE.XA(KQ)) GO TO 50
80    CONTINUE
      KP=1
      GO TO 50
C
90    A=(YY2-YY1)/(XX2-XX1)
      B=YY2-A*XX2
      X3A=(D-B)/(A-C)
      IF (X3A.LE.XS(1)) GO TO 10
      V1=V3A+(T3A-T1-G13*(Y3A-Y1)/Y13)/Q13
      TE1=T0-V1**2*(G-1.)/(2.*G*G0*R)
      SP1=SQRT(G*G0*R*TE1)
      E1A=V1/SP1
      A1=ATAN(1./SQRT(E1A**2-1.))
      IF (I.EQ.1) GO TO 100
      X3P=(X3A-X3)/X3
      Y3P=(Y3A-Y3)/Y3
      E1P=(E1A-E1)/E1
      T3P=T3A-T3
      IF (ABS(X3P).LT..0001.AND.ABS(Y3P).LT..0001.AND.ABS(E1P).LT..0001.
     1AND.ABS(T3P).LT..0001) GO TO 110
100   X3=X3A
      Y3=Y3A
      E1=E1A
      T3=T3A
      GO TO 20
C
110   CONTINUE
      DO 120 I=1,ITOT
      NSTRT=I
      XCK=X3A-XA(I)
      IF (XCK) 130,130,120
120   CONTINUE
130   CONTINUE
      RETURN
140   WRITE(6,150)
      STOP
150   FORMAT (1H0,28HTOO MANY ITERATIONS IN LOCAT)
      END
```

```
$IBFTC FLOW1
      SUBROUTINE FLOW1 (N,J,NTOT)
      REAL ML
      COMMON /B2/ XL,RL,ML,VL,TL
      COMMON /B3/ PA,PO,TO,RHOO,G,R,GO
      COMMON /B5/ REG
      COMMON /B8/ NWRITE
      COMMON /B9/ RAD,FOOT
      DIMENSION REG(1275,7), XL(75), RL(75), ML(75), VL(75), TL(75)
      IF (NWRITE.EQ.0) GO TO 10
      WRITE (6,150)
      WRITE (6,160)
      WRITE (6,170)
10    NJUMP=0
      REG(1,1)=XL(1)
      REG(1,2)=RL(1)
      REG(1,3)=ML(1)
      REG(1,4)=VL(1)
      REG(1,5)=TL(1)
      KOB=0
      IOB=1
      JOB=1
      TD=TL(1)*180.0/3.14159
      XD=XL(1)*FOOT
      RD=RL(1)*FOOT
      IF (NWRITE.NE.0) WRITE (6,180) IOB,JOB,XD,RD,ML(1),VL(1),TD,KOB
      IF (NWRITE.NE.0) WRITE (6,170)
      DO 140 I1=2,J,1
      IF (I1.GT.N) GO TO 20
      X1=XL(I1)
      X2=REG(1,1)
      Y1=RL(I1)
      Y2=REG(1,2)
      T1=TL(I1)
      T2=REG(1,5)
      V1=VL(I1)
      V2=REG(1,4)
      E1=ML(I1)
      E2=REG(1,3)
      GO TO 30
C
20    X1=XL(I1)
      X2=REG(2,1)
      Y1=RL(I1)
      Y2=REG(2,2)
      E1=ML(I1)
      E2=REG(2,3)
      V1=VL(I1)
      V2=REG(2,4)
      T1=TL(I1)
      T2=REG(2,5)
30    XX=REG(1,1)
      RX=REG(1,2)
      EX=REG(1,3)
      VX=REG(1,4)
```

```
      TX=REG(1,5)
      REG(1,1)=XL(I1)
      REG(1,2)=RL(I1)
      REG(1,3)=EL(I1)
      REG(1,4)=VL(I1)
      REG(1,5)=TL(I1)
      CALL CHAR1 (X1,X2,Y1,Y2,V1,V2,T1,T2,E1,E2,TO,G,SO,R,X3A,Y3A,V3A,T3
     1A,E3A,I)
      CALL QUAD (X1,X2,Y1,Y2,THETA)
      T1=THETA
      CALL QUAD (X1,X3A,Y1,Y3A,THETA)
      T2=THETA
      IF (T2.GE.0.0.AND.T2.LT.3.14159.AND.T1.GT.3.*3.14159/2..AND.T1.LT.
     16.28318) T1=T1-6.28318
      IF (T2-T1) 90,90,40
   40 CONTINUE
      KOB=0
      JOB=1
      IOB=I1-NJUMP
      TD=TL(I1)*180.0/3.14159
      XD=X1*FOOT
      RD=Y1*FOOT
      IF (NWRITE.NE.0) WRITE (6,180) IOB,JOB,XD,RD,E1,V1,TD,KOB
      TD=T3A*180./3.14159
      JOB=2
      XD=X3A*FOOT
      RD=Y3A*FOOT
      IF (NWRITE.NE.0) WRITE (6,180) IOB,JOB,XD,RD,E3A,V3A,TD,I
      IF (I1.GT.N) GO TO 70
      IF (I1.EQ.2) GO TO 60
      I3=I1-1
      DO 50 I2=2,I3
      X2=REG(I2,1)
      Y2=REG(I2,2)
      E2=REG(I2,3)
      V2=REG(I2,4)
      T2=REG(I2,5)
      REG(I2,1)=X3A
      REG(I2,2)=Y3A
      REG(I2,3)=E3A
      REG(I2,4)=V3A
      REG(I2,5)=T3A
      X1=X3A
      Y1=Y3A
      E1=E3A
      V1=V3A
      T1=T3A
      CALL CHAR1 (X1,X2,Y1,Y2,V1,V2,T1,T2,E1,E2,TO,G,SO,R,X3A,Y3A,V3A,T3
     1A,E3A,I)
      JOB=I2+1
      TD=T3A*180./3.14159
      XD=X3A*FOOT
      RD=Y3A*FOOT
      IF (NWRITE.NE.0) WRITE (6,180) IOB,JOB,XD,RD,E3A,V3A,TD,I
   50 CONTINUE
      XL(IOB)=X3A
```

```
      RL(IOB)=Y3A
      ML(IOB)=E3A
      VL(IOB)=V3A
      TL(IOB)=T3A
      REG(I1,1)=X3A
      REG(I1,2)=Y3A
      REG(I1,3)=E3A
      REG(I1,4)=V3A
      REG(I1,5)=T3A
      GO TO 130
C
60    XL(IOB)=X3A
      RL(IOB)=Y3A
      ML(IOB)=E3A
      VL(IOB)=V3A
      TL(IOB)=T3A
      REG(2,1)=X3A
      REG(2,2)=Y3A
      REG(2,3)=E3A
      REG(2,4)=V3A
      REG(2,5)=T3A
C
      GO TO 130
C
70    DO 80 I2=3,N
      REG(I2-1,1)=X3A
      REG(I2-1,2)=Y3A
      REG(I2-1,3)=E3A
      REG(I2-1,4)=V3A
      REG(I2-1,5)=T3A
      X1=X3A
      Y1=Y3A
      E1=E3A
      V1=V3A
      T1=T3A
      CALL CHAR1 (X1,REG(I2,1),Y1,REG(I2,2),V1,REG(I2,4),T1,REG(I2,5),E1
     1,REG(I2,3),TO,G,GO,R,X3A,Y3A,V3A,T3A,E3A,I)
      TD=T3A*180./3.14159
      XD=X3A*FOOT
      RD=Y3A*FOOT
80    IF (NWRITE.NE.0) WRITE (6,180) IOB,I2,XD,RD,E3A,V3A,TD,I
      REG(N,1)=X3A
      REG(N,2)=Y3A
      REG(N,3)=E3A
      REG(N,4)=V3A
      REG(N,5)=T3A
      XL(IOB)=X3A
      RL(IOB)=Y3A
      ML(IOB)=E3A
      VL(IOB)=V3A
      TL(IOB)=T3A
      GO TO 130
C
90    IF (I1.GT.N) GO TO 100
      GO TO 110
C
```

```
 100  IF (NWRITE.NE.0) WRITE (6,190)
      NJUMP=NJUMP+1
      GO TO 140
C
 110  IF (NWRITE.NE.0) WRITE (6,190)
      NJUMP=NJUMP+1
      JOB=1
      KOB=0
      IOB=I1-NJUMP
      TD=TL(I1)*180.0/3.14159
      XD=X1*FOOT
      RD=Y1*FOOT
      IF (NWRITE.NE.0) WRITE (6,180) IOB,JOB,XD,RD,E1,V1,TD,KOB
      X3A=REG(2,1)
      Y3A=REG(2,2)
      E3A=REG(2,3)
      V3A=REG(2,4)
      T3A=REG(2,5)
      REG(2,1)=XX
      REG(2,2)=RX
      REG(2,3)=EX
      REG(2,4)=VX
      REG(2,5)=TX
      JOB=2
      TD=REG(2,5)*180./3.14159
      XD=REG(2,1)*FOOT
      RD=REG(2,2)*FOOT
      IF (NWRITE.NE.0) WRITE (6,180) IOB,JOB,XD,RD,REG(2,3),REG(2,4),TD,
     1KOB
      DO 120 I2=3,I1
      XX=REG(I2,1)
      RX=REG(I2,2)
      EX=REG(I2,3)
      VX=REG(I2,4)
      TX=REG(I2,5)
      REG(I2,1)=X3A
      REG(I2,2)=Y3A
      REG(I2,3)=E3A
      REG(I2,4)=V3A
      REG(I2,5)=T3A
      TD=REG(I2,5)*180./3.14159
      XD=REG(I2,1)*FOOT
      RD=REG(I2,2)*FOOT
      IF (NWRITE.NE.0) WRITE (6,180) IOB,I2,XD,RD,REG(I2,3),REG(I2,4),TD
     1,KOB
      X3A=XX
      Y3A=RX
      E3A=EX
      V3A=VX
      T3A=TX
 120  CONTINUE
 130  IF (NWRITE.NE.0) WRITE (6,170)
 140  CONTINUE
      NTOT=J-NJUMP
      RETURN
C
```

```
C
C
150   FORMAT (1H1,37X,46HDATA FOR THE FLOW FIELD IN T4E SMALL REGION R1)
160   FORMAT (1H0,54X,4HMACH,22X,4HFLOW/25X,1HI,4X,1HJ,4X,2HXC,8X,2HRC,7
     1X,6HNUMBER,5X,8HVELOCITY,7X,5HANGLE,6X,4HITER/36X,4H(IN),6X,4H(IN)
     2,18X,5H(FPS),7X,9H(DEGREES))
170   FORMAT (1H0)
180   FORMAT (21X,215,3F10.5,F15.5,F12.5,17)
190   FORMAT (43X,34H RIGHT CHARACTERISTIC SKIPPED HERE)
      END
```

```
$IBFTC SEL
      SUBROUTINE SELECT (NPTS,K,KD,NS,CS,X,R,M,V,T)
      REAL M
      COMMON /B5/ REG
      COMMON /B6/ NPOINT
      DIMENSION REG(1275,7), X(75), R(75), M(75), V(75), T(75), NPOINT(5
     11)
C
      DZ=X(K)-X(1)
      N=NPTS-1
      DN=N
      DELTAZ=DZ/DN
      DELTZ1=DELTAZ/CS
      NQ=NS-1
      SN=NQ
      DN=NPTS-NS
      XS=X(1)+SN*DELTZ1
      DELTAZ=(X(K)-XS)/DN
      Z=X(1)
      REG(1,1)=X(1)
      REG(1,2)=R(1)
      REG(1,3)=M(1)
      REG(1,4)=V(1)
      REG(1,5)=T(1)
      NPOINT(1)=0
      DO 10 I=2,51
10    NPOINT(I)=NPOINT(I-1)+I-1
      DO 20 I=2,NPTS
      IF (I.GT.NS) DELTZ1=DELTAZ
      Z=Z+DELTZ1
      NJ=NPOINT(I)+1
      REG(NJ,1)=Z
      CALL AITKEN (X,R,K,KD,Z,YB)
      REG(NJ,2)=YB
      CALL AITKEN (X,M,K,KD,Z,YB)
      REG(NJ,3)=YB
      CALL AITKEN (X,V,K,KD,Z,YB)
      REG(NJ,4)=YB
      CALL AITKEN (X,T,K,KD,Z,YB)
      REG(NJ,5)=YB
20    CONTINUE
      RETURN
      END
```

```
$IBFTC FLOW
      SUBROUTINE FLOW (NZ,NY,NJ,NX,NCHECK,XLENG,NRECRD,XFINAL)
      COMMON /B3/ PA,PO,TO,RHOO,G,R,GO
      COMMON /B5/ REG
      COMMON /B6/ NP
      COMMON /B8/ NWRITE
      COMMON /B9/ RAD,FOOT
      COMMON /B13/ XS,RS,TS
      DIMENSION REG(1275,7), NP(51), XS(125), RS(125), TS(125)
      IF (NWRITE.EQ.0) GO TO 10
      WRITE (6,110)
      WRITE (6,130)
      WRITE (6,120)
      IOB=1
      JOB=1
      KOB=0
      TD=REG(1,5)/RAD
      XD=REG(1,1)*FOOT
      RD=REG(1,2)*FOOT
      WRITE (6,140) IOB,JOB,XD,RD,REG(1,3),REG(1,4),TD,KOB
      WRITE (6,120)
      IOB=2
      TD=REG(2,5)/RAD
      XD=REG(2,1)*FOOT
      RD=REG(2,2)*FOOT
      WRITE (6,140) IOB,JOB,XD,RD,REG(2,3),REG(2,4),TD,KOB
10    MY=NZ-2
      DO 70 N=NZ,NY
      IF (NCHECK.NE.1) NRECRD=N
      NS=N-2
      IF (NS.LE.0) GO TO 30
      MX=1
      IF (NZ.NE.2) MX=MY
      NW=NP(N)+1
      TD=REG(NW,5)/RAD
      JOB=1
      XD=REG(NW,1)*FOOT
      RD=REG(NW,2)*FOOT
      IF (NWRITE.NE.0) WRITE (6,140) N,JOB,XD,RD,REG(NW,3),REG(NW,4),TD,
     1KOB
      DO 20 M=MX,NS
      N1=NP(N)+M
      N2=NP(N-1)+M+1
      CALL CHAR1 (REG(N1,1),REG(N2,1),REG(N1,2),REG(N2,2),REG(N1,4),REG(
     1N2,4),REG(N1,5),REG(N2,5),REG(N1,3),REG(N2,3),TD,G,GO,R,X3A,Y3A,V3
     2A,T3A,E3A,I)
      N3=NP(N)+M+1
      REG(N3,1)=X3A
      REG(N3,2)=Y3A
      REG(N3,3)=E3A
      REG(N3,4)=V3A
      REG(N3,5)=T3A
      JOB=M+1
      TD=T3A*180./3.14159
      XD=X3A*FOOT
```

```
      RD=Y3A*FOOT
      IF (NWRITE.NE.0) WRITE (6,140) N,JOB,XD,RD,E3A,V3A,TD,I
20    CONTINUE
      GO TO 40
C
30    X3A=REG(2,1)
      Y3A=REG(2,2)
      E3A=REG(2,3)
      V3A=REG(2,4)
      T3A=REG(2,5)
40    X1=X3A
      Y1=Y3A
      T1=T3A
      E1=E3A
      V1=V3A
      N4=NP(N-1)+N-1
      X2=REG(N4,1)
      Y2=REG(N4,2)
      T2=REG(N4,5)
      CALL SURF (X1,Y1,X2,Y2,T2,T1,E1,V1,NJ,NX,X3A,Y3A,V3A,T3A,E3A,I)
      N3=NP(N)+N
      REG(N3,1)=X3A
      REG(N3,2)=Y3A
      REG(N3,3)=E3A
      REG(N3,4)=V3A
      REG(N3,5)=T3A
      TD=T3A*180./3.14159
      XD=X3A*FOOT
      RD=Y3A*FOOT
      IF (NWRITE.NE.0) WRITE (6,140) N,N,XD,RD,E3A,V3A,TD,I
      IF (NWRITE.NE.0) WRITE (6,120)
      IF (NCHECK.EQ.1) GO TO 70
      XCK=XLENG-(X3A-REG(1,1))
      IF (XCK.GT.0.0.AND.N.EQ.NY) WRITE (6,90)
      NYQ=NP(N)+1
      IF (XCK.GT.0.0.AND.N.EQ.NY) XFINAL=REG(NYQ,1)
      IF (XCK) 50,80,70
50    NE=N-1
      NF=NP(NE)+NE
      DX=XLENG-(REG(NF,1)-REG(1,1))
      DX1=REG(N3,1)-REG(NF,1)
      ZQ=XLENG+REG(1,1)
      REG(N3,1)=ZQ
      CALL AITKEN (XS,RS,NJ,NX,ZQ,YB)
      REG(N3,2)=YB
      CALL AITKEN (XS,TS,NJ,NX,ZQ,YB)
      REG(N3,5)=YB*3.14159/180.
      REG(N3,3)=REG(NF,3)+DX*(REG(N3,3)-REG(NF,3))/DX1
      REG(N3,4)=REG(NF,4)+DX*(REG(N3,4)-REG(NF,4))/DX1
      IF (NWRITE.NE.0) WRITE (6,100)
      IC=N
      N1=NP(N)+N
      N2=NP(NE)+NE
      IF (NWRITE.NE.0) WRITE (6,120)
      XD=REG(N3,1)*FOOT
      RD=REG(N3,2)*FOOT
```

```
      TD=REG(N3,5)/RAD
      IY=0
      IF (NWRITE.NE.0) WRITE (6,140) N,M,XD,RD,REG(N1,3),REG(N1,4),TD,IY
      DO 60 IX=1,NE
      IC=IC-1
      CALL CHAR1 (REG(N1,1),REG(N2,1),REG(N1,2),REG(N2,2),REG(N1,4),REG(
     1N2,4),REG(N1,5),REG(N2,5),REG(N1,3),REG(N2,3),T3,G,GO,R,X3A,Y3A,V3
     2A,T3A,E3A,I)
      N3=N1-1
      IF (IX.EQ.NE) XFINAL=X3A
      REG(N3,1)=X3A
      REG(N3,2)=Y3A
      REG(N3,3)=E3A
      REG(N3,4)=V3A
      REG(N3,5)=T3A
      TD=T3A/RAD
      XD=X3A*FOOT
      RD=Y3A*FOOT
      IF (NWRITE.NE.0) WRITE (6,140) N,IC,XD,RD,REG(N3,3),REG(N3,4),TD,I
      N1=N1-1
   60 N2=N2-1
      GO TO 80
C
   70 CONTINUE
   80 CONTINUE
      RETURN
C
C
C
   90 FORMAT (1H0,43X,34HTHE SELECTED UPSTREAM GEOMETRY AND/41X,36HAMBIE
     1NT PRESSURE PREVENT THE DESIRED/47X,26HLENGTH FROM BEING OBTAINED)
  100 FORMAT (1H0,36X,47HTHE PREVIOUS RIGHT CHARACTERISTIC IS BEYOND THE
     1/40X,41HREGION R AND IS REPLACED BY THE FOLLOWING)
  110 FORMAT (1H1,46X,28HDATA FOR THE MAIN FLOW FIELD)
  120 FORMAT (1H0)
  130 FORMAT (1H0,54X,4HMACH,22X,4HFLOW/25X,1HI,4X,1HJ,4X,2HXC,8X,2HRC,7
     1X,6HNUMBER,5X,8HVELOCITY,7X,5HANGLE,6X,4HITER/34X,4H(IN),6X,4H(IN)
     2,18X,5H(FPS),7X,9H(DEGREES))
  140 FORMAT (21X,2I5,3F10.5,F15.5,F12.5,I7)
      END
```

```
$IBFTC SKIN
      SUBROUTINE SKIN (VD,ED,CFI,TAU,TAURD,TAUR,TAURHO,TAUVD,TAUPD,RTAUD
     1X)
      COMMON /B3/ PA,PO,TO,RHOO,G,R,GO
      FUNCT1=1.+(G-1.)*ED**2/2.
      RHO=RHOO/FUNCT1**(1./(G-1.))
      CF=CFI/(1.0+.72*(G-1.0)*ED**2/2.0)**0.578
      TAU=0.5*CF*RHO*VD**2/GO
      TAUVD=0.0
      TAURD=0.0
      TAUR=0.0
      TAURHO=0.0
      TAUPD=0.0
      RTAUDX=0.0
      RETURN
      END
```

```
$IBFTC BASE1
      SUBROUTINE BASE (XD,RD,VD,M1,PB,PPHIPY,PPHIPX,AA,AB)
      REAL M1
      COMMON /B3/ PA,PO,TO,RHOO,G,R,GO
      P=PO/(1.0+(G-1.0)*M1**2/2.0)**(G/(G-1.0))
      PPHIPX=0.0
      PB=AA*P/M1**AB
      PPHIPY=RD*PB
      RETURN
      END
```

```
$IBFTC REST1
      SUBROUTINE REST (X,H,HP,HR,HRD,DDX)
      H=1.
      HP=0.0
      HR=0.0
      HRD=0.0
      DDX=0.0
      RETURN
      END
```

```
$IBFTC QUAD1
      SUBROUTINE QUAD (X1,X2,Y1,Y2,THETA)
      DX=X2-X1
      DY=Y2-Y1
      D=SQRT(DX**2+DY**2)
      ST=DY/D
      CT=DX/D
      IF (ST.GT.0.0.AND.CT.GT.0.0) GO TO 10
      IF (ST.GT.0.0.AND.CT.LT.0.0) GO TO 20
      IF (ST.LT.0.0.AND.CT.LT.0.0) GO TO 20
      IF (ST.LT.0.0.AND.CT.GT.0.0) GO TO 30
      IF (ST.EQ.0.0.AND.CT.EQ.1.0) GO TO 40
      IF (ST.EQ.0.0.AND.CT.EQ.-1.0) GO TO 50
      IF (ST.EQ.1.0.AND.CT.EQ.0.0) GO TO 60
      IF (ST.EQ.-1.0.AND.CT.EQ.0.0) GO TO 70
10    THETA=ATAN(DY/DX)
      GO TO 80
C
20    THETA=3.14159+ATAN(DY/DX)
      GO TO 80
C
30    THETA=6.28318+ATAN(DY/DX)
      GO TO 80
C
40    THETA=0.0
      GO TO 80
C
50    THETA=3.14159
      GO TO 80
C
60    THETA=3.14159/2.0
      GO TO 80
C
70    THETA=3.*3.14159/2.
80    CONTINUE
      RETURN
      END
```

```
$IBFTC CHARI
      SUBROUTINE CHARI (X1,X2,Y1,Y2,V1,V2,T1,T2,E1,E2,TO,G,GO,R,X3A,Y3A,
     1V3A,T3A,E3A,I)
C
      D1=1.0/SQRT(E1**2-1.0)
      D2=1.0/SQRT(E2**2-1.0)
      A1=ATAN(D1)
      A2=ATAN(D2)
      Q1=COS(A1)/(SIN(A1)*V1)
      Q2=COS(A2)/(SIN(A2)*V2)
      F2=SIN(T2)*SIN(A2)/SIN(T2+A2)
      G1=SIN(T1)*SIN(A1)/SIN(T1-A1)
      A13=A1
      A23=A2
      T13=T1
      T23=T2
      Q13=Q1
      Q23=Q2
      F23=F2
      G13=G1
      I=0
10    I=I+1
      X3A=(Y2-Y1+X1*SIN(T13-A13)/COS(T13-A13)-X2*SIN(T23+A23)/COS(T23+A2
     13))/(SIN(T13-A13)/COS(T13-A13)-SIN(T23+A23)/COS(T23+A23))

      Y3A=Y1+(X3A-X1)*SIN(T13-A13)/COS(T13-A13)
      Y13=(Y1+Y3A)/2.0
      Y23=(Y2+Y3A)/2.0
      IF (ABS(T13-A13).LT..314159) GO TO 20
      IF (ABS(T23+A23).LT..314159) GO TO 30
      V3A=(T1-T2+Q13*V1+Q23*V2+G13*(Y3A-Y1)/Y13+F23*(Y3A-Y2)/Y23)/(Q13+Q
     123)
      T3A=T1-Q13*(V3A-V1)+G13*(Y3A-Y1)/Y13
      GO TO 40
C
20    G13=SIN(T13)*SIN(A13)/COS(T13-A13)
      V3A=(T1-T2+Q13*V1+Q23*V2+G13*(X3A-X1)/Y13+F23*(Y3A-Y2)/Y23)/(Q13+Q
     123)
      T3A=T1-Q13*(V3A-V1)+G13*(X3A-X1)/Y13
      GO TO 40
C
30    F23=SIN(T23)*SIN(A23)/COS(T23+A23)
      V3A=(T1-T2+Q13*V1+Q23*V2+G13*(Y3A-Y1)/Y13+F23*(X3A-X2)/Y23)/(Q13+Q
     123)
      T3A=T1-Q13*(V3A-V1)+G13*(Y3A-Y1)/Y13
40    TE3A=TO-V3A**2*(G-1.0)/(2.0*G*GO*R)
      SP3A=SQRT(G*GO*R*TE3A)
      E3A=V3A/SP3A
      IF (E3A.LE.1.0.AND.I.LE.10) E3A=1.09
      D3A=1.0/SQRT(E3A**2-1.0)
      A3A=ATAN(D3A)
      IF (I.EQ.1) GO TO 50
      X3P=(X3A-X3)/X3
      Y3P=(Y3A-Y3)/Y3
      E3P=(E3A-E3)/E3
```

```
      T3P=T3A-T3
      IF (ABS(X3P).LT..0001.AND.ABS(Y3P).LT..0001.AND.ABS(E3P).LT..0001.
     1AND.ABS(T3P).LT..0001) GO TO 60
50    T13=(T1+T3A)/2.0
      T23=(T2+T3A)/2.0
      A13=(A1+A3A)/2.0
      A23=(A2+A3A)/2.0
      V13=(V1+V3A)/2.0
      V23=(V2+V3A)/2.0
      Q13=COS(A13)/(SIN(A13)*V13)
      Q23=COS(A23)/(SIN(A23)*V23)
      F23=SIN(T23)*SIN(A23)/SIN(T23+A23)
      G13=SIN(T13)*SIN(A13)/SIN(T13-A13)
      X3=X3A
      Y3=Y3A
      T3=T3A
      E3=E3A
      GO TO 10
C
60    CONTINUE
      RETURN
      END
```

```
$IBFTC SURF1
      SUBROUTINE SURF (X1,Y1,X2,Y2,T2,T1,E1,V1,N,M,X3A,Y3A,V3A,T3A,E3A,I
     1)
      DIMENSION XS(125), RS(125), TS(125)
      COMMON /B3/ PA,PO,TO,RHOO,G,R,GO
      COMMON /B13/ XS,RS,TS
      D1=1.0/SQRT(E1**2-1.0)
C
      A1=ATAN(D1)
      Q1=COS(A1)/(SIN(A1)*V1)
      G1=SIN(T1)*SIN(A1)/SIN(T1-A1)
      A13=A1
      Q13=Q1
      G13=G1
      I=0
      I1=0
      X3A=X1
      T13=T1
      A13=A1
10    I=I+1
      C=TAN(T13-A13)
      D=Y1-C*X1
20    I1=I1+1
      CALL AITKEN (XS,RS,N,M,X3A,YB)
      Y3A=YB
      CALL AITKEN (XS,TS,N,M,X3A,YB)
      T3A=YB*3.14159/180.
      A=(TAN(T2)+TAN(T3A))/2.
      B=Y2-A*X2
      IF (I1.EQ.1) GO TO 50
      X3A=(D-B)/(A-C)
      IF (X3.EQ.0.0.OR.Y3.EQ.0.0) GO TO 30
      X3P=(X3A-X3)/X3
      Y3P=(Y3A-Y3)/Y3
      GO TO 40
C
30    X3P=X3A-X3
      Y3P=Y3A-Y3
40    CONTINUE
      IF (ABS(X3P).LT..0001.AND.ABS(Y3P).LT..0001) GO TO 60
50    X3=X3A
      Y3=Y3A
      IF (I1.GE.100) GO TO 60
      GO TO 20
C
60    CONTINUE
      T13=(T1+T3A)/2.0
      Y13=(Y1+Y3A)/2.0
      V3A=V1+(G13*(Y3A-Y1)/Y13-(T3A-T1))/Q13
      TE3A=TO-V3A**2*(G-1.0)/(2.0*G*GO*R)
      SP3A=SQRT(G*GO*R*TE3A)
      E3A=V3A/SP3A
      IF (E3A.LE.1.01.AND.I.LE.20) E3A=1.05
      D3A=1.0/SQRT(E3A**2-1.0)
      A3A=ATAN(D3A)
```

```
      IF (I.EQ.1) GO TO 70
      E3P=(E3A-E3)/E3
      T3P=T3A-T3
      IF (I1.GE.100.OR.I.GE.100) GO TO 80
      IF (ABS(E3P).LT..0001.AND.ABS(T3P).LT..0001) GO TO 90
70    A13=(A1+A3A)/2.
      V13=(V1+V3A)/2.0
      Q13=COS(A13)/(SIN(A13)*V13)
      G13=SIN(T13)*SIN(A13)/SIN(T13-A13)
      X3=X3A
      Y3=Y3A
      T3=T3A
      E3=E3A
      GO TO 10
C
80    CONTINUE
      WRITE (6,100)
      STOP
C
90    CONTINUE
      RETURN
C
C
C
100   FORMAT (1H0,27HTOO MANY ITERATIONS IN SURF)
      END
```

```
$IBFTC LSQ
      SUBROUTINE LSQARE (N,X,Y,A,B)
      DIMENSION X(N), Y(N)
C
C     LEAST SQUARE FIT TO A STHRAGHT LINE   Y=A*X + B
C
C     FORM SUMS
C
      SX=0.0
      SY=0.0
      SXY=0.0
      SX2=0.0
      DO 10 I=1,N
      SX=SX+X(I)
      SY=SY+Y(I)
      SXY=SXY+X(I)*Y(I)
      SX2=SX2+X(I)**2
10    CONTINUE
      SXQ2=SX**2
      AN=N
C
C     CALCULATE CONSTANTS
C
      A=(AN*SXY-SY*SX)/(AN*SX2-SXQ2)
      B=(SY-A*SX)/AN
      RETURN
      END
```

```
$IBFTC AITKEN
      SUBROUTINE AITKEN (X,Y,N,K,XB,YB)
C
CAITKEN INTERPOLATION SUBROUTINE
C      CALLING SEQUENCE....
C      CALL AITKEN(X,Y,N,K,XB,YB)
C         X IS A ONE DIMENSIONAL ARRAY OF INDEPENDENT
C            VARIABLE(INCREASING OR DECREASING)
C         Y IS A ONE DIMENSIONAL ARRAY OF DEPENDENT
C            VARIABLE
C         N IS NO. OF X,Y PAIRS
C         K IS DEGREE OF INTERPOLATING POLYNOMIAL  (MAX = 10 )
C         YB IS INTERPOLATED RESULT
C         XB IS INDEP. VARIABLE ARGUMENT
C
      DIMENSION X(N), Y(N), XX(11), YY(11)
      K1=K+1
      IF (X(N)-X(1)) 100,10,10
10    IF (XB-X(1)) 20,20,30
20    LL=0
      GO TO 190
C
30    IF (X(N)-XB) 40,40,50
40    LL=N-K1
      GO TO 190
C
50    LL=1
      LU=N
60    IF (LU-LL-1) 170,170,70
70    L1=(LL+LU)/2
      IF (X(L1)-XB) 80,80,90
80    LL=L1
      GO TO 60
C
90    LU=L1
      GO TO 60
C
100   IF (XB-X(1)) 110,20,20
110   IF (X(N)-XB) 120,40,40
120   LL=1
      LU=N
130   IF (LU-LL-1) 170,170,140
140   L1=(LL+LU)/2
      IF (X(L1)-XB) 150,160,160
150   LU=L1
      GO TO 130
C
160   LL=L1
      GO TO 130
C
170   LL=LL-(K1+1)/2
      IF (LL) 20,190,180
180   IF (LL+K1-N) 190,190,40
190   DO 200 I=1,K1
      I1=LL+I
```

```
      XX(I)=X(I1)-XB
200   YY(I)=Y(I1)
      DO 210 I=1,K
      DU 210 J=I,K
210   YY(J+1)=(1./(XX(J+1)-XX(I)))*(YY(I)*XX(J+1)-YY(J+1)*XX(I))
      YB=YY(K1)
      RETURN
      END
$DATA
```

UNCLASSIFIED
Security Classification

DOCUMENT CONTROL DATA - R & D

(Security classification of title, body of abstract and indexing annotation must be entered when the overall report is classified)

1. ORIGINATING ACTIVITY (Corporate author) Purdue University Lafayette, Indiana 47907	2a. REPORT SECURITY CLASSIFICATION UNCLASSIFIED 2b. GROUP

3. REPORT TITLE
DESIGN OF MAXIMUM THRUST PLUG NOZZLES FOR FIXED INLET GEOMETRY

4. DESCRIPTIVE NOTES (Type of report and inclusive dates)
Technical Report covering period 1 September 1966 to 31 August 1969

5. AUTHOR(S) (First name, middle initial, last name)
Robert P. Humphreys, H. Doyle Thompson, and Joe D. Hoffman

6. REPORT DATE	7a. TOTAL NO. OF PAGES	7b. NO. OF REFS
June 1970	222	35

8a. CONTRACT OR GRANT NO. Air Force F33615-67-C-1068 b. PROJECT NO. BPSN: 7(63 301206 6205214) c. d.	9a. ORIGINATOR'S REPORT NUMBER(S) 9b. OTHER REPORT NO(S) (Any other numbers that may be assigned this report) AFAPL-TR-70-47

10. DISTRIBUTION STATEMENT
This document is subject to special export controls and each transmittal to foreign governments or foreign nationals may be made only with prior approval of AFAPL, Wright-Patterson AFB, Ohio

11. SUPPLEMENTARY NOTES	12. SPONSORING MILITARY ACTIVITY
	Air Force Aero Propulsion Laboratory Wright-Patterson Air Force Base, Ohio

13. ABSTRACT

The techniques of the calculus of variations ~~have been~~ used to determine the configuration of an optimum thrust plug nozzle. The problem is formulated for a fixed thrust injection angle and cowl lip radius, and the resulting plug contour is then an optimum for a given upstream geometry. The optimum values of the injection angle and cowl lip radius are determined by a parametric study. The analysis is carried out for rotational and irrotational flows and includes boundary layer effects. A method is presented for each of the problem formulations to determine if a given contour is an optimum and a relaxation technique is used to obtain a solution to the irrotational flow problem.

A computer program which makes use of the design equations for the irrotational flow problem is developed and described. This program is used to carry out a parametric study to determine the optimum cowl lip radius and injection angle when the plug length is fixed. The resulting optimum nozzle is compared to one designed by Rao's Method. The importance of determining the base pressure accurately is illustrated and an example of scramjet nozzle optimization is presented.

DD FORM 1 NOV 65 1473 (PAGE 1)
S/N 0101-807-6811

UNCLASSIFIED
Security Classification

A-31408

14 KEY WORDS	LINK A		LINK B		LINK C	
	ROLE	WT	ROLE	WT	ROLE	WT
Scramjet Technology						
Exhaust Nozzle						
Optimum Nozzle Design						
Method of Characteristic						
Boundary Layer						
Calculus of Variations						
Numerical Relaxation Technique						
Computer Program						
Plug Nozzles						

DD FORM 1 NOV 65 1473 (BACK)